1-1-2015

Cardiolipin Regulates Mitophagy Through The Pkc Pathway

Zheni Shen
Wayne State University,

CARDIOLIPIN REGULATES MITOPHAGY THROUGH THE PKC PATHWAY

by

ZHENI SHEN

DISSERTATION

Submitted to the Graduate School

of Wayne State University,

Detroit, Michigan

in partial fulfillment of the requirements

for the degree of

DOCTOR OF PHILOSOPHY

2015

MAJOR: BIOLOGICAL SCIENCES

Approved by:

_____

Advisor Date

_____

_____

_____

_____

DEDICATION

To my loving parents, husband Yanhua Zhang, for all their love and support & my dear daughter Faith for bringing me so much happiness

ACKNOWLEDGMENTS

I would like to extend my deepest gratitude to my advisor Professor Miriam L. Greenberg for her continuous support and outstanding guidance throughout my work. She not only taught me numerous scientific knowledge and writing skills, but also taught me many virtues that will benefit me throughout my life. I can write pages to express how much I respect and appreciate her.

My sincere appreciation to my committee members, Professor Karen A. Beningo, Professor Victoria H. Meller and Professor David H. Kessel, for their precious time, valuable advice, and continuous support throughout my graduate studies.

I am very grateful to former and present members of the Greenberg group, especially Dr. Cunqi Ye and Dr. Shuliang Chen for all the valuable scientific discussions and technical suggestions, and Dr. Jingming Zhou, Dr. Amit Joshi, Dr. Vinay Patil, and Dr. Rania Deranieh for sharing their knowledge and experience. And I would express my appreciation to my colleagues: Yiran Li, Wenjia Lou, Vaishnavi Raja, Wenxi Yu, Shyamala Jadhav, Michael Salsa, Jiajia Ji, and Keanna L. McCain for their generous help and friendship.

The friendship and enormous help of Alexander N. Gasparski with my graduate studies and scientific writing is greatly acknowledged.

I am very grateful to my parents for all their love, support and efforts in guiding me to the right path in life. My heartfelt appreciation goes to my husband Yanhua Zhang for his love, and unconditional support. Finally, my blessings and thanks go to my daughter Faith, for the hope and love that she brings into my life.

TABLE OF CONTENTS

CHAPTER **PAGE**

DEDICATION ii

ACKNOWLEDGEMENTS iii

LIST OF TABLES v

LIST OF FIGURES vi

CHAPTER 1 – INTRODUCTION 1

CHAPTER 2 – LOSS OF CARDIOLIPIN LEADS TO DEFECTIVE MITOPHAGY 19

Introduction 19

Methods and Materials 23

Results 32

Discussion 44

CHAPTER 3 – DEFECTIVE MITOPHAGY IN crd1Δ MAY RESULT FROM DECREASED MAPK PATHWAYS 47

Introduction 47

Methods and Materials 51

Results 59

Discussion 73

CHAPTER 4 - FUTURE DIRECTIONS 76

REFERENCES 104

ABSTRACT 135

AUTOBIOGRAPHICAL STATEMENT 137

LIST OF TABLES

TABLE **PAGE**

Table 2.1 Yeast strains and plasmids used in Chapter 2.....26

Table 2.2 Real-time PCR primers used in Chapter 2…….27

Table 3.1 Yeast strains used in Chapter 3 52

Table 3.2 Antibodies used in determining MAPK pathway activation.....58

Table 4.1 Deletion strains used in the mini SGA.....82

LIST OF FIGURES

FIGURE **PAGE**

Figure 1.1 CL synthesis and remodeling pathway in Saccharomyces cerevisiae. ..2

Figure 2.1 Deletion of UTH1 rescues (A) the vacuole morphology defect of crd1Δ at 37℃, (B) the vacuole acidification defect of crd1 at 37℃ ..... ……33

Figure 2.2 Deletion of autophagy/mitophagy genes does not rescue *crd1Δ* growth defect at 37℃ 35

Figure 2.3 *crd1Δ* is (A) synthetically lethal with atg8Δ and atg18Δ at 36℃, (B) synthetically sick with *atg32Δ* at 36℃.....36

Figure 2.4 Insertion of GFP into the IDH1 gene locus.....37

Figure 2.5 Delivery of mitochondria to the vacuole in response to increased temperature is inhibited in *crd1Δ* 39

Figure 2.6 Increased temperature triggers increased upregulation of *ATG8* expression in *crd1Δ* cells 40

Figure 2.7 Decreased mitophagy in *crd1Δ* cells.....42

Figure 2.8 Decreased mitophagy in *crd1Δ* cells expressing Idh1-GFP 43

Figure 3.1 The PKC and HOG pathways regulate different stages of mitophagy.49

Figure 3.2 Construction of the pYPGK18-*PTP2* and pYPGK18-*PTP3* overexpression plasmids.....54

Figure 3.3 Deletion of HOG pathway genes is synthetically lethal with *CRD1* deletion 61

Figure 3.4 Overexpression of the negative regulators of the HOG pathway is synthetically lethal with *CRD1* deletion.....62

Figure 3.5 (A) Decreased Hog1p phosphorylation in the *crd1Δ* mutant, (B) Translocation of activated Hog1p is not affected in *crd1Δ*. 64

Figure 3.6 Heat stress does not (A) trigger phosphorylation in the BY4742 background, (B) induce the translocation of GFP tagged Hog1p into the nucleus in the BY4742 background 65

Figure 3.7 (A) The PKC pathway is decreased in *crd1Δ*, (B) Upregulation of the PKC pathway rescues the *crd1Δ* growth defect 67

Figure 3.8 Upregulation of the PKC pathway rescues the delivery of mitochondria into vacuole in crd1Δ after induction of mitophagy.....69

Figure 3.9 Upregulation of the PKC pathway rescues mitophagy in *crd1Δ* 71

Figure 3.10 200 mM NaCl rescues *crd1Δ* temperature sensitivity 72

Figure 4.1 1 M sorbitol induces Hog1p activation in *crd1Δ* at elevated temperature 80

Figure 4.2 Deletion of *ANP1*, *PTC7*, *OSM1* or *DOG2* does not abrogate the rescue of *crd1Δ* temperature sensitivity by sorbitol.....83

Figure 4.3 Deletion of *ATG8* does not rescue the vacuole enlargement triggered by elevated temperature in *crd1Δ* 85
Figure 4.4 Rapamycin triggers enlargement of vacuoles in both WT and *crd1Δ*, which is not rescued by deletion of *ATG8* 87
Figure 4.5 The FAB pathway and its regulation 89
Figure 4.6 Deletion of *FIG4* partially rescues *crd1Δ* temperature sensitivity 91
Figure 4.7 *crd1Δ* exhibits normal PI3P localization at the vacuolar membrane 93
Figure 4.8 Normal vacuolar localization of $PI(3,5)P_2$ in *crd1Δ* 94
Figure 4.9 Overexpression of *FAB1* and *VAC7* does not rescue *crd1Δ* temperature sensitivity 96
Figure 4.10 Deletion of *ENA1* does not affect *crd1Δ* temperature sensitivity 99
Figure 4.11 Inadequate *ENA1* upregulation in *crd1Δ* compared to WT, at elevated temperature 101
Figure 4.12 Overexpression of *ENA1* does not rescue *crd1Δ* temperature sensitivity 102

CHAPTER 1

INTRODUCTION

Parts of this chapter have been submitted for publication to the journal *BioMed Research International*.

Cardiolipin (CL), the signature phospholipid of mitochondrial membranes, is crucial for mitochondrial function and is involved in various cellular processes outside of the mitochondria. The importance of CL in cardiovascular health is underscored by the life-threatening genetic disorder Barth syndrome (BTHS), which manifests clinically as cardiomyopathy, skeletal myopathy, neutropenia, and growth retardation. In addition to BTHS, CL is linked to various cardiovascular diseases (CVDs), including cardiomyopathy, atherosclerosis, myocardial ischemia-reperfusion injury, heart failure and Tangier disease. The link between CL and CVDs may possibly be explained by the physiological roles of CL in pathways that have cardioprotective function, such as autophagy/mitophagy and the mitogen-activated protein kinase (MAPK) pathways. My dissertation work focuses on elucidating how CL influences mitophagy and MAPK pathways. This knowledge may contribute to our understanding of the function of this important lipid, and may ultimately identify novel therapeutic strategies to treat CVDs and improve heart performance.

1. CL and CL synthesis

CL contains two phosphatidyl moieties joined by a central glycerol backbone, forming a dimeric structure (De Bruijn, 1966). Thus, unlike other phospholipids that contain two fatty acyl chains linked to glycerol, CL has four acyl chains. Considering the potential combinations of fatty acyl groups on CL, a large number of CL species may be possible. However, in most organisms and tissues, the fatty acyl composition of CL is unique and specific. For example, bacterial CL contains both saturated and monounsaturated fatty acyl chains that are composed of 14–19 carbons (Kito et al., 1972). In eukaryotes, CL mainly contains monounsaturated and diunsaturated fatty acyl chains that consist of 16–18 carbons (Schlame et al., 1993). In mammals, CL acyl species vary in different tissues, but the most abundant species in the heart is tetralinoleoyl CL. In yeast, the predominant fatty acyl species of CL are oleic acid and palmitoleic acid (Schlame et al., 1993). While CL plays critical roles in mitochondrial biogenesis, fusion and fission, respiration and protein import (Joshi et al., 2009), it is also involved in various cellular processes outside of the mitochondria. These include, but are not limited to cell wall biogenesis (Zhong et al., 2005), vacuole homeostasis (Chen et al., 2008b), ageing (Zhou et al., 2009), the cell cycle (Chen et al., 2010), and apoptosis (Li et al., 2015).

Unlike mitochondrial membrane lipids that are synthesized in the endoplasmic reticulum, *de novo* synthesis of CL occurs exclusively in the inner membrane of the mitochondria (Hostetler et al., 1972) in a series of well-characterized steps that are conserved from yeast to higher eukaryotes (Tian et al., 2012). The first step in the CL biosynthetic pathway is the conversion of phosphatidic acid (PA) to CDP-diacylglycerol

(CDP-DAG), which is catalyzed in the inner membrane by CDP-DAG synthase encoded by *TAM41* (Deprez et al., 2002; Kutik et al., 2008; Tamura et al., 2013). The *PGS1*-encoded phosphatidylglycerolphosphate (PGP) synthase catalyzes transfer of the phosphatidyl group from CDP-DAG to a glycerol-3-phosphate molecule to generate PGP (Chang et al., 1998b). PGP is subsequently dephosphorylated to phosphotidylglycerol (PG) by PGP phosphatase, encoded by *PTPMT1* in mammals (Xiao et al., 2011; Zhang et al., 2011) and *GEP4* in yeast (Osman et al., 2010). The final step in the biosynthetic pathway is carried out by CL synthase, encoded by *hCLS1* in human cells (Chen et al., 2006; Houtkooper et al., 2006; Lu et al., 2006) and by *CRD1* in yeast (Chang et al., 1998a; Jiang et al., 1997; Tuller et al., 1998). In this step, a second phosphatidyl group is added to PG from another CDP-DAG molecule, generating CL (Hostetler et al., 1972; Houtkooper et al., 2006; Malhotra et al., 2009).

The acyl composition of CL varies in different tissues, and the CL remodeling process is responsible for the CL acyl group exchange following CL *de novo* synthesis. CL remodeling may occur through two mechanisms (Ye et al., 2014b). In the two-step mechanism, CL is first deacylated to monolyso-CL (MLCL) by phospholipases (Lands, 1960). In yeast, the only CL-specific phospholipase is encoded by *CLD1* (Beranek et al., 2009), while in mammals, several phospholipases are reported to have CL-hydrolyzing activities, including $iPLA_2\beta$, $iPLA_2\gamma$, $cPLA_2$, and $sPLA_2$ (Buckland et al., 1998; Dennis et al., 2011; Hsu et al., 2013). MLCL is reacylated to remodeled CL by the transacylase tafazzin, encoded by the tafazzin gene (*TAZ/G4.5*) located on Xq28 in human cells (Bione et al., 1996) and by *TAZ1* in yeast (Gu et al., 2004; Vaz et al.,

2003). Acyltransferases encoded by *ALCAT1* (Cao et al., 2004) and *MLCLAT1* (Taylor and Hatch, 2009) have also been described in mammalian cells. In the one-step mechanism, CL remodeling occurs by direct transacylation (Xu et al., 2003; Yamashita et al., 1997). Mutations in tafazzin perturb CL remodeling and cause the life-threatening genetic disorder Barth syndrome (BTHS) (Barth PG et al., 1983), which is discussed below.

The CL synthesis and remodeling pathway in my research model, *Saccharomyces cerevisiae*, is shown in Fig. 1.1.

2. Relationship between CL and CVD

2.1 CL and cardiomyopathy

2.1.1 Barth syndrome

The most direct link between CVD and CL is seen in BTHS, an X-linked genetic disorder of CL remodeling caused by tafazzin mutations. BTHS manifests clinically as cardiomyopathy, skeletal myopathy, neutropenia, and growth retardation (Barth et al., 1999). More than 160 mutations in the tafazzin gene have been identified in BTHS patients (Chen et al., 2002; D'Adamo et al., 1997; Hijikata et al., 2015). These mutations result in loss of function of tafazzin, leading to decreased cellular CL, increased MLCL, and altered CL fatty acyl composition (Schlame et al., 2003; Schlame et al., 2002; Valianpour et al., 2002). Total CL is decreased to about 80% in BTHS platelets and skeletal muscle and 20% in cardiac tissue (Schlame et al., 2002). CL species vary in different tissues. Tetralinoleoyl-CL (L4-CL) is the most abundant

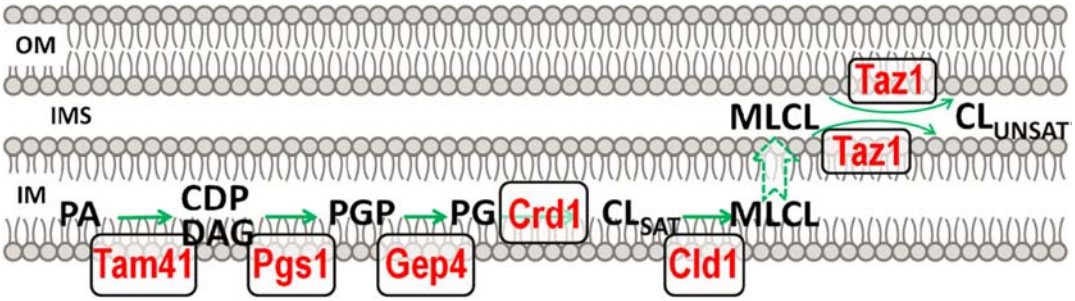

Fig. 1.1 Cardiolipin synthesis and remodeling pathway in *Saccharomyces cerevisiae.* Cited from Ye et al. 2014b. Cited from Ye et al. 2014b. The first reaction of CL de novo synthesis is the conversion of phosphatidic acid (PA) to CDP-diacylglycerol (CDP-DAG) by the mitochondrial CDP-DAG synthase Tam41. The committed step of CL synthesis is catalyzed by Pgs1, which converts CDP-DAG to phosphatidylglycerolphosphate (PGP). PGP is subsequently dephosphorylated to phosphatidylglycerol (PG) by the GEP4-encoded PGP phosphatase. CL synthase, encoded by CRD1, condenses PG and CDP-DAG to form CL. CL synthesized de novo has primarily saturated acyl chains (CLSAT). CLSAT is deacylated by the CL-specific phospholipase Cld1 to monolysocardiolipin (MLCL), which is reacylated by tafazzin (the TAZ1 gene product) to CL containing more unsaturated acyl chains (CLUNSAT). All the CL biosynthetic enzymes are localized in the mitochondrial inner membrane (IM), whereas tafazzin is localized in the outer face of the (IM) and the inner face of the outer membrane (OM). IMS: intermembrane space.

CL species in heart, skeletal muscle and most other tissues, whereas acyl species such as arachidonic and docosahexaenoic acids are found in brain (Cheng et al., 2008; Houtkooper and Vaz, 2008; Schlame and Ren, 2006). L4-CL is absent in BTHS, while increases in other CL species are present (Schlame et al., 2003; Schlame et al., 2002; Valianpour et al., 2002).

Understanding the cellular function and molecular mechanisms of CL remodeling may provide better treatment options for BTHS patients (Ye et al., 2014b). Tafazzin deficiency results in decreased CL, increased MLCL, and altered CL species, any of which may cause the pathology in BTHS. Recent findings in yeast indicate that deletion of Cld1p-mediated deacylation rescues growth and lifespan defects in tafazzin deficient cells (Baile et al., 2013; Ye et al., 2014a). Because the *cld1* mutation restored CL levels without generating remodeled CL, these findings suggest that decreased total CL and/or increased MLCL, but not decreased remodeled CL, causes the defects associated with tafazzin deficiency. Inhibiting CL deacylation may, thus, be a potential strategy to treat BTHS patients.

2.1.2 Dilated cardiomyopathy with ataxia (DCMA) syndrome

DCMA syndrome is an autosomal recessive genetic disorder that is characterized by early onset dilated cardiomyopathy with conduction defects, non-progressive cerebellar ataxia, testicular dysgenesis, growth failure, and 3-methylglutaconic aciduria (Davey et al., 2006). These clinical manifestations are similar to phenotypes found in BTHS. Patients with DCMA have a common mutation, a G→C

base substitution within a splice site of the *DNAJC19* gene (Davey et al., 2006). DNAJC19 protein localizes to the mitochondria and shares sequence and location similarity with yeast Tim14, an essential subunit of the TIM23 complex (D'Silva et al., 2003; Mokranjac et al., 2003). TIM23 is required for the import of protein precursors from the cytoplasm into the mitochondrial matrix and inner membrane (Rehling et al., 2003). This suggests that the DCMA phenotype may result from defective mitochondrial protein import. Interestingly, loss of CL also leads to defective mitochondrial protein import (Eilers et al., 1989; Endo et al., 1989; Endo and Schatz, 1988; Gebert et al., 2009; Jiang et al., 2000). Therefore, it is interesting to speculate that defective mitochondrial protein import may be common to DCMA and BTHS. A recent study suggests that CL may play a role in the pathogenesis of DCMA (Richter-Dennerlein et al., 2014). DNAJC19 protein is reported to form the PHB/DNAJC19 complex with prohibitin, a ring-like scaffold protein located in the mitochondrial inner membrane. The PHB/DNAJC19 complex modulates CL remodeling by regulating tafazzin activity. Depletion of *DNAJC19* does not affect CL or MLCL levels but alters the acyl chain composition of CL (Richter-Dennerlein et al., 2014). However, if the cause of DCMA is due to defective protein import, altered CL fatty acyl species, or a combination of the two remains unknown.

2.1.3 Diabetic cardiomyopathy

Diabetes is a metabolic disease characterized by increased levels of glucose in the blood over a prolonged period. It is due to either poor insulin production (type I) or

insulin resistance with β-cell dysfunction (type II) (He and Han, 2014). Diabetic complications are characterized by a group of diseases derived from microvascular and macrovascular damage, including diabetic cardiomyopathy, myonecrosis, stroke, peripheral vascular disease, nephropathy, retinopathy and encephalopathy (Nathan, 1993). Diabetes doubles the risk of CVD, of which diabetic cardiomyopathy is the leading cause of mortality. Diabetic cardiomyopathy is characterized by altered lipid composition and mitochondrial dysfunction in the diabetic myocardium (Han et al., 2000). In the early stages of pathological development in the type II diabetic mouse model, a sharp decrease in total cardiac CL is observed (Han et al., 2005). In addition to a decrease in the whole cell CL content, there is also a shift from the predominant fatty acyl species, L4-CL (18:2) to longer and polyunsaturated fatty acids, due to aberrant CL remodeling (Han et al., 2007). Strikingly, these alterations are similar to changes observed in the type I model of diabetes. In type II diabetic mice, treatment with the antidiabetic drug rosiglitazone restored total CL, L4-CL, and polyunsaturated CL levels (Pan et al., 2006). Impairment of CL synthesis plays a causal role in mitochondrial dysfunction (Koshkin and Greenberg, 2002; Mileykovskaya and Dowhan, 2014a; Pfeiffer et al., 2003), and mitochondrial dysfunction is associated with the pathogenesis of diabetic CVD, especially the sequential events following silent myocardial ischemia in diabetics (Sack, 2009). Thus, the sharp decrease in total cardiac CL and the altered CL fatty acyl species in the early stages of diabetic pathogenesis may play a key role in the progression of this disease.

2.2 CL is associated with other CVDs

In addition to its role in cardiomyopathy, CL has been linked to other CVDs, including atherosclerosis, Tangier disease, myocardial ischemia-reperfusion and heart failure.

Atherosclerosis is a form of arteriosclerosis in which an artery wall thickens due to chronic invasion and further accumulation of white blood cells (WBC), remnants of dead cells, cholesterol, and triglycerides (Ross, 1993). Oxidized CL (oxCL) was found to accumulate both in rabbit and human atherosclerotic lesions (Tuominen et al., 2006), and in the aortic root of mice fed a high fat diet (Zhong et al., 2014). Increased anti-oxCL IgG (Lopez et al., 2003; Marai et al., 2008; Türkoğlu et al., 2008) and IgM (Su et al., 2013; Türkoğlu et al., 2008) antibodies are associated with atherosclerosis development. oxCL is recognized as a natural antigen that stimulates pro-inflammatory effects in the artery and promotes formation of atherosclerotic plaques (Bochkov et al., 2010; Marai et al., 2008). However, some studies purport that autoantibodies to oxCL may serve a protective role against the onset and development of atherosclerosis (Frostegård et al., 2014; Su et al., 2006). The seemingly contradictory findings regarding the role of anti-oxCL antibodies in atherosclerosis may reflect the influence of other factors, including age, gender and existing diseases. The anti-coagulation protein annexin A5 has been reported to bind to and inhibit the pro-inflammatory effects of oxCL (Wan et al., 2014), providing the basis of a promising therapeutic strategy for oxCL-positive atherosclerosis.

Tangier disease (TD) is another genetic disorder that may be linked to CL. TD is

a disorder of cholesterol efflux and lipid metabolism characterized by a nearly complete absence of plasma high-density lipoproteins (HDLs), atherosclerosis, peripheral neuropathy and an increased risk for developing CVD (Fredrickson, 1964; Oram, 2000). The genetic cause of TD is mutations of the ABCA1 gene, which is located on chromosome 9 (Rust et al., 1999). ABCA1 encodes a highly conserved ATP binding cassette transporter that belongs to a subfamily of ABC transporters. The ABCA subfamily is involved in lipoprotein metabolism and lipid transport across the plasma membrane (Knight, 2004). Researchers propose that a physical interaction between apoA-I and ABCA1 results in the formation of a phospholipid-apoA-I complex that promotes cholesterol efflux (Wang et al., 2001). Three phospholipids, including CL and lysoCL 1 and 2 (LC_1 and LC_2), which together contribute only a small fraction of the total cellular phospholipid content, were found to be enriched up to five-fold in TD fibroblasts compared to wild type (WT) cells (Fobker et al., 2001). This finding suggests that phospholipid and cholesterol efflux may be co-regulated and, therefore, dually impaired in TD cells. Additionally, it is possible that increased CL may play an as yet uncharacterized regulatory role in cholesterol trafficking and efflux.

In addition to the above disorders, the CL profile is altered in both myocardial ischemia-reperfusion injury and heart failure. Myocardial ischemia occurs when the myocardium does not receive sufficient blood flow, resulting in cell death and further irreversible injury (Carden and Granger, 2000). Restoration of circulation in ischemic myocardium exacerbates the injury (Carden and Granger, 2000). In the early stages of myocardial ischemia, there is an increase in reactive oxygen species (ROS).

During and post ischemia-reperfusion, ROS is thought to trigger lipid peroxidation as well as damage to cellular macromolecules and the electron transport chain, which together lead to apoptosis, necrosis and tissue damage (Ferrari et al., 1991; Kalogeris et al., 2014; Kloner et al., 1989). Unsaturated CL acyl species in the mitochondrial inner membrane that are close to the site of ROS generation are vulnerable to oxidative damage. Consistent with this, total CL was decreased and peroxidized CL was increased in the rat heart during ischemia-reperfusion (Paradies et al., 1999). A study of ischemia-reperfusion in rabbit heart reported that reduction of total CL was due in large part to a significant decrease in CL in the subsarcolemmal mitochondria, whereas CL in the interfibrillar mitochondria was unchanged (Lesnefsky et al., 2001). The levels of all other phospholipids remained unaffected in the same study. Decreased CL was shown to have an impact on electron transport chain complexes I (Paradies et al., 2004), III (Petrosillo et al., 2003), and IV (Paradies et al., 1999). The enzyme activies of these complexes in mitochondria from the ischemic rat heart was restored by the addition of exogenous CL, but not by other phospholipids or peroxidized CL (Paradies et al., 1999). In summary, a feedback loop appears to be formed, in which CL is damaged by ischemia-reperfusion-induced ROS, and damaged CL leads to impairment of electron transport chain complexes, resulting in the generation of more ROS. In addition, the fact that membranes containing peroxidized CL are more permeable to apoptosis factors (Korytowski et al., 2011) may suggest a route through which ROS triggers apoptosis and tissue damage.

Heart failure (HF) occurs when the heart is not able to contract efficiently enough

to pump blood to meet the body's needs. The major clinical symptoms of HF include edema, shortness of breath and lack of energy. HF is usually the end stage of CVD, including cardiomyopathy, heart attack, cardiac valvular disease, atrial fibrillation, and high blood pressure (McMurray and Pfeffer). In both the spontaneously hypertensive HF rat (SHHF) and human HF patients, decreased tafazzin mRNA levels were observed, concomitant with compensatory increases in the activity of phosphatidylglycerolphosphate synthase and MLCL acyltransferase (Saini-Chohan et al., 2009). However, studies of the CL profile in HF are controversial. While most studies report a significant reduction of total CL and L4-CL in human HF (Chatfield et al.; Le et al., 2014; Sparagna et al., 2007) and in the rat HF model (Reibel et al., 1986; Sparagna et al., 2007), one study reported an unchanged CL profile in a rat model with intracoronary microembolization-induced HF (Rosca et al., 2011). It is likely that different HF pathogenesis mechanisms lead to varying degrees of CL profile change and mitochondrial damage.

3 CL plays a role in cellular events and pathways that are important for maintaining cardiovascular health

3.1 Autophagy/mitophagy

Autophagy refers to the cellular process in which cytoplasmic contents are delivered to the lysosome or vacuole for degradation. Autophagy is further classified into selective and nonselective autophagy (Nair and Klionsky, 2005). Various types of selective autophagy have been identified, including mitophagy, pexophagy, lipophagy, nucleophagy, lysophagy, reticulophagy/ER-phagy and ribophagy (Okamoto, 2014).

Mitophagy is the selective degradation of mitochondria by autophagy (Wang and Klionsky, 2011). Mitophagy and autophagy are generally not distinguished in studies of CVD and will be discussed together here.

In the heart, autophagy is an important housekeeping process and is essential for maintaining cardiac health (Moyzis et al., 2015). Autophagic activity declines with age, and decreased or impaired autophagy leads to accumulation of proteins and damaged mitochondria, contributing to cardiac aging (Linton et al.). In addition, deletion of *ATG5*, the gene encoding a protein that regulates phagophore expansion, is known to result in cardiomyopathy in mice (Nakai et al., 2007).

As discussed above, decreased CL causes impairment of the electron transport chain complexes I (Paradies et al., 2004), III (Petrosillo et al., 2003) and IV (Paradies et al., 1999), resulting in mitochondrial dysfunction. In response to mitochondrial damage, mitophagy increases as an adaptive and protective strategy to eliminate damaged mitochondria (Frank et al., 2012; Narendra et al., 2008). Therefore, I undertook the study in this thesis to investigate if the loss of CL leads to altered mitophagy.

3.2 CL and MAPK pathways

3.2.1 PKC pathway

Protein kinase C (PKC) is a family of protein kinases that regulate the function of other proteins through specific phosphorylation of hydroxyl groups on threonine and serine residues. Human cells have fifteen PKC isozymes (Mellor and Parker,

1998). Over-stimulation of PKCα, PKCβ, PKCδ or PKCε results in hypertrophy of cardiomyocytes through activation of the extracellular signal-related kinase (ERK) pathway (Steven P. Marso and Stern, 2003). However, during ischemia preconditioning, PKCα, PKCδ, PKCε and PKCη have been shown to translocate to the active membrane pool and perform cardioprotective functions (Steven P. Marso and Stern, 2003). Activation of PKCδ results in intracellular pH changes and viability protection; activation of PKCη protects against myocardial stunning; activation of both PKCδ and PKCη provides global myocardial protection against necrosis, acidosis, and myocardial stunning (Meldrum et al.). Blocking the phosphatidylinositol-specific phospholipase C (PI-PLC)-induced translocation of PKCα, PKCε, and PKCη during ischemia impairs myocardial recovery (Munakata M et al., 2002). Therefore, PKC isozymes have dual functions in the pathogenesis and progression of CVD. However, unlike other PKC isozymes that affect different CVDs, PKCη is mainly reported to play a cardioprotective role during ischemia.

Yeast has only one PKC (Pkc1p). Human PKCη is the only human PKC isozyme that can complement the defects caused by deletion of *PKC1* in yeast through activation of the same protein kinase cascade (Nomoto S et al., 1997). This suggests that PKCη shares both functional and structural homology with Pkc1p. A previous study in yeast showed that loss of PG, the precursor of CL, leads to defects in the activation of the PKC pathway (Zhong et al., 2007). Extrapolating from the finding in yeast that the CL precursor is required for PKC pathway activation, the cardioprotective role of PKCη activation during ischemia preconditioning may be dependent on CL. In yeast,

PKC activation is also required for mitophagy (Mao et al., 2011), another cardioprotective process. Thus, to investigate how CL plays a role in maintaining cardiovascular health, it is necessary to determine if CL is required for PKC pathway activation.

3.2.2 HOG pathway

The high osmolarity glycerol (HOG) pathway is a highly conserved MAPK pathway that mediates the cellular response to hyperosmotic shock. In yeast, the HOG pathway consists of two stress-sensing branches, SLN1 and SHO1 branches (Saito and Tatebayashi, 2004). Both branches are cascades that lead to phosphorylation of Hog1p, the yeast homolog of the mammalian MAPK p38, which functions in the inflammatory and stress responses (Raingeaud et al., 1995). Phosphorylation activates Hog1p and promotes translocation into the nucleus. The phosphorylated protein (pHog1p) induces transcription of *GPD1*, and *GPP2*, which encode glycerol-3-phosphate dehydrogenase and glycerol-3-phosphate phosphatase, respectively (Rep et al., 2000). These enzymes are involved in the production of glycerol, the cytosolic accumulation of which counteracts osmotic stress. Activated Hog1p also regulates intracellular ion homeostasis by phosphorylating the C-termini of Nha1p, the Na+/H+ antiporter on the plasma membrane, and Tok1p, the potassium channel on the plasma membrane (Proft and Struhl, 2004). In addition to regulating glycerol biogenesis and ion homeostasis, pHog1p regulates the transcription of about 600 genes, resulting in cellular adaptation to various stresses (O'Rourke and Herskowitz, 2004).

A previous study showed that CL mutants exhibit vacuole defects that are characterized by enlarged vacuoles and loss of vacuole acidification (Chen et al., 2008b). The vacuole defects were rescued by deletion of *NHX1*, which encodes the Na+/H+ and K+/H+ exchanger, suggesting that ion homeostasis is perturbed in CL mutants. The vacuole defects were also rescued by supplementation with 1 M sorbitol, a HOG pathway stimulant, suggesting that osmoregulation may be perturbed in CL mutants. Because the HOG pathway functions in both osmoregulation and intracellular ion homeostasis, it is necessary to determine if the HOG pathway is perturbed in CL mutants.

4 *Saccharomyces cerevisiae* as my research model

As discussed above, CL biosynthesis is highly conserved from yeast to humans. The yeast *taz1Δ* mutant exhibits respiratory and metabolic deficiencies similar to those in human BTHS cells (Chen et al., 2008a; Gu et al., 2004; Ma et al., 2004). In addition, the availability of null mutants for each step of CL synthesis facilitates studies to elucidate CL function, which are not easily carried out in higher eukaryotes. For example, the finding that growth and respiratory defects of the yeast *taz1* mutant are rescued by deletion of *CLD1*, which restores CL/MLCL levels without generating remodeled CL, suggests that CL/MLCL levels are more important for mitochondrial function than CL acyl composition (Baile et al., 2014; Ye et al., 2014a). This study could not be carried out in mammalian cells, as CL phospholipases have not been characterized in mammals.

Most of the studies described in this thesis utilize the *crd1Δ* null mutant, in which the gene for CL synthase is deleted. The *crd1Δ* mutant has no CL and accumulates the CL precursor, PG. I also utilized the yeast genome deletion collection, which facilitated me to carry out genetic interaction studies. The genetic and molecular tools of the yeast model enabled me to carry out my analysis of the role of CL in mitophagy and the MAPK pathways.

5 Project outline

The goal of my doctoral research was to investigate the role of CL in cellular events and pathways that are required for maintaining cardiovascular health. I specifically focused on the role of CL in mitophagy, and the mechanism underlying this connection.

The study described in Chapter 2 shows that the loss of CL leads to defective mitophagy. Synthetic lethality with autophagy/mitophagy mutants suggested that mitophagy may be deficient in *crd1Δ*. Microscopic examination of mitophagy revealed decreased translocation of GFP-tagged mitochondrial protein into the vacuole of *crd1Δ* cells. This was confirmed by immunoblotting detection of free GFP, which was generated by cleavage of GFP-tagged mitochondrial protein after it was delivered into the vacuole by mitophagy. These findings indicated that mitophagy is decreased in CL deficient cells.

Chapter 3 describes a possible mechanism underlying defective mitophagy in *crd1Δ*. It is known that the PKC pathway is required for early stages of mitophagy and

the HOG pathway is required for later stages (Mao et al., 2011). My studies showed that *crd1Δ* growth defects are exacerbated by downregulation of the HOG pathway and rescued by upregulating the PKC pathway, suggesting that these MAPK pathways may be defective in CL mutants. Consistent with this, Western blot experiments showed decreased phosphorylation of Slt2p and Hog1p in *crd1Δ*, indicating defective activation of the PKC and HOG pathways. Interestingly, upregulation of PKC rescued defective mitophagy in *crd1Δ*. These results suggest that the mechanism underlying defective mitophagy in *crd1Δ* cells is defective MAPK function.

Although the findings of my dissertation research shed light on the role of CL in pathways known to be important for maintaining cardiovascular health, the story is far from over. Chapter 4 describes exciting experiments that can be done to elucidate the mechanism underlying the role of CL in mitophagy and the MAPK pathways. In addition, follow up experiments are proposed to continue preliminary studies of the role of CL in vacuole homeostasis.

CHAPTER 2

LOSS OF CARDIOLIPIN LEADS TO DEFECTIVE MITOPHAGY

Introduction

Cardiolipin (CL) is the signature lipid of mitochondrial membranes. It plays an important role in mitochondrial function through interacting with various mitochondrial membrane proteins, including electron transport chain (ETC) complex proteins that are components of complex I (Fry and Green, 1981; Mileykovskaya and Dowhan, 2014b), complex III (Fry and Green, 1981; Pfeiffer et al., 2003; Zhang et al., 2002; Zhang et al., 2005), complex IV (Pfeiffer et al., 2003; Zhang et al., 2002; Zhang et al., 2005), complex V (Gohil et al., 2004), cytochrome c (Ranieri et al., 2015) and transporter proteins such as the ADP-ATP carrier (Beyer K and M., 1985), pyruvate carrier (Paradies and Ruggiero, 1988) and phosphate carrier (Kadenbach et al., 1982). Loss of CL leads to impaired mitochondrial function, including defective respiration (Schlame and Ren, 2006), decreased mitochondrial membrane potential (Jiang et al., 2000) and impaired mitochondrial protein import (Gebert et al., 2009; Jiang et al., 2000). Additional cellular functions of CL outside of mitochondria are continuously being explored.

In studies described in this chapter, I investigated the role of CL in mitophagy. Mitophagy is the selective degradation of mitochondria through autophagy (Wang and Klionsky, 2011). Autophagy is the cellular process in which cytoplasmic contents are delivered into the lysosome or vacuole for degradation. According to the different ways by which cargos are delivered to the lysosome/vacuole for degradation, autophagy is

classified as macroautophagy, microautophagy, and chaperone-mediated autophagy (Shintani and Klionsky, 2004). Autophagy is further classified as selective or nonselective, depending on whether specific cargo is selected (Nair and Klionsky, 2005). Various types of selective autophagy have been identified (Okamoto, 2014), among which mitophagy is the selective degradation of mitochondria (Wang and Klionsky, 2011). In the heart, autophagy is essential for maintaining cardiac health (Moyzis et al., 2015). Impairment of the process by deletion of *ATG5* has been demonstrated to cause cardiomyopathy in mice (Nakai et al., 2007), linking abnormal autophagy to cardiomyopathy.

Cardiomyocytes have a remarkably high mitochondrial density that comprises about 30% of the total intracellular volume (Maack and O'Rourke, 2007). This allows cardiomyocytes to produce ATP quickly to satisfy the high demand for energy. Even subtle alterations in mitochondrial function or membrane potential can cause a significant change in cardiomyocyte energy production and further harm cardiovascular health. In response to mitochondrial damage, mitophagy increases as an adaptive and protective strategy (Frank et al., 2012; Narendra et al., 2008). Therefore, I carried out studies to determine if loss of CL, which perturbs numerous mitochondrial functions, leads to altered mitophagy.

Genetic interaction analysis is a very powerful approach to study gene function. Rescue of a mutant phenotype by deletion of another gene identifies suppression of the mutant phenotype. Exacerbation of a mutant phenotype to lethality by deletion of another gene is defined as synthetic lethality, which suggests that the two genes may

work in redundant pathways. I predicted that genetic interaction analysis between autophagy/mitophagy genes and *CRD1* would shed light on the role of CL in mitophagy.

Although mitophagy occurs via both macro- and micro-autophagy (Kanki et al., 2009c; Kiššová et al., 2007; Nowikovsky et al., 2007; Okamoto et al., 2009), degradation of mitochondria via macro-autophagy is the dominant process when mitophagy is triggered by nitrogen starvation or glucose deprivation (Kiššová et al., 2007). During macro-mitophagy, mitochondria are recognized as the cargo that is brought to the phagophore assembly site (PAS), where the double-membrane of the phagophore expands and closes to form a mature mitophagosome that contains mitochondria. Macro-mitophagy adapts the general autophagy core machinery, which involves various autophagy-related (ATG) proteins, including the Atg1p/Atg13p complex, Atg9p, Atg18p-Atg2p complex, Atg8p conjugation system (Atg3p, Atg4p, Atg7p, and Atg8p), and the Atg12 ubiquitin-like conjugation system (Atg5p, Atg7p, Atg10p, Atg12p, and Atg16p) (Köfinger et al., 2015; Reggiori et al., 2005; Reggiori et al., 2004; Sakoh-Nakatogawa et al., 2015; Suzuki et al., 2001; Suzuki et al., 2007; Xie and Klionsky, 2007). Atg8p is the yeast homolog of mammalian LC3, and it is conjugated to phosphatidylethanolamine (PE) (Kirisako et al., 1999). Atg8p-PE coats the mitophagosome membrane during membrane elongation. Phosphatidylinositol 3-phosphate (PI3P) is another important lipid that constitutes the mitophagosome membrane (Gillooly et al., 2000). Atg18p binds to PI3P and regulates the retrieval of Atg9p from PAS, and normal transport of Atg9p between PAS and the peripheral site is essential in PI3P synthesis on the mitophagosome membrane (Reggiori et al.,

2005). Thus, Atg8p and Atg18p are essential proteins in the general autophagy core machinery.

The mitochondrial outer membrane protein Atg32p plays a key role in selecting mitochondria as the specific cargo. When mitophagy is triggered, Atg32p is phosphorylated (Aoki et al., 2011). Then it interacts with Atg11p, which directs mitochondria to the PAS, where an Atg32–Atg11–Atg8 initiator complex is formed (Aoki et al., 2011; Farré et al., 2013). When an intact mitophagosome is formed and delivered to the vacuole, the mitophagosome outer membrane fuses with the vacuole membrane and releases the mitochondria wrapped by the mitophagosome inner membrane into the vacuole lumen for degradation.

In this chapter, I investigated if loss of CL in the *crd1Δ* mutant leads to altered mitophagy. Deletion of autophagy/mitophagy genes exacerbated the *crd1Δ* growth defect. Mito-GFP marker tracking experiments and Western detection of free GFP, the mitophagy product, both showed inhibited mitophagy in *crd1Δ* compared to WT. These findings suggest that CL plays a novel role in mitophagy.

Methods and materials

Yeast strains and growth media

The *Saccharomyces cerevisiae* strains used in this work are listed in Table 2.1. Yeast extract peptone dextrose (YPD) medium contained yeast extract (1%), peptone (2%), and glucose (2%). Synthetic complete (SC) medium contained lab-made vitamin-free yeast nitrogen base without amino acids (Difco protocol, 0.17%), ammonium sulfate (0.5%), glucose (2%), vitamins, and the following amino acids: adenine (20.25 mg/liter), arginine (20 mg/liter), histidine (20 mg/liter), leucine (60 mg/liter), lysine (200 mg/liter), methionine (20 mg/liter), threonine (300 mg/liter), tryptophan(20 mg/liter), and uracil (20 mg/liter). Synthetic drop-out medium contained all ingredients mentioned above except the amino acid used as the selective marker. Synthetic lactate (SL) medium contained lab-made vitamin free yeast nitrogen base without amino acids (Difco protocol, 0.17%), ammonium sulfate (0.5%), and lactate (2%). Solid medium contained agar (2%).

Construction of deletion mutants and strains that express GFP-tagged mitochondrial proteins

Deletion mutants were constructed as follows. The entire open reading frame of the target gene was replaced by a *KanMX4* cassette via homologous recombination in the wild type (WT) strain. The *KanMX4* cassette was amplified by polymerase chain reaction (PCR), using the pUG6 plasmid, which contains the *KanMX4* cassette, as the

template. The amplification primers consisted of 50 nucleotides that were identical to either the upstream or the downstream flanking region of the target gene at the 5' end and 21 nucleotides that annealed to the *KanMX4* gene at the 3' end. For construction of the single mutants with the target mitophagy gene deleted, the PCR product was transformed into the WT strain by electroporation. For construction of the double mutants with both *CRD1* and the target mitophagy gene deleted, the PCR product was transformed into the *crd1Δ* strain by electroporation. Transformants were selected on YPD plates with 200 μg/ml G418. Deletion of the target gene was confirmed by PCR using primers that amplify the original target gene.

To monitor mitophagy in both WT and *crd1Δ* strains, the mitochondrial matrix protein Idh1p in both strains was tagged by GFP as previously described (Kanki et al., 2009a). The pFA6a-GFP (S65T)-HIS3MX6 plasmid (kindly provided by Dr. Daniel Klionsky, University of Michigan) was used as the PCR template to amplify a DNA fragment that encodes GFP with *HIS3* as the selective marker. The primers consisted of 50 nucleotides that were identical to either the upstream or the downstream flanking region of the *IDH1* ending code (TAA) at the 5' end and 20 nucleotides that annealed to the GFP sequence on the plasmid at the 3' end. The sequences of these primers are 5'-CTTCTACTACTGACTTCACGAATGAAATCATCAACAAATTATCTAC CATGCGGATCCCCGGGTTAATTAA-3' and 5'-AATTTGAACACACTTAAGTTGCAG AACAAAAAAAAGGGGAATTGTTTTCAGAATTCGAGCTCGTTTAAAC-3'. The PCR product was then transformed into both WT and *crd1Δ* cells in the BY4742 and FGY genetic backgrounds by electroporation, and inserted into the end of the *IDH1* locus

via homologous recombination. The transformants that express *IDH1-GFP* were selected on SC his$^-$ medium. Correct GFP insertion was confirmed by PCR analysis, using confirmation primers 5'-ATGCTGTCTTCGAACCAGGTT-3' and 5'-AGTTCATCCATGCCATGTGT-3'.

Another approach to construct strains containing GFP-tagged mitochondria was to transform the pCu416-*IDP1-GFP* plasmid that expresses *IDP1-GFP* (kindly provided by Dr. Hagai Abeliovich, Hebrew University) into WT and *crd1Δ*, by electroporation. Transformants carrying the plasmid encoding *IDP1-GFP* were selected on SC ura$^-$ medium.

Single colony formation analysis

Cells were pre-cultured in YPD at 30˚C to the mid-log phase. The absorbance at 550 nm (A_{550}) of the liquid culture was determined using a spectrophotometer (Beckman). Cell aliquots were centrifuged and pellets were resuspended in YPD to adjust the A_{550} value to 10 units per ml. 10 µl of the above sample were added to 990 µl of water. 10 µl of the 100X diluted sample were placed on a hemocytometer for cell counting using light microscopy at a magnification of 1000 X. Based on cell number, cell aliquots with A_{550} of 10 were adjusted again and serial diluted to 2000 cells/ml, from which 100 µl suspension that contained about 200 cells were plated on a YPD plate and incubated at 30˚C, 36˚C or 37˚C for 3 days. The ability of single cells to form colonies was evaluated at 30˚C, 36˚C or 37˚C.

Table 2.1 Yeast strains and plasmids used in Chapter 2

Strain/plasmid	Characteristics or genotype	Source or reference
FGY3 (WT)	MAT α, *ura3-52, lys2-801, ade2-101, trp1Δ1, his3Δ200, leu2Δ1*	Jiang et al., 1997
FGY2 (*crd1Δ*)	MAT α, *ura3-52, lys2-801, ade2-101, trp1Δ1, his3Δ200, leu2Δ1, crd1Δ*::*URA3*	Jiang et al., 1997
FGY3 *atg8Δ*	Derivative of FGY3, *atg8Δ*::*KanMX4*	This study
FGY2 *atg8Δ*	Derivative of FGY2, *atg8Δ*::*KanMX4*	This study
FGY3 *atg18Δ*	Derivative of FGY3, *atg18Δ*::*KanMX4*	This study
FGY2 *atg18Δ*	Derivative of FGY2, *atg18Δ*::*KanMX4*	This study
FGY3 *atg32Δ*	Derivative of FGY3, *atg32Δ*::*KanMX4*	This study
FGY2 *atg32Δ*	Derivative of FGY2, *atg32Δ*::*KanMX4*	This study
FGY3 *atg21Δ*	Derivative of FGY3, *atg21Δ*::*TRP1*	This study
FGY3 *atg18Δatg21Δ*	Derivative of FGY3, *atg18Δ*::*KanMX4*, *atg21Δ*::*TRP1*	This study
FGY2 *atg18Δatg21Δ*	Derivative of FGY2, *atg18Δ*::*KanMX4*, *atg21Δ*::*TRP1*	This study
FGY3-*IDH1-GFP*	Derivative of FGY3, in which *GFP* is inserted into the *IDH1* gene locus	This study
FGY2-*IDH1-GFP*	Derivative of FGY2, in which *GFP* is inserted into the *IDH1* gene locus	This study
BY4742	MATα, *his3Δ1, leu2Δ0, lys2Δ0, ura3Δ0*	Euroscarf [a]
VGY1 (BY4742 *crd1Δ*)	MATα, *his3Δ1, leu2Δ0, lys2Δ0, ura3Δ0, crd1Δ*::*URA3*	Gohil et al., 2005
BY4742-*IDH1-GFP*	Derivative of BY4742, in which *GFP* is Inserted into the *IDH1* gene locus	This study
BY4742 *crd1Δ-IDH1-GFP*	Derivative of BY4742 *crd1Δ*::*KanMX4*, in which *GFP* is Inserted into the *IDH1* gene locus	This study
pFA6a-GFP(S65T)-His3MX6	Derivative of pFA6a- His3MX6	Kanki et al., 2009a
pCu416-*IDP1-GFP*	Derivative of pCu416, expresses GFP-tagged *IDP1* from *CUP1* promoter	Journo et al., 2009

[a] Euroscarf, European *Saccharomyces cerevisiae* Archive for Functional analysis.

Table 2.2 Real-time PCR primers used in Chapter 2

Gene	Primers	Sequence
ACT1	Forward	TCGTGCTGTCTTCCCATCTATCG
	Reverse	CGAATTGAGAGTTGCCCCAGAAG
ATG8	Forward	ACCTTACCGTAGGGCAATTTG
	Reverse	CCCGTCCTTATCCTTGTGTTC

FM 4-64 and quinacrine staining

FM 4-64 staining was performed as previously described (Conboy and Cyert, 2000) with minor revisions. Cell aliquots equivalent to an A_{550} of 1.0 were harvested by centrifugation, resuspended in 100 µl YPD, and incubated at 37˚C or 39˚C with 0.16 mM FM4-64 for 15 min. Cells were pelleted and washed once with 37˚C YPD or 39˚C YPD and then resuspended in 500 µl YPD of the same temperature for 30 min. The cell suspension was centrifuged and the supernatants were discarded. The cell pellets were resuspended in 100 µl YPD, from which 3 µl were applied to the microscope slide and observed using epifluorescence microscopy using the filter for red fluorescence.

Quinacrine staining was performed as previously described (Roberts et al., 1991), with minor revisions. Cell aliquots equivalent to an A_{550} of 1.0 were harvested by centrifugation and resuspended in 500 µl YPD (containing 2 mM quinacrine and buffered to pH 7.6 with 0.5M Na2HPO4) prewarmed to 37˚C or 39˚C. After a 5 min incubation, cells were pelleted and washed once with 500 µl 2% glucose that had been buffered to pH 7.6 with 0.5M Na_2HPO4. The cell suspension was pelleted again and resuspended in 100 µl 2% glucose at pH 7.6, from which 3 µl were applied to a microscope slide and observed using epifluorescence microscopy using the filter for green fluorescence.

Detection of mitophagy using fluorescence microscopy

Microscopic analyses were performed using an Olympus BX41 epifluorescence

microscope. Images were captured by an Olympus Q-Color3 digital charge-coupled device camera operated by QCapture2 software. All pictures were taken at a magnification of 1000X. To induce mitophagy, cells expressing *IDH1- GFP* were cultured in SC medium to the mid-log phase, pelleted and resuspended in 5 ml SL medium with a starting A_{550} of 0.5. They were then cultured for 18 hours and observed using epifluorescence microscopy. An increase in the signal of mito-GFP in the vacuole indicated induction of mitophagy. In addition, cells were also treated with elevated temperature. Both WT-*IDH1-GFP* and *crd1Δ-IDH1-GFP* were cultured in YPD medium to the mid-log phase at 30˚C and then switched to 39˚C for 8 hours. Cells were then observed using epifluorescence microscopy, using the filter for green fluorescence.

Western blot

Whole cell extracts were prepared as previously described (Kanki et al., 2009a) with minor changes. Cell pellets equivalent to 1.5 A_{550} units were collected and resuspended in 1 ml 10% trichloroacetic acid (TCA). Samples were incubated for 10 min on ice and proteins were pelleted by centrifugation at 4˚C, 15,000 rpm for 10 min. The pellets were washed twice with 1 ml of ice-cold acetone and air-dried at room temperature. The air-dried cell pellets were resuspended in 75 µl sample buffer, which consisted of 150 mM Tris-HCl with pH 8.8, 6% SDS, 25% glycerol, 6 mM EDTA, and disrupted by vortexing for 3 min in the presence of 75 µl acid-washed glass beads. Following this step, the samples were heated at 100°C for 3 min and then centrifuged at 4˚C, 7,000 rpm for 30 s to pellet the glass beads. 18 µl of the supernatants that

contained the proteins were mixed with 6 μl 4X loading dye (80% bromophenol blue and 20% β-mercaptoethanol) and loaded into a 12% SDS-polyacrylamide gel for electrophoresis. The proteins were then transferred to a PVDF membrane with 0.2 μm pores following the standard semidry Western blot transfer procedure. After blotting in TBST-milk (TBS containing 1% TWEEN 20 and 0.5% milk), the membranes were incubated in TBST-milk with mouse anti-YFP monoclonal antibody (JL-8, Clontech) at a 1:3000 dilution at 4°C overnight. After washing with TBST (TBS containing 1% TWEEN 20) for 4 times, 8 min per time, the membranes were incubated in 0.5% TBST-milk with the secondary antibody, HRP-conjugated goat anti-mouse IgG (Santa Cruz), at a 1:5000 dilution for 1 h at room temperature. After washing with TBST 4 more times, 8 min per time, the membrane was covered with Pierce™ ECL Plus Western Blotting Substrate reagent. To detect the signal of GFP, the HyBlot ES® Autoradiography film was exposed to the PVDF membrane and then developed. Idh1-GFP and cleaved GFP were detected as bands of 68 kDa and 28 kDa, respectively.

Real-Time PCR (RT-PCR)

Both WT-*IDH1-GFP* and *crd1Δ-IDH1-GFP* strains in the FGY background were cultured in 10 ml YPD medium to the mid-log phase at 30˚C and then switched to 39˚C for 8 hours. Cells were harvested and total RNA was extracted using the RNeasy Mini kit (QIAGEN). This procedure removed possible contaminating genomic DNA. cDNAs were synthesized using the Transcriptor First Strand cDNA synthesis kit (Roche Diagnostics) following the manufacturer's protocol. RT-PCR was performed

in a 96-well plate using Brilliant III Ultra-Fast SYBR Green QPCR Master Mix (Agilent Technologies). Duplicates for each sample were included. The primers used for RT-PCR are listed in Table 2.2. *ACT1* was used as the internal control. The mRNA level of the target gene was normalized to *ACT1* mRNA levels. PCR reactions were performed at 95°C for 10 min for denaturation and then 40 cycles that consisted of 30 s at 95°C and 60 s at 56°C.

Results

Deletion of autophagy/mitophagy genes exacerbates the temperature sensitivity of *crd1Δ*

Previous studies have shown that loss of CL leads to impaired mitochondrial function, including defective respiration (Schlame and Ren, 2006), decreased mitochondrial membrane potential (Jiang et al., 2000) and impaired mitochondrial protein import (Gebert et al., 2009; Jiang et al., 2000). It is known that mitophagy increases as an adaptive and protective strategy in response to damage of mitochondria to eliminate damaged organelles (Frank et al., 2012; Narendra et al., 2008). A previous study in our lab found that, at elevated temperature, CL mutants exhibit not only growth defects but also vacuole defects characterized by enlarged vacuoles and loss of vacuole acidification (Chen et al., 2008b). The mechanism underlying the vacuole defects in the CL mutants are unknown. Because increased autophagy leads to a large influx of membrane and contents to the vacuole, resulting in increased vacuole size (Baba M et al., 1994; Baba et al., 1995; Takeshige K et al., 1992), I originally hypothesized that loss of CL might lead to increased mitophagy to eliminate the damaged mitochondria at elevated temperature. In addition, my preliminary study found that deletion of *UTH1*, a gene that is involved in cell wall biogenesis and may play a role in mitophagy, rescued both the vacuole defects and the temperature sensitivity of *crd1Δ* (Fig. 2.1), seeming to support my hypothesis that the vacuole defects in the CL mutants may be due to increased mitophagy.

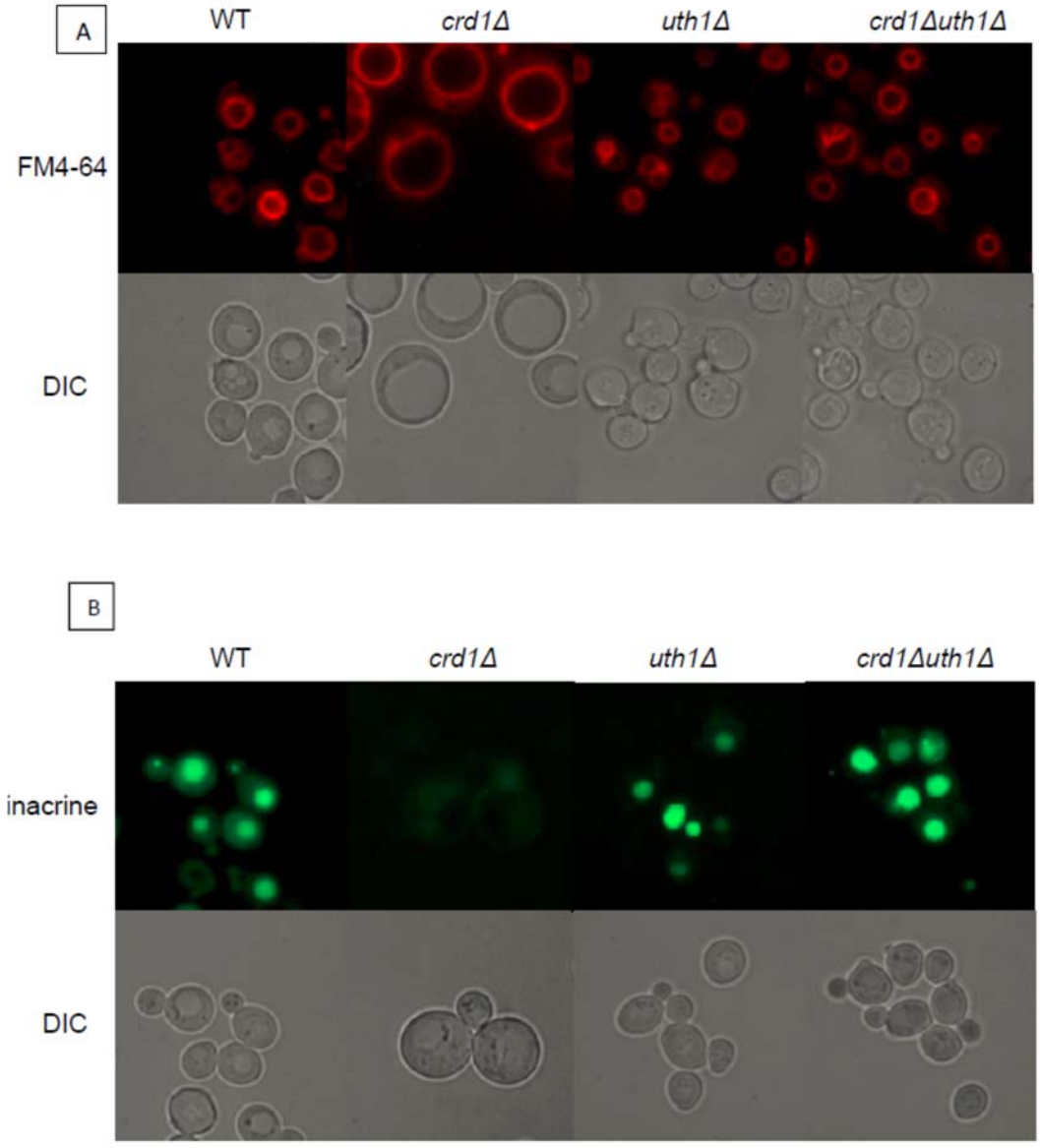

Fig. 2.1 (A) Deletion of *UTH1* rescues the vacuole morphology defect of *crd1Δ* at 37°C Cells were pre-cultured at 30 ℃ to the early log phase and then transferred to 37℃ for 8 hours. FM 4-64 staining was performed and cells were observed using fluorescence microscopy. **(B) Deletion of *UTH1* rescues vacuole acidification defect of *crd1* at 37°C** Cells were pre-cultured at 30 ℃ to the early log phase and then transferred to 37℃ for 8 hours. Quinacrine staining was performed and cells were observed using fluorescence microscopy.

To test this hypothesis, I decided to determine if there was genetic interaction between *CRD1* and autophagy/mitophagy genes. The rationale for this is that, deletion of autophagy/mitophagy genes should block excessive mitophagy and rescue the phenotype of *crd1Δ*. I constructed single mutants of mitophagy genes in the FGY background, including *atg8Δ*, *atg18Δ*, *atg21Δ*, *atg32Δ*, double mutants of *crd1Δ* and *atg8Δ*, *atg18Δ*, *atg21Δ*, *atg32Δ*, and the triple mutant *crd1Δatg18Δatg21Δ*. Temperature sensitivity of these strains was examined. Surprisingly, deletion of autophagy/mitophagy genes did not rescue (Fig. 2.2) but rather exacerbated the temperature sensitivity of *crd1Δ* (Fig. 2.3). Compared to deletion of the mitophagy-specific gene *ATG32*, deletion of general autophagy genes, including *ATG8* and *ATG18*, caused more severe exacerbation of *crd1Δ* temperature sensitivity. These findings suggested that mitophagy may be decreased in *crd1Δ*.

Delivery of mitochondria to the vacuole in response to increased temperature is inhibited in *crd1Δ*

WT-*IDH1-GFP* and *crd1Δ-IDH1-GFP* strains in the FGY background were constructed as described in the 'Methods and materials' section (Fig. 2.4). These strains express an endogenous Idh1 protein that is tagged with GFP at the C terminus and is localized in mitochondria. After culture in YPD medium to the mid-log phase at 30˚C, WT-*IDH1-GFP* and *crd1Δ-IDH1-GFP* were switched to 39˚C for 8 hours. Cells were then observed using epifluorescence microscopy. Accumulation of GFP was observed in the vacuole of WT cells, suggesting that elevated temperature

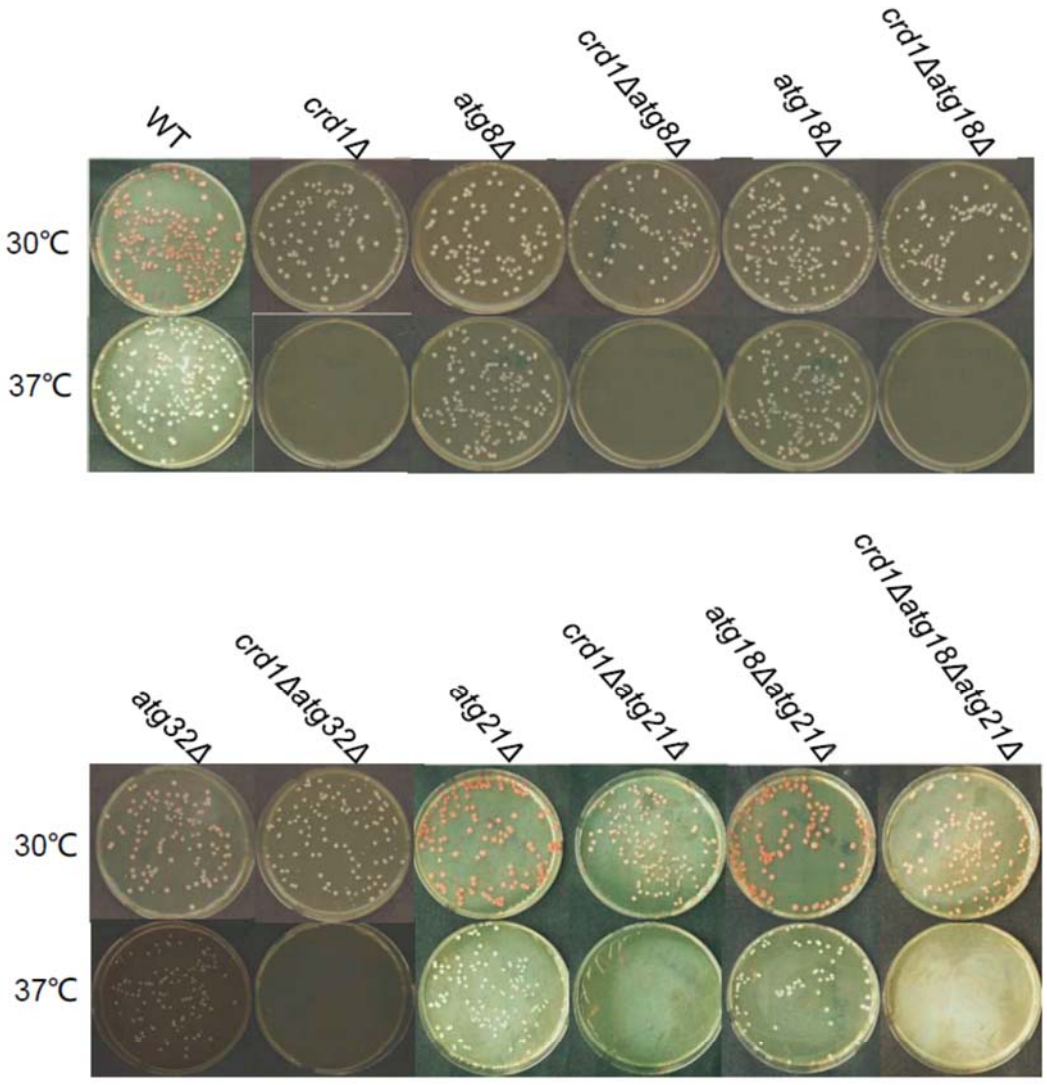

Fig. 2.2 Deletion of autophagy/mitophagy genes does not rescue *crd1Δ* growth defect at 37℃. Cells were pre-cultured in YPD liquid at 30°C to the mid-log phase. About 200 cells of each strain were plated on YPD and incubated at the indicated temperature for 3 days.

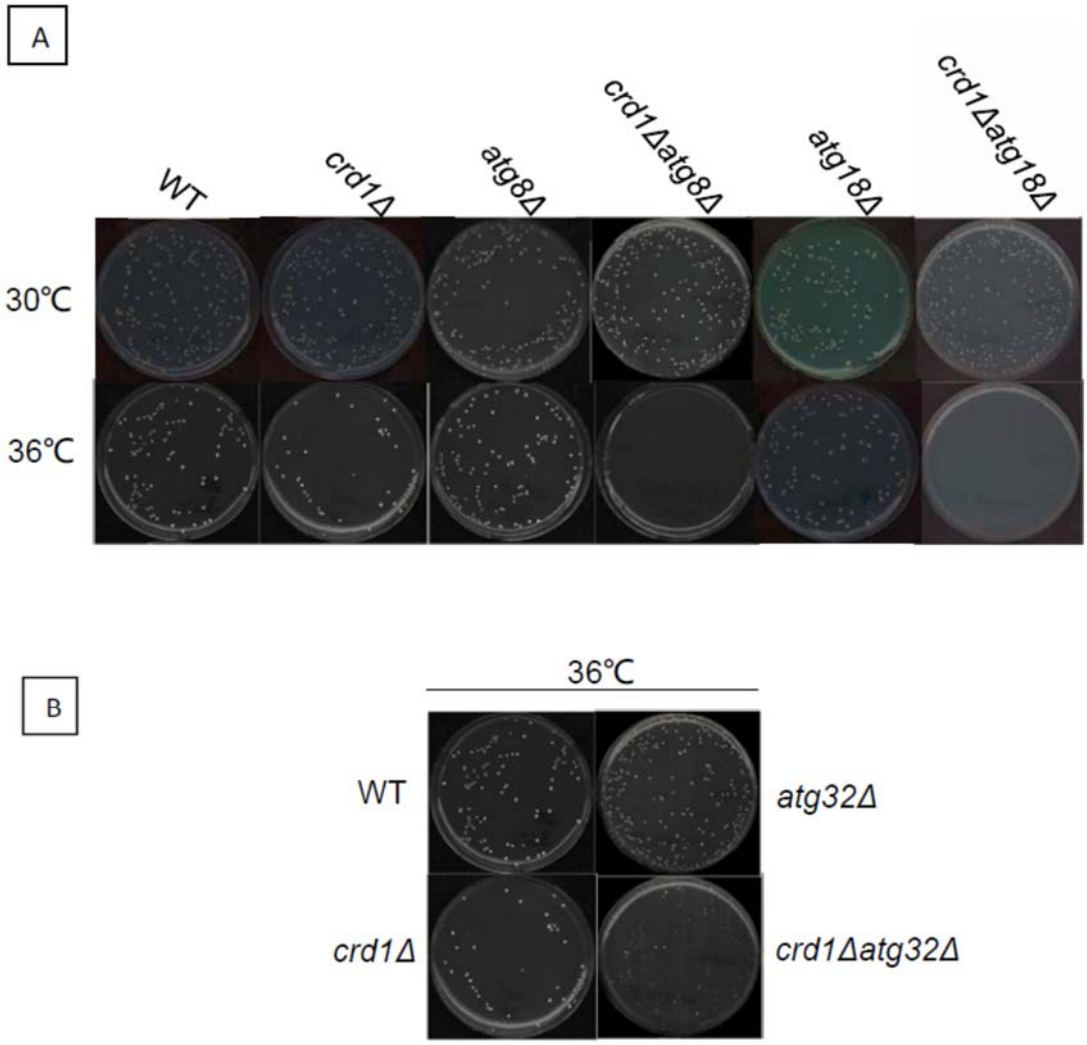

Fig. 2.3 (A) *crd1Δ* is synthetically lethal with *atg8Δ* and *atg18Δ* at 36℃. (B) *crd1Δ* is synthetically sick with *atg32Δ* at 36℃. Cells were pre-cultured in YPD liquid at 30˚C to the mid-log phase. About 200 cells of each strain were plated on SC complete plates and incubated at the indicated temperature for 3 days.

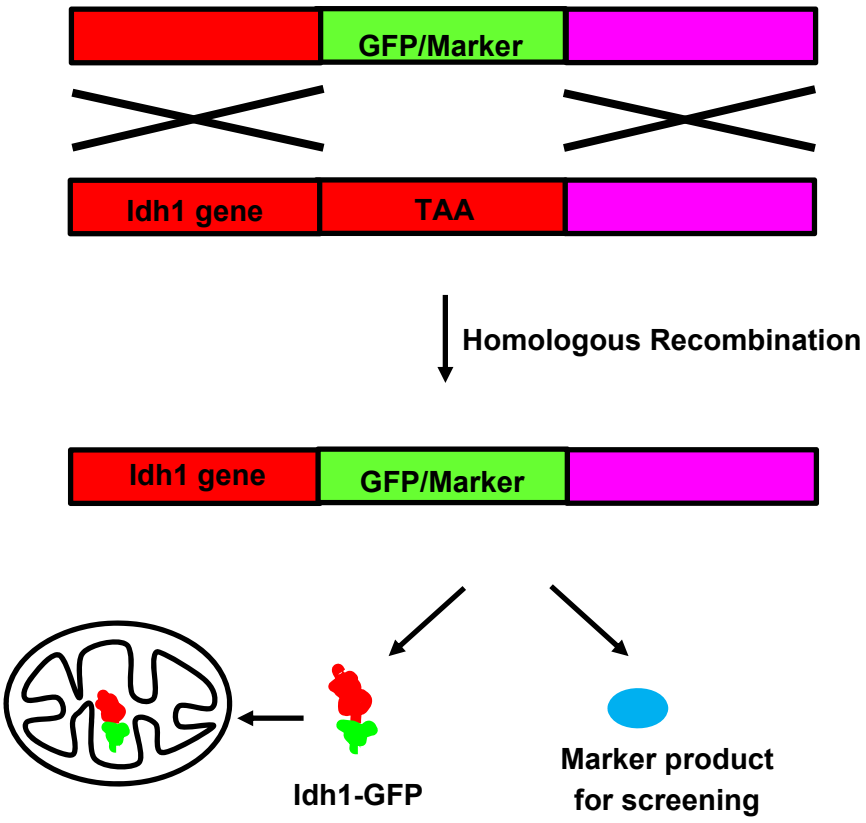

Fig. 2.4 Insertion of GFP into the *IDH1* gene locus. Strains expressing an endogenous Idh1 protein tagged with GFP at the C terminus were constructed as described in the 'Methods and materials' section.

induced delivery of Idh1-GFP tagged mitochondria into the vacuole of WT cells for degradation. However, translocation of *crd1Δ* mitochondria into the vacuole was not observed, suggesting that mitophagy was inhibited in *crd1Δ* cells (Fig. 2.5).

A recent study reported that *transcription of ATG8* positively regulates the size of the *autophagosome* (Backues et al., 2012) and reflects the extent of autophagy induction (Gasch et al., 2000; Kirisako et al., 1999). When autophagy is triggered, expression of *ATG8* is induced more than 10-fold (Gasch et al., 2000; Kirisako et al., 1999). Expression of *ATG8* was determined in both WT and *crd1Δ* cells at 30˚C and after switching to 39˚C for 8 hours. *ATG8* mRNA levels in WT and *crd1Δ* were comparable at 30˚C. Interestingly, *ATG8* expression increased 3-fold in WT cells at 39˚C compared to that at 30˚C, while it increased 6.7-fold in *crd1Δ* cells at 39˚C compared to that at 30˚C (Fig. 2.6). Expression of *ATG8*, the essential gene for mitophagy and non-selective autophagy, was upregulated in both WT and *crd1Δ* at elevated temperature. However, the increase was greater in *crd1Δ* than in WT cells, suggesting that, in *crd1Δ*, there is a greater need to initiate mitophagy, or that non-selective autophagy may be upregulated to compensate for the decrease of mitophagy.

Induction of mitophagy is inhibited in *crd1Δ* cells

Based on the finding that the delivery of mitochondria into the vacuole is inhibited in *crd1Δ* compared to WT in response to elevated temperature, I predicted that mitophagy is decreased in *crd1Δ* compared to WT. Because elevated temperature has not been previously shown to trigger mitophagy, and mitophagy has not been studied

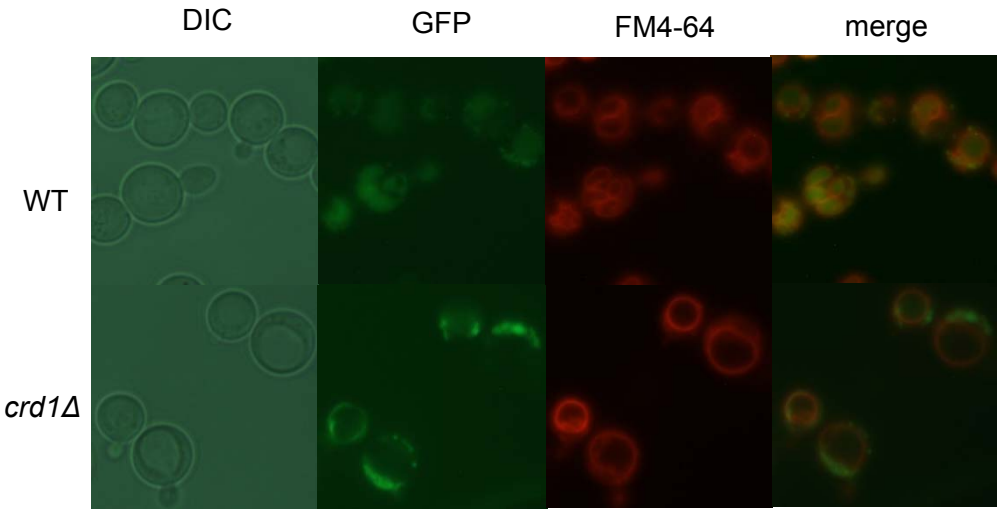

Fig. 2.5 Delivery of mitochondria to the vacuole in response to increased temperature is inhibited in *crd1Δ.* WT and *crd1Δ* cells expressing an endogenous Idh1 protein that is tagged with GFP at the C terminus were cultured in YPD medium to the mid-log phase at 30˚C, shifted to 39˚C for 8 hours and observed using fluorescence microscopy.

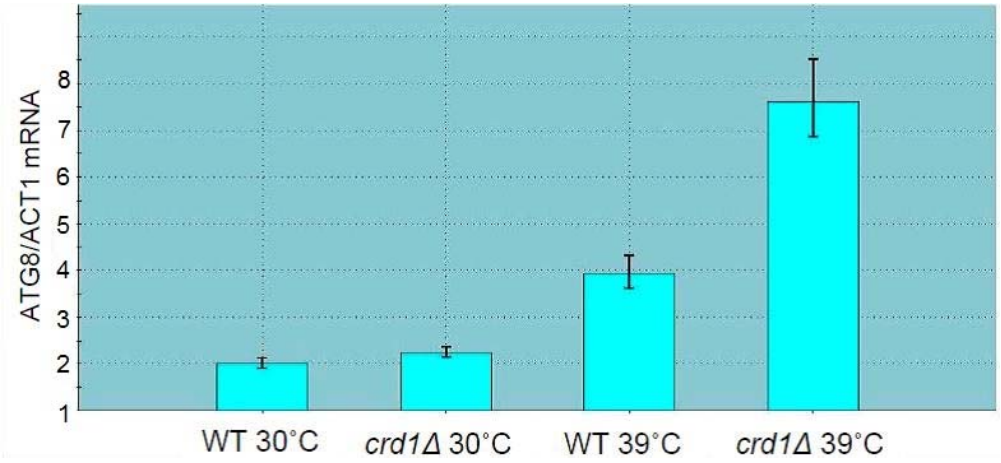

Fig. 2.6 Increased temperature triggers increased upregulation of *ATG8* expression in *crd1Δ* cells. WT and *crd1Δ* cells were cultured in YPD medium to the mid-log phase at 30˚C and divided into two groups: one group was kept growing in 30˚C for 8 hours while the other group was shifted to 39˚C for 8 hours. *ATG8* expression was determined by RT-PCR.

in the FGY genetic background, I constructed WT-*IDH1-GFP* and *crd1Δ-IDH1-GFP* strains in the BY4742 background, which is widely used in mitophagy studies (Kanki et al., 2009b). WT-*IDH1-GFP* and *crd1Δ-IDH1-GFP* cells were cultured in SC medium to the mid-log phase at 30˚C, harvested, washed twice and resuspended in SL medium, which has been shown to induce mitophagy (Wu and Tu, 2011). After 18 hours, cells were observed using epifluorescence microscopy. Similar to the result seen in the FGY genetic background, accumulation of GFP was observed in the vacuole of WT but not *crd1Δ* cells, suggesting that mitophagy is inhibited in *crd1Δ* (Fig 2.7 A). To exclude the possibility that the observed differences were specific to the Idh1-GFP protein, I constructed WT and *crd1Δ* strains that have the GFP-tagged mitochondrial protein Idp1p exogenously expressed from the pCu416-*IDP1-GFP* plasmid. As seen in *IDH1-GFP* strains (Fig 2.7 B), accumulation of Idp1-GFP was observed in the vacuole of the WT but not *crd1Δ* cells, suggesting that mitophagy was inhibited in *crd1Δ* cells.

To confirm the microscopic finding, the release of free GFP from Idh1-GFP was determined in WT-*IDH1-GFP* and *crd1Δ-IDH1-GFP* strains by Western blot. Cells were cultured in SC medium to the mid-log phase at 30˚C, harvested, washed twice and resuspended in SL medium. After 5, 6 or 7 hours, proteins were extracted as described in the ‘Methods and materials’ section. As seen in Fig. 2.8, 6 hours after transferring to SL medium, a GFP band was detectable in WT cells. In contrast, the signal from *crd1Δ* cells was barely detectable. Taken together, these findings indicate that mitophagy is inhibited in *crd1Δ*.

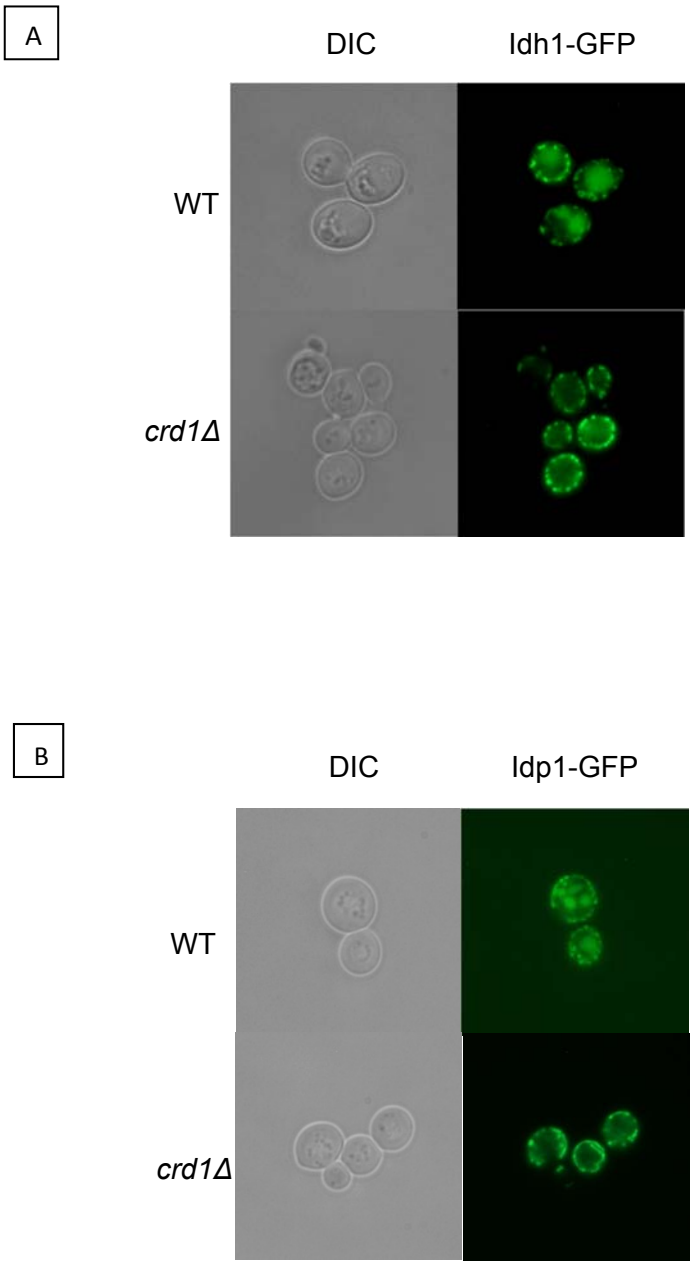

Fig. 2.7 Decreased mitophagy in *crd1Δ* cells. WT and *crd1Δ* cells expressing an endogenous Idh1-GFP (A) or exogenous Idp1-GFP (B) were cultured in SC medium to the mid-log phase at 30˚C and shifted to SL for 18 hours. Cells were observed using fluorescence microscopy.

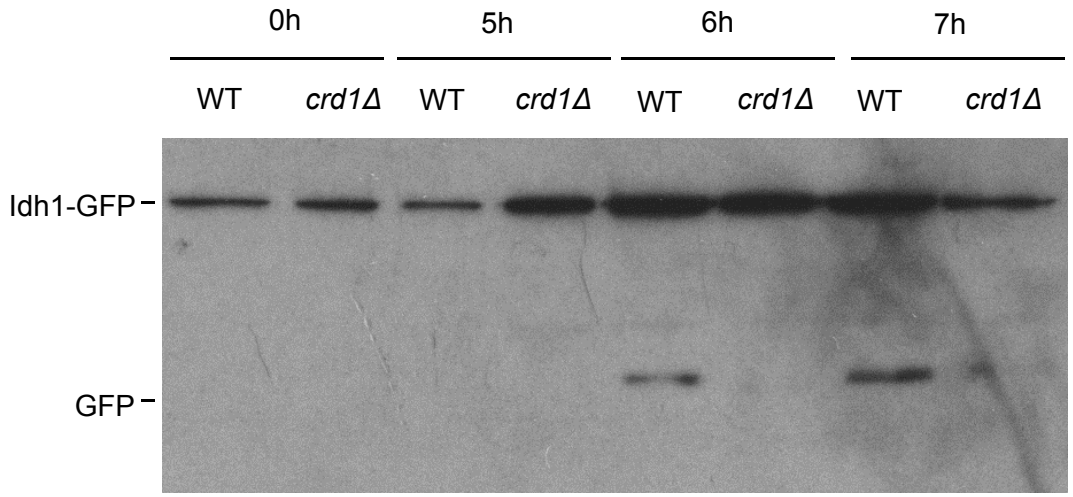

Fig. 2.8 Decreased mitophagy in *crd1Δ* cells expressing Idh1-GFP. WT and *crd1Δ* cells carrying the GFP-tagged *IDH1* gene were pre-cultured in SC medium to the mid-log phase at 30˚C and shifted to SL medium for 5, 6 or 7 hours. Aliquots were taken at the indicated times. Immunoblotting was done with anti-YFP antibody and the positions of full-length Idh1-GFP and free GFP are indicated.

Discussion

In this chapter, I addressed the question of how loss of CL in the *crd1Δ* mutant affects mitophagy. My findings indicate that CL deficiency leads to decreased mitophagy. This conclusion is based on the findings that 1) deletion of autophagy/mitophagy genes exacerbated *crd1Δ* growth defects, 2) GFP-tagged mitochondria were not detected in the vacuole of *crd1Δ* in response to mitophagy induction, and 3) in *crd1Δ*, there was decreased level of free GFP, which is cleaved from Idh1-GFP after the mitochondria are delivered to the vacuole for degradation in response to mitophagy induction.

The finding of decreased mitophagy seemed to contradict my preliminary finding that deletion of *UTH1* rescued both vacuole defects and temperature sensitivity in *crd1Δ*. *UTH1* was first linked to mitophagy by the finding that the *uth1Δ* mutant was resistant to rapamycin, the inducer of autophagy (Camougrand et al., 2003). This was further supported by the report of Kissova et al. (Kissová et al., 2004), which showed loss of colocalization of mitochondria and vacuole in *uth1Δ* after rapamycin treatment. However, Western analysis of degradation of mitochondria as determined by free GFP was not carried out in this study. More recently, Uth1p was found on the mitochondrial inner membrane, not in the outer membrane as previously predicted, and is dispensable for post-log-phase and rapamycin-induced mitophagy (Welter et al., 2013). Based on this recent finding, rescue of *crd1Δ* by deletion of *UTH1* is unrelated to mitophagy but more likely due to rescue of cell wall biogenesis defects, as CL mutants exhibit defects in cell wall biogenesis and in maintenance of cell integrity (Zhong et al.,

2005).

Interestingly, compared to deletion of the mitophagy specific gene, deletion of general autophagy genes that are required in both nonselective autophagy and mitophagy exacerbated *crd1Δ* growth defects to a more severe extent. As seen in Fig.2.3 A, *crd1Δ* is synthetically lethal with *atg8Δ* and *atg18Δ*. In contrast, *crd1Δ* is synthetically sick with *atg32Δ*, as seen in Fig.2.3 B. The explanation for this may be that CL is specifically involved in mitophagy, not nonselective autophagy. Thus, nonselective autophagy may function normally in *crd1Δ*, and damaged mitochondria may be delivered into vacuole for degradation as cargo in the nonselective autophagosome. If nonselective autophagy is also blocked by deletion of *ATG8* or *ATG18*, cells will not be able to get rid of damaged mitochondria, resulting in cell death. If mitophagy is further impaired by deletion of *ATG32*, damaged mitochondria may be eliminated by nonselective autophagy, resulting in a sick but not lethal phenotype.

The possibility that nonselective autophagy in *crd1Δ* may not be compromised may explain the greater increase in *ATG8* gene expression in *crd1Δ* cells compared to WT as seen in Fig. 2.6. Non-optimal growth temperatures likely result in a higher rate of formation of aberrant mitochondria and respiratory-deficient petite mutants. Furthermore, yeast mitochondrial protein synthesis is more thermolabile than cytoplasmic protein synthesis (Walker, 1998). It has been reported that exposure to elevated temperature induces mitochondrial swelling (Ma et al., 2004). These factors may account for increased *ATG8* expression and mitophagy at elevated temperature in WT. When CL mutants are exposed to elevated temperature, mitochondrial swelling

may be more pronounced than in WT cells (Ma et al., 2004). Thus, it is reasonable to speculate that increased *ATG8* expression in *crd1Δ* is necessary to increase mitophagy in order to eliminate damaged mitochondria. Another possibility is that *crd1Δ* cells upregulate nonselective autophagy to a greater extent than WT cells to compensate for decreased mitophagy.

In summary, studies in this chapter suggest that loss of CL may lead to decreased mitophagy, which may account at least in part for the temperature sensitivity of the *crd1Δ* mutant. Previous studies indicate that the PKC and HOG MAPK pathways are required for mitophagy (Mao et al., 2011). To understand the underlying mechanism of decreased mitophagy in *crd1Δ*, I carried out targeted genetic interaction analysis between *CRD1* and the genes of the MAPK pathways, which is described in Chapter 3. The findings in this chapter provide novel insights into the cellular functions of CL outside of mitochondria.

.

CHAPTER 3

DEFECTIVE MITOPHAGY IN *crd1Δ* MAY RESULT FROM DECREASED MAPK PATHWAYS

Introduction

The studies described in Chapter Two suggest that perturbation of CL synthesis leads to defective mitophagy. Mitophagy is regulated by different pathways from those that control nonselective autophagy. Nonselective autophagy is regulated by at least four signaling pathways, including the Ras/cAMP-dependent protein kinase A (PKA) (Budovskaya et al., 2004; Zhou et al., 2009), the target of rapamycin (TOR) (Li et al., 2012; Yorimitsu et al., 2007), Sch9 (Li et al., 2012; Yorimitsu et al., 2007) and Pho85 pathways. Mitophagy is specifically regulated by two MAPK pathways: the PKC and HOG pathways (Li et al., 2012; Mao et al., 2011). The studies described in this chapter were undertaken to determine if these MAPK pathways are affected by the loss of CL, and if defective mitophagy in *crd1Δ* is due to altered PKC and HOG pathways.

PKC is a MAPK pathway that regulates cell wall integrity in yeast. Cell wall integrity signaling is induced in response to various environmental stimuli, including heat stress, hypo-osmotic shock, mating pheromone, and agents that cause cell wall stress (Herskowitz, 1995; Levin and Errede, 1995). Wsc1p and Mid2p are plasma membrane sensors that trigger Pkc1p, which conveys the signal downstream to Bck1p, Mkk1p/ Mkk2p and Slt2p through a kinase cascade (Heinisch et al., 1999) (Fig. 3.1). In response to induction of mitophagy, Slt2p is dually phosphorylated on threonine and tyrosine residues (Mao et al., 2011). Deletion of the PKC pathway genes *BCK1*, *MKK1/MKK2*, and *SLT2* leads to defective mitophagy, suggesting the involvement of

the PKC pathway in mitophagy. However, deletion of *RLM1* and *SWI4*, genes encoding the downstream effectors of phosphorylated Slt2p (pSlt2p), does not alter mitophagy in WT cells. In addition, pSlt2p remains in the cytosol during mitophagy, suggesting that, other than conveying the signal downstream, pSlt2p may directly play a role in a relatively early stage of mitophagy (Fig. 3.1). As described in Chapter 2, mitophagy is inhibited in *crd1Δ*, but the mechanism underlying the inhibition is not understood. The finding that loss of PG, the precursor of CL, leads to defective activation of the PKC pathway (Zhong et al., 2007) provides a clue to the potential mechanism underlying inhibited mitophagy in *crd1Δ*. It is necessary to investigate if CL is required for PKC pathway activation and further regulation of mitophagy.

The HOG pathway is a MAPK pathway that mediates the cellular response to osmotic stress. It consists of two stress sensing branches, SLN1 and SHO1 (Saito and Tatebayashi, 2004). While both branches are triggered by osmotic stress, only the SHO1 signaling is triggered by heat stress (Winkler et al., 2002). Sln1p and Sho1p are transmembrane osmosensors located within the plasma membrane. In response to osmotic stress, Sln1p conveys the signal downstream to Ypd1p, Ssk1p and Ssk2p/Ssk22p. In response to either osmotic or heat stress, Sho1p conveys the signal to Cdc42p, Ste20p and Ste11p/Ste50p. The MAPKKKs Ssk2p/Ssk22p and Ste11p trigger the same downstream MAPKK, Pbs2p. The MAPK Hog1p is dually phosphorylated by activated Pbs2p (Fig. 3.1). When Hog1p is phosphorylated, it translocates into the nucleus and induces transcription of up to 600 genes for cellular adaptation to stress, including the genes that function in the synthesis of glycerol

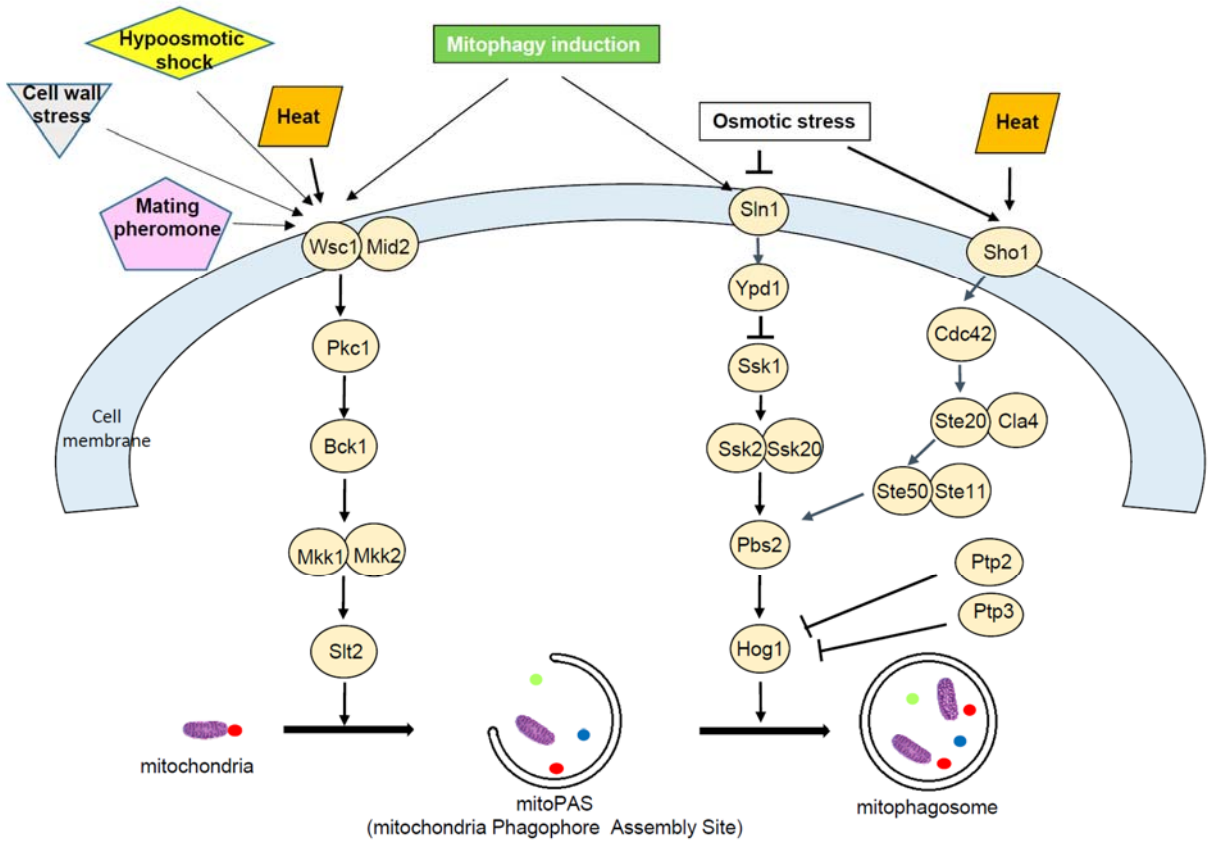

Fig. 3.1 The PKC and HOG pathways regulate different stages of mitophagy. Revised from Mao et al. 2011.

(O'Rourke and Herskowitz, 2004). Alternatively, phosphorylated Hog1p (pHog1p) remains in the cytosol under certain conditions, including high temperature and mitophagy induction (Mao et al., 2011; Winkler et al., 2002). Deletion of *HOG1*, *PBS2* and *SSK1*, leads to defective mitophagy, suggesting the involvement of the SLN1 signaling of the HOG pathway in mitophagy. However, deletion of *SKO1*, *HOT1* and *SMP1*, genes encoding the downstream effectors of pHog1p, does not alter mitophagy in WT cells (Mao et al., 2011). In addition, Hog1 is phosphorylated and remains in the cytosol after induction of mitophagy, suggesting that pHog1p may directly play a role in the cytosol at a relatively late stage of mitophagy (Fig. 3.1). As described in Chapter 2, mitophagy is inhibited in *crd1Δ*. Thus, it is necessary to investigate if the HOG pathway is perturbed in *crd1Δ*.

In the studies described in this chapter, I investigated the effect of CL deficiency on the HOG and PKC pathways. This study suggests that both pathways are defective when there is a loss of CL. Interestingly, upregulation of the PKC pathway rescues mitophagy in *crd1Δ*, indicating that decreased mitophagy in *crd1Δ* may result from an impaired PKC pathway.

Methods and materials

Yeast strains and growth media

The *Saccharomyces cerevisiae* strains used in this work are listed in Table 3.1. Yeast extract peptone dextrose (YPD) medium, synthetic complete (SC) medium, synthetic drop-out medium (SC ura$^-$, SC leu$^-$) and synthetic lactate (SL) medium were described in Chapter Two. YPDS medium was YPD medium supplemented with 1 M sorbitol. Sporulation medium contained potassium acetate (1%), glucose (0.05%), and essential amino acids. Solid medium contained agar (2%) for solidification.

Construction of deletion mutants

An established *MAT*α *crd1Δ* mutant with *CRD1* replaced by the dominant selectable marker *URA3* was used as the query strain. Single mutants that have a single HOG pathway gene deleted were obtained from the deletion collection generated in the BY4741 (*MAT*a) background (Research Genetics). The gene mutated in each strain was replaced by a kanamycin (geneticin) resistance marker (*KanMX4*). After *crd1Δ* was mated with each of these deletion strains, diploids were selected on SC met$^-$ lys$^-$ double drop-out medium, and sporulation was induced on sporulation medium. Double mutant meiotic progeny were selected on SC ura$^-$ drop-out medium with 200 mg/liter geneticin, as described (Tong et al., 2001). Growth of the double mutants was examined at various temperatures to identify genetic interactions between *CRD1* and the HOG pathway genes.

Table 3.1 Yeast strains used in Chapter 3

Strain/plasmid	Characteristics or genotype	Source or reference
BY4742 (WT)	MATα, *his3Δ1, leu2Δ0, lys2Δ0, ura3Δ0*	Euroscarf [a]
VGY1 (BY4742 *crd1Δ*)	Derivative of BY4742 , *crd1Δ*::*URA3*	Gohil et al., 2005
BY4742 *sho1Δ*	Derivative of BY4742, *sho1Δ*:: *KanMX4*	This study
VGY1*sho1Δ*	Derivative of BY4742, *crd1Δ*::*URA3, sho1Δ*::*KanMX4*	This study
BY4742 *ssk1Δ*	Derivative of BY4742, *ssk1Δ*:: *KanMX4*	This study
VGY1*ssk1Δ*	Derivative of BY4742, *crd1Δ*::*URA3, ssk1Δ*::*KanMX4*	This study
BY4742 *ste50Δ*	Derivative of BY4742, *ste50Δ*::*KanMX4*	This study
VGY1*ste50Δ*	Derivative of BY4742, *crd1Δ*::*URA3, ste50Δ*::*KanMX4*	This study
BY4742 *hog1Δ*	Derivative of BY4742, *hog1Δ*::*KAN*	This study
VGY1*hog1Δ*	Derivative of BY4742, *crd1Δ*::*URA3, hog1Δ*::*KanMX4*	This study
BY4742 WT-*IDH1-GFP*	Derivative of BY4742, in which *IDH1* gene is chromosomally tagged with GFP	This study
BY4742 *crd1Δ*- *IDH1-GFP*	Derivative of BY4742 *crd1Δ*::*KanMX4*, in which *IDH1* gene is chromosomally tagged with GFP	This study
pYPGK18	2µm, *LEU2*	Vaz et al., 2003
pYPGK18-*PTP2*	Derivative of pYPGK18, expresses *PTP2* from PGK1 promoter	This study
pYPGK18-*PTP3*	Derivative of pYPGK18, expresses *PTP3* from PGK1 promoter	This study
pYCp50	CEN, *URA3*	Helliwell et al., 1998
pYCp50-*PKC1* ^{R398P}	Derivative of pYCp50, expresses *PKC1* ^{R398P} from PGK1 promoter	Helliwell et al., 1998
pRS352	2µm, *URA3*	Helliwell et al., 1998
pRS352-*BCK1-20*	Derivative of pRS352, expresses *BCK1-20* from PGK1 promoter	Helliwell et al., 1998
pPS1739-HOG1-GFP	CEN, *URA3*, HOG1-GFP	Ferrigno et al., 1998

Plasmid construction

To construct the *PTP2* overexpression plasmid, a sequence of 2250 base pairs that contains the entire open reading frame of *PTP2* was amplified from yeast genomic DNA using KpnI-tagged forward primer *PTP2*fr-f (5'-GG GGTACCATTGATGGATCGCATAGCACAG-3') and XbaI-tagged reverse primer *PTP2*fr-r (5'- CGC TCTAGA TTAACAAGGTAACGCGTTCTTTATC -3'). After being cut by the restriction enzyme KpnI and XbaI, the PCR product was ligated downstream of the *PGK1* promoter on the pYPGK18 (2um, *LEU2*) plasmid (Fig 3.2).

To construct the *PTP3* overexpression plasmid, a sequence of 2751 base pairs that contains the entire open reading frame of *PTP3* was amplified from yeast genomic DNA using EcoRI-tagged forward primer *PTP3*fr-f (5'-CCGGAATTC GAACATGAAGGACAGTGTAGACTGC-3') and BamHI-tagged reverse primer *PTP3*fr-r (5'-CGCGGATCCGCCTAACTATTGTGGCAATTCTTTC-3'). After being cut by the restriction enzyme KpnI and XbaI, the PCR product was ligated downstream of the *PGK1* promoter on the pYPGK18 (2um, *LEU2*) plasmid (Fig 3.2).

Single colony formation and spotting

Single colony formation experiments were performed as described in Chapter Two.

Spotting experiments were performed as follows. Cells were pre-cultured in SC drop-out liquid medium at 30˚C to the mid-log phase. The A_{550} of the cells was determined using a spectrometer (Beckman). Cell aliquots were centrifuged and pellets were resuspended in SC leu$^-$ medium adjusted to an A_{550} of 10 units per ml. A

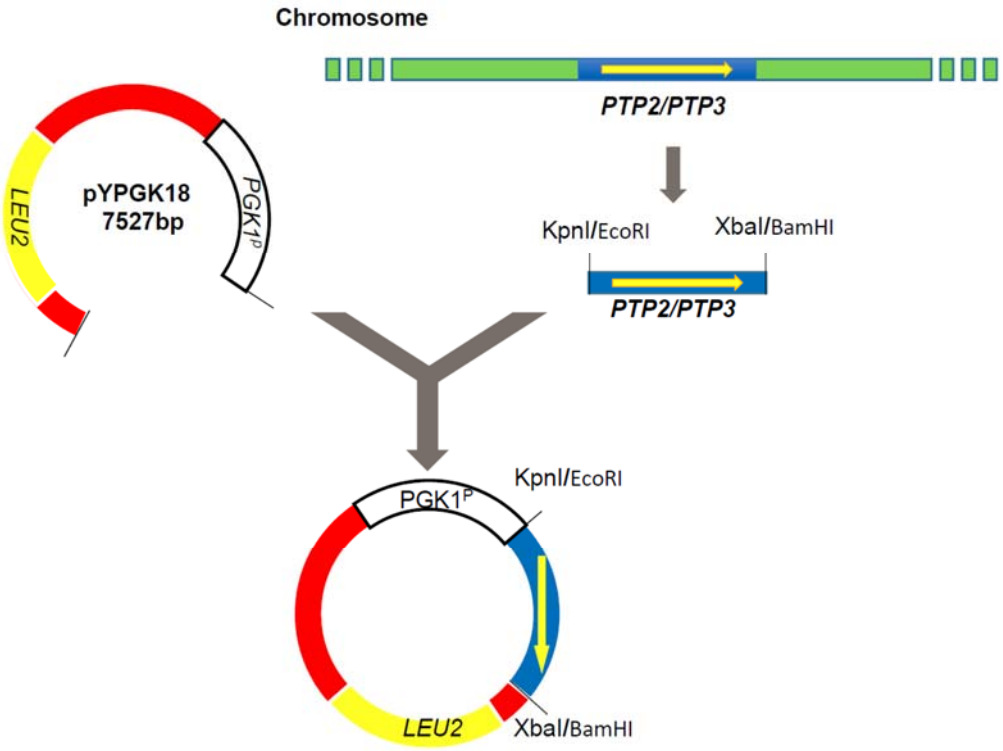

Fig. 3.2 Construction of the pYPGK18-*PTP2* and pYPGK18-*PTP3* overexpression plasmids. The detailed procedure was described in the 'Methods and materials' section.

100X diluted sample was added onto a hemocytometer for cell counting using light microscopy. Based on the cell counting result, cell aliquots were adjusted to $2x10^8$ cells/ml. The cell aliquots were then diluted in a 10X serial dilution. Cells were spotted on SC drop-out plates with the most diluted spot containing 2000 cells and the plates were incubated at experimental temperatures for 2 days. The appearance of visible growth at various temperatures was evaluated.

Fluorescence and microscopic analysis

Microscopic analysis was performed using an Olympus BX41 epifluorescence microscope. Images were captured by an Olympus Q-Color3 digital charge-coupled camera operated by QCapture2 software. All pictures were taken at 1000x magnification.

The method used to detect mitophagy by monitoring the translocation of GFP-tagged mitochondria was described in Chapter Two. The same procedure was performed in BY4742 WT-*IDH1-GFP* and *crd1Δ-IDH1-GFP* strains that were transformed with either pYcp50 empty vector or pYcp50::*PKC1*^{R398}, which overexpresses a constitutively activated Pkc1p.

To visualize the translocation of phosphorylated Hog1p, WT and *crd1Δ* cells in the BY4742 background were transformed with the pPS1739 plasmid, which expresses *HOG1*-GFP (kindly provided by Dr. Pamela Silver, Harvard Medical School). Transformants were cultured in SC ura$^-$ liquid medium and grown to an A_{550} of 1.0. The cells were treated with different conditions (39°C or 0.5 M NaCl) and observed using

epifluorescence microscopy using a green fluorescence filter. Translocation of phosphorylated Hog1p was determined by the accumulation of GFP inside the nucleus.

Western blot

Western blot analysis to detect Idh1-GFP and cleaved free GFP was described in Chapter Two.

To detect Slt2p and pSlt2p by Western blot, whole cell extracts were prepared as previously described (Hoppins et al., 2011) with minor changes. Mid-log phase cells were diluted to an A_{550} of 0.3 and grown at 30°C or 39°C. After culture at different temperatures for 2 hours, cells at an A_{550} of 1 were collected, washed with 1 ml ice-cold sterile water and resuspended in 1 ml 0.255 M NaOH BME buffer, which consisted of 0.255 M NaOH, 1% β-mercaptoethanol, and 0.86 ml sterile distilled water. The samples were incubated for 10 min on ice and 138 µl 72% TCA were added. The samples were incubated on ice for another 10 min and then pelleted by centrifugation at 4˚C, 15000 rpm for 10 min. The pellets were washed once with 500 µl of ice-cold acetone, spun down at 4˚C, 15000 rpm for 5 min and then air-dried at room temperature. The air-dried cell pellets were resuspended in 50 µl MURB buffer, which consisted of 100 mM MES (PH 7.0), 1% SDS, 3 M urea, 10% β–ME and 35 µl ddH_2O. 9 µl of each sample were mixed with 3 µl 4X loading dye (80% bromophenol blue and 20% β-mercaptoethanol) and loaded into a 10% SDS-polyacrylamide gel for electrophoresis. The transferring and blotting steps were described in Chapter Two.

The primary and secondary antibodies used to recognize dually phosphorylated pSlt2p and total Slt2p are listed in Table 3.2.

To detect Hog1p and pHog1p by Western blot, whole cell extracts were prepared as described (Li et al., 2012). The primary and secondary antibodies used to recognize phosphorylated pHog1p and total Hog1p are listed in Table 3.2.

Table 3.2 Antibodies used in determining MAPK pathway activation

Protein	Primary Antibody	Secondary Antibody	Band size
pSlt2p	anti-phospho-p44/42 MAPK (Thr202/Tyr204) mouse IgG (Cell signaling)	HRP-conjugated goat anti-mouse IgG (Santa Cruz)	2 bands ~ 55 kDa
Slt2p	anti-Slt2p goat IgG (Santa Cruz)	HRP-conjugated donkey anti-goat IgG (Santa Cruz)	1 band ~ 55 kDa
pHog1p	anti-phospho-p38 rabbit IgG (antibody 3D7; Cell Signaling)	HRP-conjugated goat anti-rabbit IgG (Santa Cruz)	1 band ~ 49 kDa
Hog1p	anti-Hog1p goat IgG (antibody yC-20, Santa Cruz)	HRP-conjugated donkey anti-goat IgG (Santa Cruz)	1 band ~ 49 kDa

Results

Down-regulation of the HOG pathway exacerbates the *crd1Δ* growth defect.

In Chapter Two, I reported that, under mitophagy inducing conditions, *crd1Δ* exhibited decreased mitophagy compared to WT. The HOG pathway is an upstream regulator of mitophagy. Deletion of the HOG pathway genes *HOG1* and *PBS2* leads to defective mitophagy (Mao et al., 2011). pHog1p appears to stay in the cytosol to play a role in a relatively late stage of mitophagy. Thus, I investigated the possibility that the HOG pathway is perturbed in *crd1Δ*.

For this purpose, I determined if there is genetic interaction between *CRD1* and HOG pathway genes. The yeast deletion collection facilitated construction of double mutants (Tong et al., 2001). *crd1Δ* was mated with *sho1Δ*, *ssk1Δ*, *ste50Δ* and *hog1Δ* mutants. Tetrads were obtained subsequent to sporulation, and haploids were acquired via tetrad dissection. Haploids containing mutations in both *CRD1* and one of the four HOG pathway genes were selected by uracil prototrophy (*crd1Δ* mutation) and geneticin resistance (HOG pathway mutation). *crd1Δ* in the BY4742 background cannot form colonies from single cells plated on YPD at 40°C, which is a permissive temperature for WT (Jiang *et al*., 1999; Zhong *et al*., 2004). At 38˚C and 39˚C, *crd1Δ* cells form smaller colonies than WT. Based on this growth phenotype, genetic interaction was assessed at elevated temperature. Growth of double mutants at 40°C was considered rescue of the *crd1Δ* growth defect, while inability to grow at 38˚C or 39˚C indicated exacerbation of the *crd1Δ* growth defect.

While *crd1Δ* cells formed colonies at 39˚C, *crd1Δssk1Δ* did not. *crd1Δste50Δ*,

crd1Δsho1Δ, *crd1Δhog1Δ* did not form colonies even at 38˚C (Fig. 3.3), suggesting that mutants of *SSK1*, *STE50, SHO1*, and *HOG1* genetically interact with *crd1Δ*. To determine if down-regulation of the HOG pathway leads to exacerbation of the *crd1Δ* growth defect, *PTP2* and *PTP3*, which negatively regulate the HOG pathway, were overexpressed in *crd1Δ*. Serial diluted *crd1Δ* cells containing empty vector or overexpressing PTP2 or PTP3 were spotted on leu$^-$ plates and incubated at 30˚C - 38˚C. The growth defect of *crd1Δ* was exacerbated by overexpression of *PTP2* and *PTP3* (Fig. 3.4). These data suggest that downregulation of the HOG pathway leads to exacerbation of the *crd1Δ* growth defect, and the HOG pathway may be perturbed in *crd1Δ*.

Loss of CL leads to decreased Hog1p phosphorylation without perturbing activated Hog1p translocation

Downregulation of the HOG pathway leads to exacerbation of the *crd1Δ* growth defect, suggesting that the HOG pathway may be altered in *crd1Δ* cells. To determine if Hog1p phosphorylation is perturbed in *crd1Δ*, I induced Hog1p activation with 0.5 M NaCl for 5 min, and analyzed Hog1p phosphorylation by Western blot, using a monoclonal antibody against dually phosphorylated p38, as described (Li et al., 2012; Zhou et al., 2009). Compared to WT cells, Hog1p activation was decreased in *crd1Δ* in response to osmotic stress (Fig. 3.5 A). To determine if translocation of activated Hog1p was perturbed in *crd1Δ*, WT and *crd1Δ* cells were transformed with the pPS1739 plasmid containing *HOG1*-GFP. The cells were cultured in SC ura$^-$ liquid

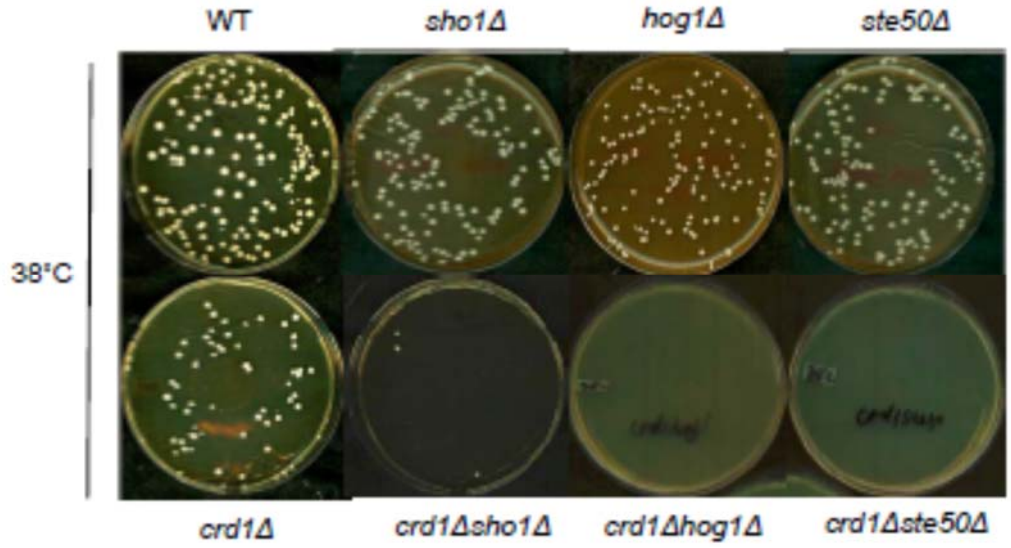

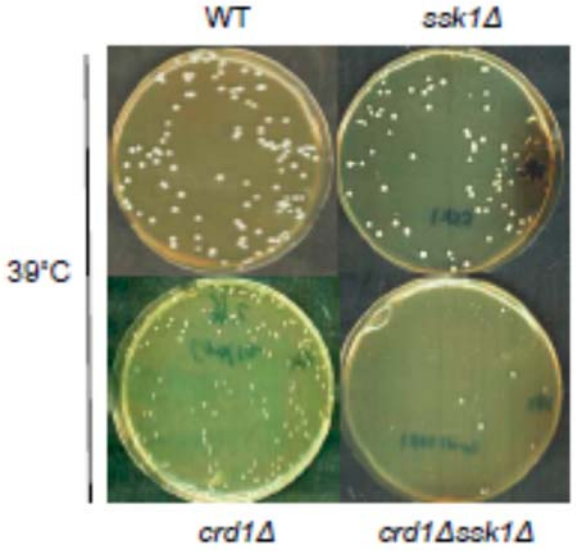

Fig. 3.3 Deletion of HOG pathway genes is synthetically lethal with *CRD1* deletion. Cells were pre-cultured in liquid YPD at 30˚C to the mid-log phase. 200 cells of each strain were plated on YPD plates and incubated at 38˚C or 39˚C for 3 days.

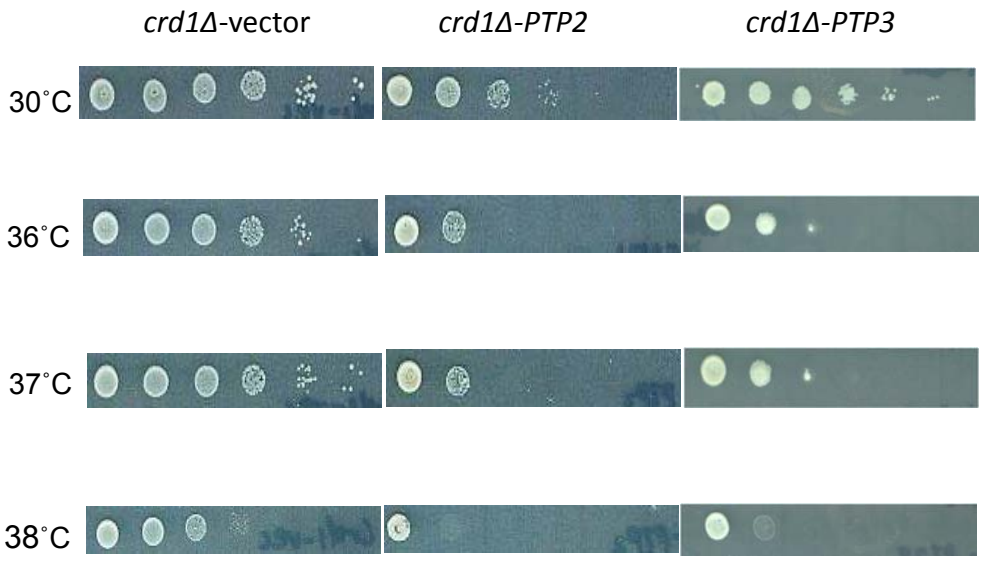

Fig. 3.4 Overexpression of the negative regulators of the HOG pathway is synthetically lethal with *CRD1* deletion. Cells were pre-cultured in liquid SC leu$^-$ at 30˚C to the mid-log phase. Cell aliquots were adjusted to 2x10^8 cells/ml and then diluted in a 10X serial dilution. Cells were spotted on SC leu$^-$ plates with the most diluted spot containing 2000 cells, and the plates were incubated at 30˚C, 36˚C, 37˚C or 38˚C for 2 days.

medium to an A_{550} of 1 and treated with 0.5 M NaCl for 5 min. Fluorescence microscopy showed no difference between WT and *crd1Δ* in the translocation of activated Hog1p after NaCl treatment (Fig. 3.5 B).

Heat stress does not activate Hog1p in WT and does not rescue decreased Hog1p phosphorylation in *crd1Δ*

Both branches of the HOG pathway are triggered by activation of the corresponding membrane-bound sensors (Sho1p or Sln1p) in response to osmotic stress. A previous publication has shown that heat stress triggers the HOG pathway via the SHO1 but not the SLN1 signaling (Winkler A, 2002). Surprisingly, Hog1p phosphorylation was not observed in WT or *crd1Δ* in response to heat stress (Fig. 3.6 A). The translocation of Hog1-GFP in response to heat stress was also not observed. WT and *crd1Δ* cells containing the pPS1739 plasmid were pre-cultured in liquid YPD at 30˚C to the mid-log phase, switched to 39˚C for 10 min and observed using epifluorescence microscopy. Consistent with the Western blot result, the translocation of Hog1-GFP into the nucleus was not observed in either WT or *crd1Δ* (Fig. 3.6 B), suggesting that heat stress does not trigger Hog1p activation or translocation in the BY4742 background.

Upregulation of the PKC pathway rescues the *crd1Δ* growth defect

As mentioned above, a previous study in yeast demonstrated that activation of the PKC pathway is decreased in *pgs1Δ* (Zhong et al., 2007). Deletion of *PGS1* causes loss of both PG and CL. Thus, I investigated if there is decreased activation of PKC

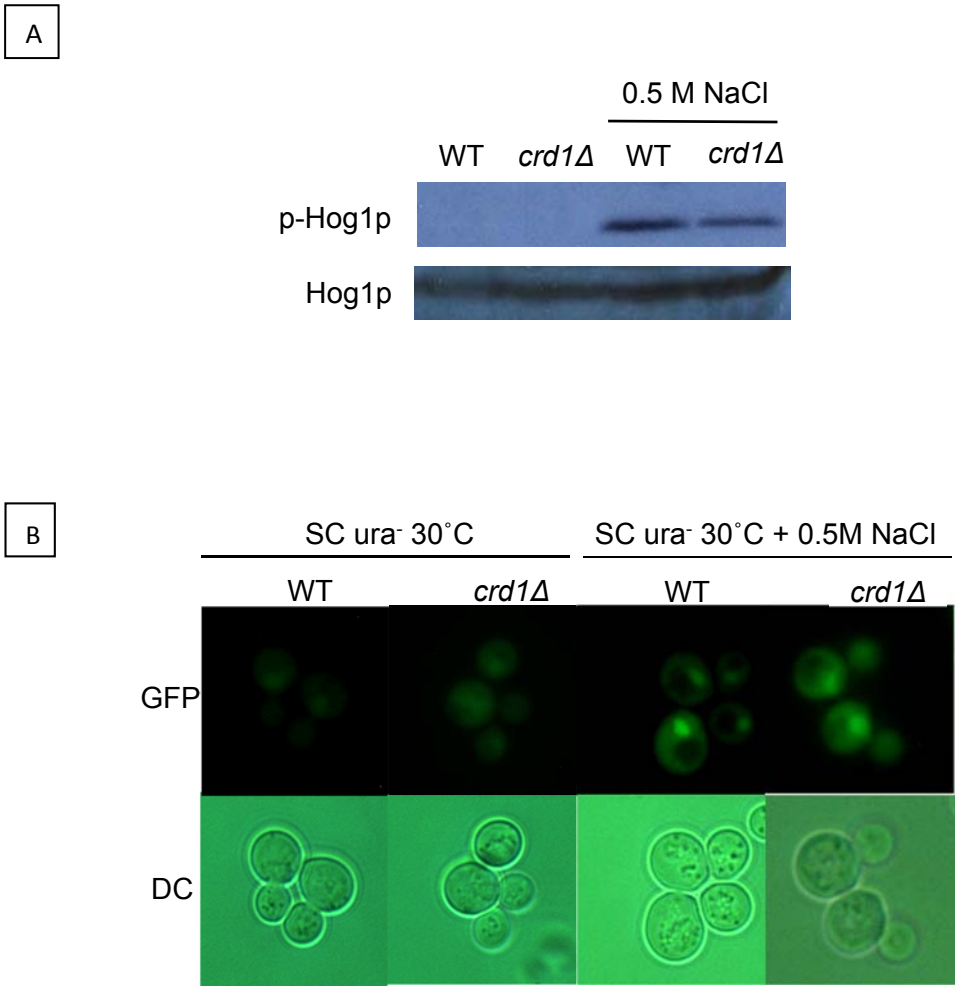

Fig. 3.5 (A) Decreased Hog1p phosphorylation in the *crd1Δ* mutant. Cells were pre-cultured in liquid YPD at 30˚C to the mid-log phase and treated with 0.5 M NaCl for 5 min. Dually phosphorylated Hog1p and total Hog1p protein were detected by Western blot, as described previously (Zhou et al., 2009). **(B) Translocation of activated Hog1p is not affected in *crd1Δ***. WT and *crd1Δ* were transformed with the plasmid pPS1739, from which Hog1p fused to GFP was expressed. Cells were grown in SC ura$^-$ to an A_{550} of 1, treated with 0.5 M NaCl for 5 min and then observed using epifluorescence microscopy.

A

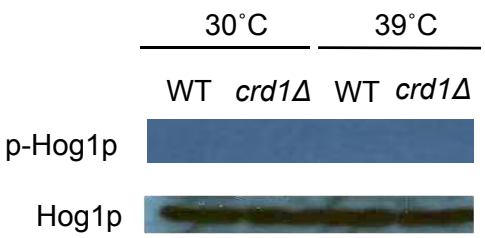

B

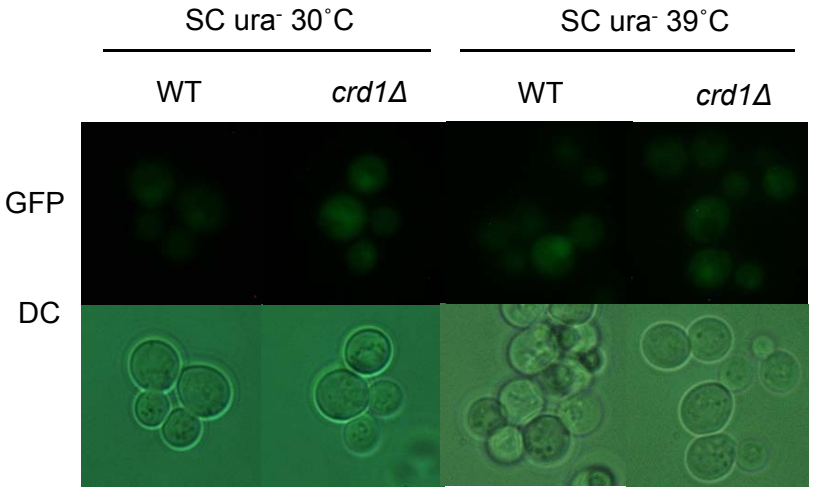

Fig. 3.6 (A) Heat stress does not trigger phosphorylation in the BY4742 background. Cells were pre-cultured in YPD at 30˚C to the mid-log phase and switched to 39˚C for 5 min. Dually phosphorylated Hog1p and total Hog1p proteins were detected by Western blot, as described previously (Zhou et al., 2009). **(B) Heat stress does not induce the translocation of GFP tagged Hog1p into the nucleus in the BY4742 background.** WT and *crd1Δ* were transformed with the plasmid pPS1739, on which HOG1 is fused to GFP. Cells were grown in SC ura$^-$ to an A_{550} of 1, switched to 39˚C, and observed using epifluorescence microscopy.

pathway in *crd1Δ*, which has PG but not CL. For this purpose, I examined the activation state (dual phosphorylation) of Slt2p in response to elevated temperature in isogenic WT, *crd1Δ* and *pgs1Δ* cells in the BY4742 background by Western blot. Because *pgs1Δ* in the FGY background requires sorbitol for survival at even 30°C, to exclude any influence caused by sorbitol, I also determined the Slt2p phosphorylation in *pgs1Δ* in this background, supplemented with 1 M sorbitol. Cells were pre-cultured in YPD at 30˚C to the mid-log phase, diluted to an A_{550} of 0.3, and grown at 30°C or 39˚C for 2 hours. Whole cell extracts were prepared, and dually phosphorylated Slt2p and total Slt2p proteins were detected by Western blot, as described in the 'Methods and materials' section. Dual phosphorylation of Slt2p in WT was detected after the cells were cultured for 2 hours at 39˚C. Slt2p dual phosphorylation was decreased in *crd1Δ* and almost absent in *pgs1Δ* and *pgs1Δ* supplemented with sorbitol, which indicates decreased PKC pathway activation in the CL mutants (Fig. 3.7 A). To upregulate the PKC pathway, *crd1Δ* was transformed with a vector expressing constitutively activated Bck1 (*BCK1-20*) or Pkc1 (PKC^{R398P}). Consistent with the Western blot result, spotting experiments demonstrated that *crd1Δ* temperature sensitivity was rescued by plasmids expressing constitutively activated Bck1 or Pkc1 (Fig. 3.7 B), suggesting that upregulation of the PKC pathway rescues the *crd1Δ* growth defect.

Upregulation of the PKC pathway rescues defective mitophagy in *crd1Δ*

As mentioned above, activation of the PKC and HOG pathways are required for

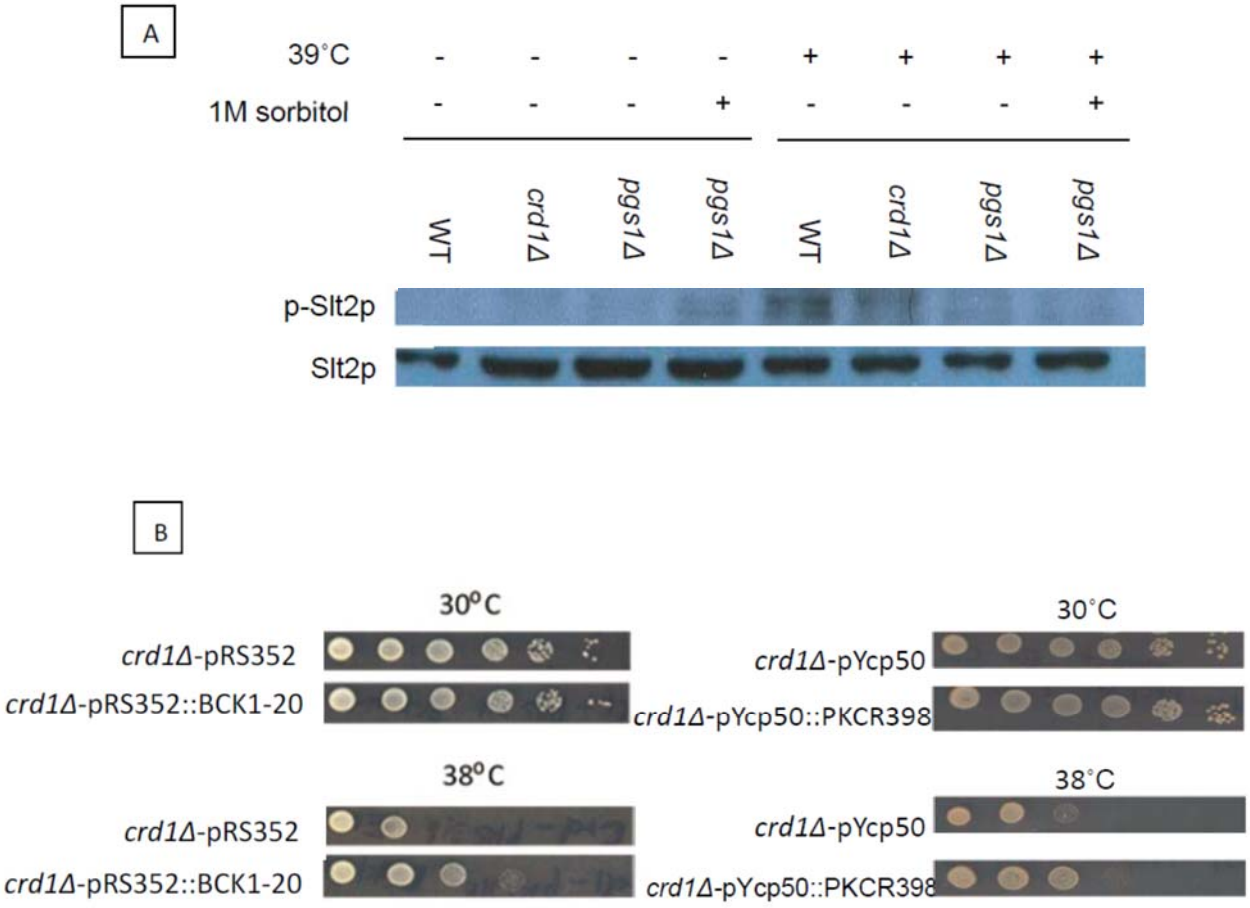

Fig 3.7 (A) The PKC pathway is decreased in *crd1Δ*. Cells were pre-cultured in liquid YPD at 30˚C to the mid-log phase, diluted to an A_{550} of 0.3, and treated with increased temperature or sorbitol for 2 hours. Whole cell extracts were prepared and dually phosphorylated Slt2p and total Slt2p protein were detected by Western blot. **(B) Upregulation of the PKC pathway rescues the *crd1Δ* growth defect.** Cells containing overexpression plasmids that upregulate the PKC pathway (*BCK1-20* and $PKC1^{R398}$) were cultured in SC ura$^-$ medium at 30˚C to the mid-log phase. Cells were diluted, spotted on SC ura$^-$ plates, and incubated at 30˚C or 38˚C for 2 days.

mitophagy (Mao et al., 2011). Therefore, I investigated a possible causal relationship between decreased MAPK pathways and inhibited mitophagy in *crd1Δ*.

Upregulation of the PKC pathway was achieved in WT-*IDH1-GFP* and *crd1Δ-IDH1- GFP* strains in the BY4742 background by transfecting the cells with plasmid carrying the $PCK1^{R398}$ gene, which encodes a constitutively activated Pkc1p. WT-*IDH1-GFP* and *crd1Δ-IDH1-GFP* cells containing either empty vector or vector expressing $PCK1^{R398}$ were pre-cultured in liquid SC ura$^-$ medium, harvested, washed twice, and resuspended in SL medium at a starting A_{550} of 0.5. After 18 hours, cells were observed using epifluorescence microscopy. As predicted, accumulation of GFP was observed in the vacuole of WT-*IDH1-GFP* cells containing either the empty vector or vector expressing $PKC1^{R398P}$. GFP accumulation was not observed in *crd1Δ-IDH1-GFP* cells containing the empty vector. Interestingly, accumulation of GFP was observed in *crd1Δ-IDH1-GFP* cells containing the vector that expresses the $PKC1^{R398P}$ gene, suggesting that mitochondria were delivered into the vacuole of this strain (Fig. 3.8).

The release of free GFP, a byproduct of mitophagy, was determined by Western blot of WT-*IDH1-GFP* and *crd1Δ-IDH1-GFP* strains containing either an empty vector or a vector expressing $PCK1^{R398}$. Cells were cultured in liquid SC ura$^-$ medium to the mid-log phase at 30˚C, harvested, washed twice and resuspended in SL medium at a starting A_{550} of 0.5. After 6 hours, proteins were extracted as described previously. Consistent with the finding of the microscopic examination experiment, the Western blot showed a strong free GFP band in WT cells containing either the empty vector or

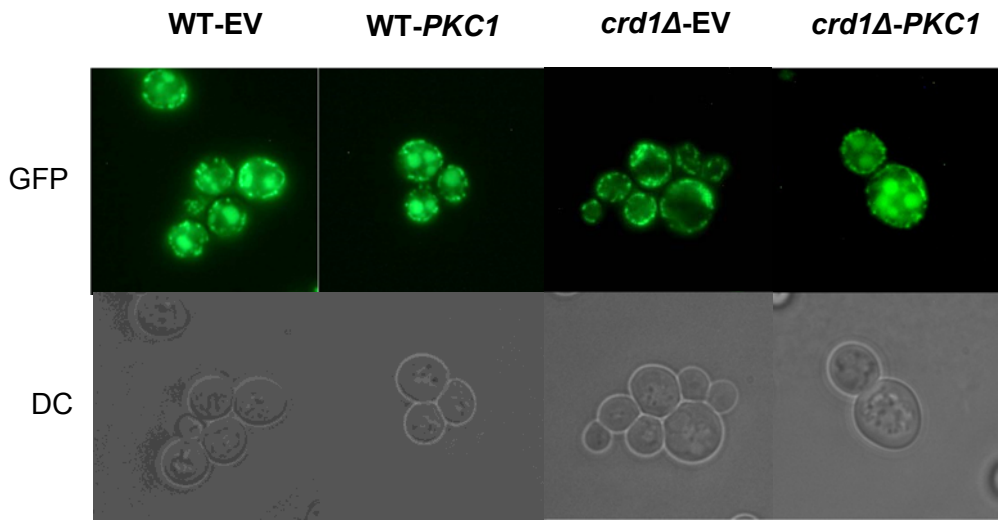

Fig.3.8 Upregulation of the PKC pathway rescues the delivery of mitochondria into vacuole in *crd1Δ* after induction of mitophagy. WT-*IDH1-GFP* and *crd1Δ-IDH1-GFP* cells containing either an empty vector or a vector expressing $PKC1^{R398P}$ were cultured in SC ura^- medium to the mid-log phase at 30˚C, washed and shifted to SL for 18 hours. Cells were then observed with fluorescence microscopy.

the vector expressing *PKC1*^{R398P}, but only a very faint free GFP band in *crd1Δ-IDH1-GFP* containing the empty vector, indicating that mitophagy is defective in *crd1Δ* cells. However, a strong free GFP band that is comparable to that detected in WT-ev and WT-PKC strains was observed in *crd1Δ-IDH1-GFP* cells containing the vector that expresses *PKC1*^{R398P}, suggesting that PKC rescued mitophagy in this strain (Fig. 3.9).

The HOG pathway stimulants rescues the *crd1Δ* growth defect

A constitutively activated HOG pathway causes lethality, and cannot be used to study mitophagy in *crd1Δ*. Although it is difficult to test if there is direct causal relationship between a decreased HOG pathway and defective mitophagy in *crd1Δ*, indirect evidence suggests that upregulating the HOG pathway may rescue the *crd1Δ* growth defect. A previous study demonstrated that the addition of 1 M sorbitol, a HOG pathway stimulant, rescued *crd1Δ* growth and vacuole defects (Chen et al., 2008b). Our present study established that 200 mM NaCl, another HOG pathway activator, similarly rescued *crd1Δ* temperature sensitivity (Fig. 3.10). However, more direct evidence is needed to conclude that a decreased HOG pathway inhibits mitophagy in *crd1Δ*.

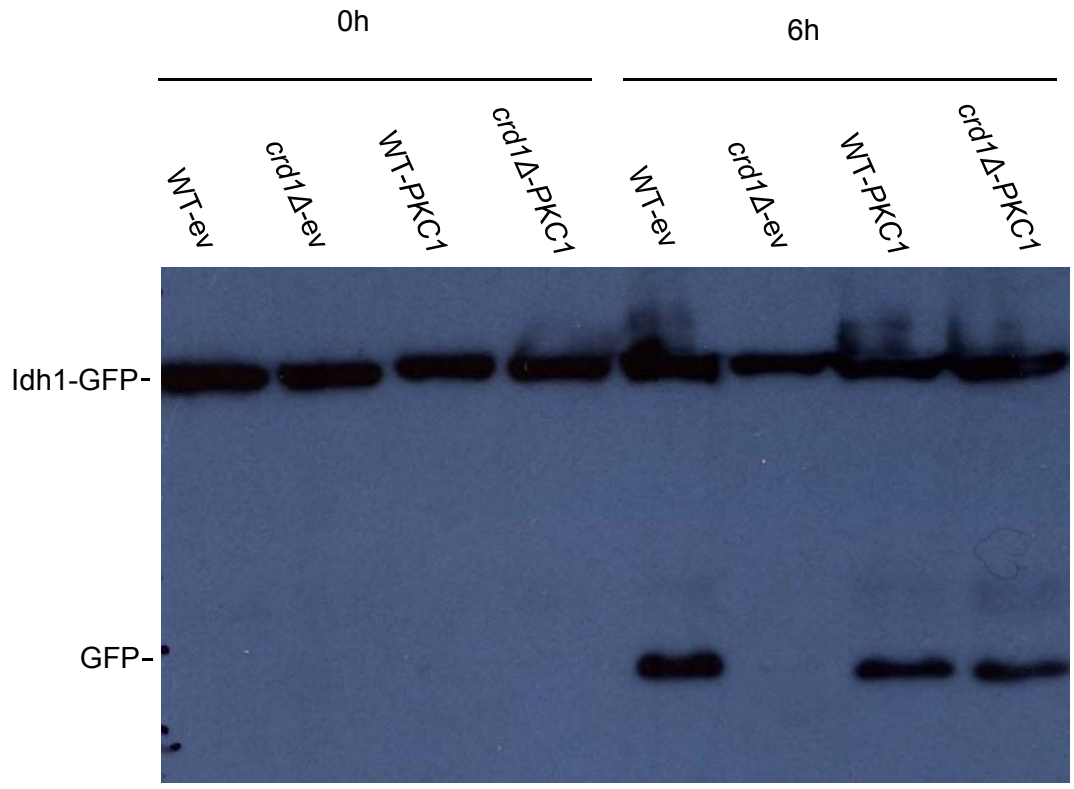

Fig. 3.9 Upregulation of the PKC pathway rescues mitophagy in *crd1Δ*. WT-*IDH1-GFP* and *crd1Δ-IDH1-GFP* cells containing either an empty vector or a vector expressing *PKC1*^{R398P} were cultured in SC ura$^-$ medium to the mid-log phase at 30˚C, washed and shifted to SL. Samples were taken before shift to SL medium and at 6 hours post-shift. Immunoblotting was done with an anti-GFP antibody and the positions of full-length Idh1-GFP and free GFP are as indicated.

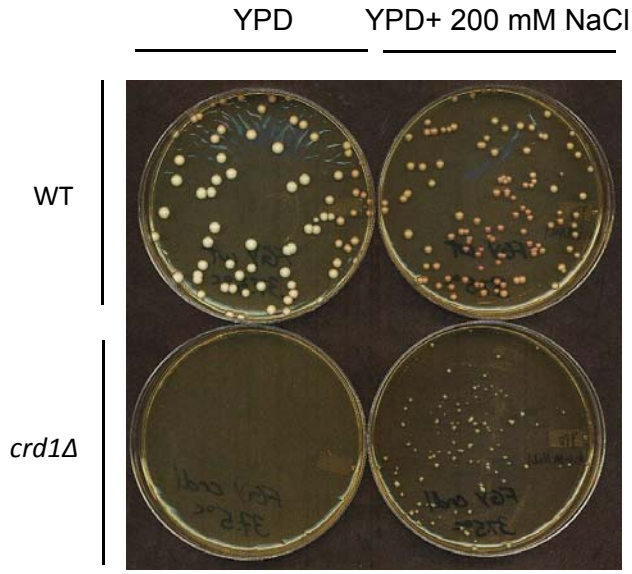

Fig. 3.10 200 mM NaCl rescues *crd1Δ* temperature sensitivity. WT and *crd1Δ* cells in the FGY background were pre-cultured in YPD liquid at 30˚C to the mid-log phase. 200 cells were plated on a YPD plate with or without 200 mM NaCl. Plates were then incubated at 37.5˚C for 3 days.

Discussion

In this chapter, I addressed the hypothesis that loss of CL leads to perturbation of the HOG and PKC pathways, which causes defective mitophagy in *crd1Δ*. Consistent with this hypothesis, the *crd1Δ* mutant exhibited decreased phosphorylation of Hog1p in the presence of osmotic stress and decreased phosphorylation of Slt2p in the presence of heat stress, suggesting defective activation of both the HOG and PKC pathways in *crd1Δ*. As expected, *pgs1Δ* treated with heat stress also exhibited largely decreased phosphorylation of Slt2p. I demonstrated that upregulation of the PKC pathway rescued the growth defect in *crd1Δ*, as well as the accumulation of GFP labeled mitochondria and cleaved GFP in the vacuole of *crd1Δ-IDH1-GFP*. This suggests that upregulation of the PKC pathway rescued mitophagy in *crd1Δ*, supporting the hypothesis that defective mitophagy in *crd1Δ* may be due to defective activation of the PKC pathway.

Based on the previous findings that *crd1Δ* exhibits defective activation of the HOG pathway, which is required for mitophagy, upregulation of this pathway may rescue mitophagy in *crd1Δ*. However, constitutive activation of the HOG pathway causes cell lethality. It was previously shown that 1 M sorbitol, a HOG pathway stimulant, rescues the *crd1Δ* growth and vacuole defects (Chen et al., 2008b). In addition, I found that 200 mM NaCl, which also stimulates the HOG pathway, rescued *crd1Δ* temperature sensitivity (Fig. 3.8). These findings provide a clue that upregulating the HOG pathway may rescue the *crd1Δ* growth defect. However, sorbitol and NaCl also regulate cellular ion homeostasis, which may account for rescue of *crd1Δ* defects.

Although ion homeostasis may be perturbed in *crd1Δ*, it would not be the sole cause of the growth defect, because upregulation of the PKC pathway, which does not affect ion regulation, rescued the *crd1Δ* growth defect.

As mentioned in Chapter Two, there was very little free GFP detected by Western blot in whole cell extracts from *crd1Δ-IDH1-GFP* after induction of mitophagy. Consistent with this, the phosphorylation of Slt2p and Hog1p upon induction by heat or osmotic stress was decreased but not fully blocked. Slt2p and Hog1p phosphorylation was detectable after stimulation, which might explain the faint band of free GFP detected in *crd1Δ-IDH1-GFP* cells 7 hours after mitophagy induction (Fig. 2.8). If the HOG pathway is fully blocked, the late stage of mitophagy may be disrupted. Upregulation of the PKC pathway, which regulates the early stage of mitophagy, may not rescue mitophagy in *crd1Δ* under these conditions.

Because *crd1Δ* is synthetically lethal with mutants of SLN1 and SHO1 branches, decreased activation of both branches may occur in *crd1Δ*. To address this possibility, Hog1p activation in double mutants with deletion of *CRD1* and a gene from either branch should be compared to that of *crd1Δ*. For example, if *sho1Δ* exacerbates the Hog1p activation defect in *crd1Δ*, this would suggest that CL may be required for activation of SLN1 signaling.

Translocation of pHog1p into the nucleus was not affected in *crd1Δ* cells. Surprisingly, elevated temperature did not induce phosphorylation or the translocation of Hog1p into the nucleus. This conflicts with the finding of Winkler, who reported that heat stress induced Hog1p activation (Winkler et al., 2002), but it may be explained by

the fact that our studies were performed using strains from different backgrounds. Heat activation of the HOG pathway is likely to be strain dependent.

In summary, the studies described in this chapter suggest that the loss of CL may lead to decreased PKC and HOG pathways, and that a defective PKC pathway may account for impaired mitophagy in the *crd1Δ* mutant. The findings in this chapter provide novel insights into the cellular function of CL. It is tempting to speculate that upregulation of the PKC pathway may be a potential treatment strategy for BTHS patients.

CHAPTER 4

FUTURE DIRECTIONS

The studies described in this thesis provide novel insights into the cellular functions of CL beyond the confines of mitochondria, including mitophagy and the PKC and HOG pathways. While my studies showed that loss of CL leads to defective mitophagy, which may be due to decreased function of MAPK pathways, much remains to be unveiled. To elucidate the mechanism linking defective mitophagy and MAPK pathways in CL-deficient cells, as well as the mechanism underlying the role of CL in vacuolar morphology and acidification, future studies should address the following questions:

1. Does nonselective autophagy function normally in *crd1Δ* ?

In Chapter 2, I showed that CL deficiency leads to decreased levels of mitochondria and cleaved GFP in the vacuole, suggesting defective mitophagy in *crd1Δ* cells. However, deletion of *ATG8* or *ATG18*, the general autophagy genes required for both nonselective autophagy and mitophagy, exacerbated the *crd1Δ* growth defect to a greater extent than deletion of the mitophagy specific gene, *ATG32*, (Fig. 2.3). I hypothesize that CL is specifically required for mitophagy, not for nonselective autophagy. Accordingly, if nonselective autophagy is unaffected in *crd1Δ*, damaged mitochondria can be enclosed in nonselective autophagosomes and delivered to the vacuole for degradation. However, if nonselective autophagy in *crd1Δ*

is blocked by deletion of *ATG8* or *ATG18*, the cell will not be able to remove damaged mitochondria. This would result in cell death, consistent with synthetic lethality of *crd1Δ* and *atg8Δ*. This hypothesis is further supported by the finding that expression of *ATG8* in *crd1Δ* is two-fold higher than in WT at 39˚C (Fig. 2.6), suggesting that nonselective autophagy is upregulated in *crd1Δ*.

If nonselective autophagy is functional in *crd1Δ* cells, stimulation by rapamycin might be expected to rescue *crd1Δ* growth defects. To test this possibility, rapamycin was added to YPD plates and temperature sensitivity of *crd1Δ* and WT in the FGY background was examined at 36.5°C and 37°C. WT cells were unable to grow at elevated temperature in the presence of rapamycin concentrations greater than 1 nM. 0.01-1 nM rapamycin did permit growth of WT cells, while 0.5 nM rapamycin induced a slight rescue of *crd1Δ* temperature sensitivity at elevated temperature (data not shown). Future experiments are necessary to explain why only 0.5 nM rapamycin rescued *crd1Δ* growth defects. Rapamycin is an antifungal antibiotic, which inhibits the target of rapamycin complex 1 (TOR1). In addition to negatively regulating autophagy and transcription of stress responsive genes, TOR1 positively regulates ribosome biogenesis, global translation initiation, and nutrient import. Thus, the effect of rapamycin is like a double-edged sword: it increases autophagy while inhibiting ribosome biogenesis, global translation initiation, and nutrient import, resulting in cell lethality. With additional growth defects, *crd1Δ* may be more sensitive to rapamycin than WT. The toxicity of 0.5-1 nM rapamycin may overwhelm the benefits of increased nonselective autophagy induced by these concentrations in *crd1Δ*. *crd1Δ* may tolerate

rapamycin less than 0.5 nM. However, levels of nonselective autophagy triggered by these concentrations may be inadequate to remove the majority of damaged mitochondria. 0.5 nM rapamycin may be an optimal concentration that can trigger enough nonselective autophagy to remove the majority of the damaged mitochondria.

To definitively ascertain if nonselective autophagy is functional in CL deficient cells, direct monitoring of nonselective autophagy in *crd1Δ* is required. An engineered protein Pho8Δ60 has been designed for this purpose (Noda and Klionsky, 2008). Pho8Δ60 lacks the N-terminal transmembrane domain of Pho8 (alkaline phosphatase) that targets the endoplasmic reticulum; thus, the mutated protein remains in the cytosol and is only delivered to the vacuole through nonspecific autophagy. After entering the vacuole lumen, the alkaline phosphatase activity of Pho8Δ60 is proteolytically activated. Therefore, enzyme activity of Pho8Δ60 reflects the level of nonspecific autophagy. To determine if nonselective autophagy is upregulated to compensate for defective mitophagy in *crd1Δ* cells, the Pho8Δ60 assay should be performed.

2. Which branch of the HOG pathway is defective in *crd1Δ*?

As described in Chapter 3, loss of CL leads to decreased Hog1p phosphorylation without perturbing activated Hog1p translocation. However, it is not known if decreased Hog1p phosphorylation is due to perturbation of the SHO1 or SLN1 branch, or perhaps to both.

If loss of CL leads to defective SHO1 signaling, downregulating SLN1 signaling

will exacerbate decreased Hog1p activation in *crd1Δ.* In this situation, with 0.5 M NaCl, *crd1Δssk1Δ* (*SSK1* is required for SLN1 signaling) should have less Hog1p activation than *crd1Δ*, while *crd1Δsho1Δ* should have comparable Hog1p activation with *crd1Δ*. If loss of CL leads to defective SLN1 signaling, downregulating SHO1 signaling will exacerbate the decreased Hog1p activation in *crd1Δ.* In this situation, with 0.5 M NaCl, *crd1Δsho1Δ* should have less Hog1p activation than *crd1Δ*, while *crd1Δssk1Δ* should have comparable Hog1p activation with *crd1Δ*. However, if CL is required for activation of both branches, then the Hog1p activation in both *crd1Δsho1Δ* and *crd1Δssk1Δ* will be less than that of *crd1Δ*.

In summary, comparing Hog1p activation in *crd1Δ*, *crd1Δsho1Δ* and *crd1Δssk1Δ* by Western blot should help to identify which HOG branch is defective in *crd1Δ*.

3. How does sorbitol rescue *crd1Δ* growth and vacuole defects?

A previous study in our lab showed that 1 M sorbitol restores both growth and vacuole defects in *crd1Δ* by a mechanism not yet identified (Chen et al., 2008b). As shown in Fig. 4.1, 1 M sorbitol upregulates the HOG pathway at 39˚C, which might be the mechanism underlying rescue of *crd1Δ* temperature sensitivity and vacuole defects by sorbitol. However, the possibility that 1 M sorbitol restores the defects of *crd1Δ* via stimulating other osmotic regulatory pathways is not excluded. To address this question, my previous labmate Shuliang Chen and I carried out a targeted screen of osmotic regulatory mutants to identify those that abrogated sorbitol-mediated rescue of *crd1Δ*. Double mutants of *CRD1* and the genes shown in Table 4.1 were constructed.

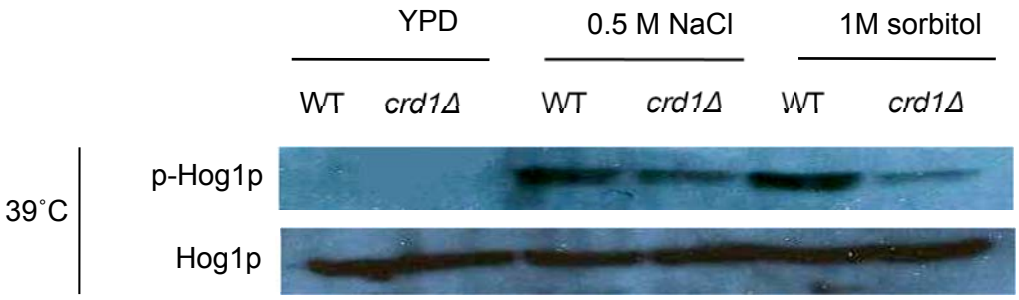

Fig. 4.1 1 M sorbitol induces Hog1p activation in *crd1Δ* at elevated temperature. Cells were pre-cultured in YPD at 30˚C to mid-log phase and switched to 39˚C for 5 min and at the same time treated with either 0.5 M NaCl (positive control) or 1 M sorbitol. The dually phosphorylated Hog1p and total Hog1p proteins were detected by Western blot, as described previously (Zhou et al., 2009).

Failure of sorbitol to rescue the double mutant indicated that the query gene is required for sorbitol-mediated rescue of *crd1Δ*.

A search of the *Saccharomyces* Genome Database identified 57 nonessential genes that are involved in the HOG or other osmotic stress pathways (Table 4.1). A targeted synthetic genetic array (SGA) was performed as described (Zhou et al., 2009). Single mutants of the stress response genes were mated with *crd1Δ*, diploids were sporulated, and progeny containing mutations in both *CRD1* and each of the query genes were selected by geneticin resistance (mutation of the query gene) and uracil prototrophy (*CRD1* mutation). Double mutants were confirmed by PCR.

Four of the double mutants were tested, including *crd1Δanp1Δ*, *crd1Δptc7Δ*, *crd1Δosm1Δ* and *crd1Δdog2Δ*. All were rescued by 1 M sorbitol at elevated temperature (Fig.4.2). This indicates that the corresponding genes are not required for sorbitol rescue. 53 double mutants remain to be tested. The screen for double mutants that cannot grow on YPD or YPD supplemented with 1 M sorbitol at elevated temperature is an interesting direction to pursue in future studies.

4. What is the mechanism underlying the vacuole defects in *crd1Δ* ?

A previous study in our lab found that, at elevated temperature, CL mutants exhibit enlarged vacuoles and loss of vacuole acidification (Chen et al., 2008b). The observed decrease in V-ATPase activity and proton pumping in *crd1Δ* may explain the loss of acidification of the vacuole. However, the mechanism underlying the enlarged vacuole morphology remains unknown. The following studies aimed to address the

Table 4.1. Deletion strains used in the mini SGA

Standard name	Standard name	Standard name
YHR078W	*SSK2*	*POR1*
HKR1	*VAC7*	*YPR1*
NBP2	*PTC2*	*PTC7*
GRE1	*PBS2*	*HSP12*
PTC1	*GRE2*	*PPZ2*
IZH2	*SSK1*	*PPZ1*
OSM1	*NHX1*	*YML131W*
ANP1	*FIG4*	*PTC3*
MSN1	*GON7*	*ZNF1*
GLO1	*GRE3*	*DOG2*
RVS161	*GPD1*	*MSB2*
SKN7	*YNL190W*	*POR2*
STE50	*PAI3*	*HOT1*
SHO1	*AGP2*	*AQY2*
MPC3	*PTP3*	*RVS167*
PCK2	*PTP2*	*STE11*
SIP18	*HIR1*	*YAR1*
SMP1	*RRD2*	*STL1*
SKO1	*YJL144W*	*GPP1*

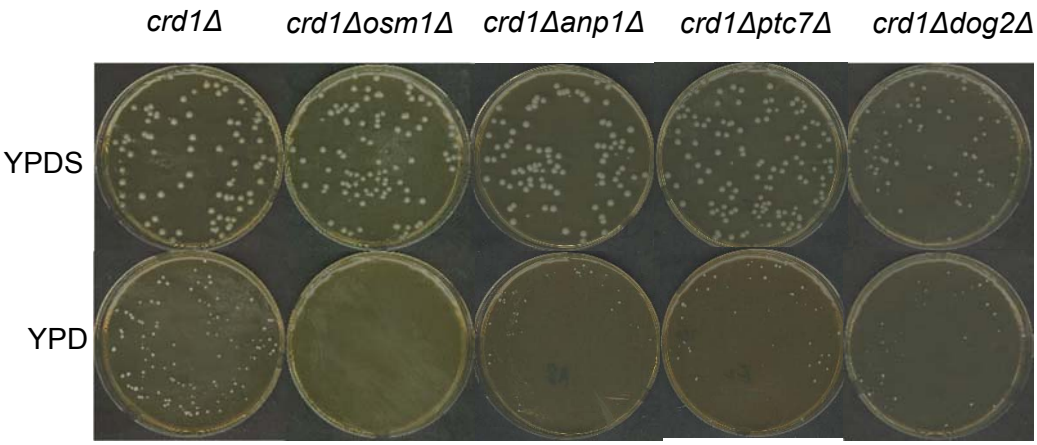

Fig. 4.2 Deletion of *ANP1*, *PTC7*, *OSM1* or *DOG2* does not abrogate the rescue of *crd1Δ* temperature sensitivity by sorbitol. Cells were pre-cultured in liquid YPD at 30˚C to the mid-log phase. Approximately 200 cells of each strain were plated on YPD or YPDS plates and incubated at 39.5°C for 3 days.

potential mechanism of vacuole morphology defects in *crd1Δ.*

4.1 Increased nonselective autophagy may not be the cause of vacuole enlargement

As described in Chapter 2, elevated temperature triggers increased expression of the general autophagy gene, *ATG8*, in both *crd1Δ* and WT (Fig. 2.6). In addition, at 39°C, *ATG8* expression is two-fold greater in *crd1Δ* than in WT. Although mitophagy is defective in *crd1Δ*, nonselective autophagy may not be affected, as discussed in Chapter 2. Because autophagy is the source of a large influx of lipid membrane and cellular contents to the vacuole (Baba M et al., 1994; Baba et al., 1995; Takeshige K et al., 1992)**,** it is reasonable to speculate that increased nonselective autophagy may be the cause of vacuole enlargement in *crd1Δ*.

If enlargement of the vacuole in *crd1Δ* at elevated temperature is due to increased nonselective autophagy, deletion of the nonselective autophagy genes should rescue the vacuole morphology defect of *crd1Δ*. To address this possibility, the effect of deleting nonselective autophagy genes on vacuole morphology of *crd1Δ* cells was determined. As seen in Fig. 4.3, *crd1Δatg8Δ* exhibited enlarged vacuoles similar to *crd1Δ*, indicating that blocking nonselective autophagy does not rescue the vacuole enlargement triggered by elevated temperature in *crd1Δ*.

In addition, if increased nonselective autophagy causes vacuole enlargement, triggering nonselective autophagy should lead to enlarged vacuoles in WT and *crd1Δ* at optimal temperature. To address this hypothesis, rapamycin, a stimulant of

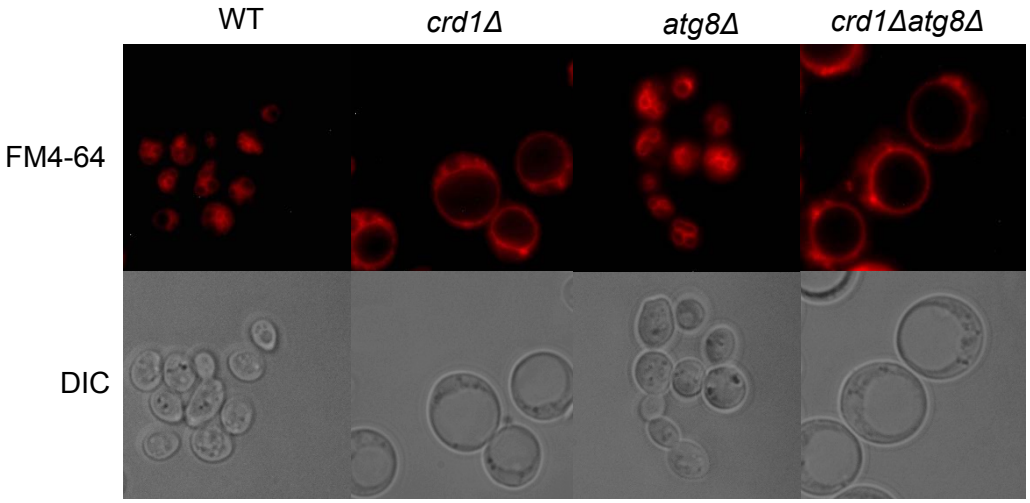

Fig. 4.3 Deletion of *ATG8* does not rescue the vacuole enlargement triggered by elevated temperature in *crd1Δ*. Cells were pre-cultured at 30 ℃ to the early log phase and then transferred to 37℃ at a starting A_{550} of 0.5 for 8h. FM4-64 staining was performed and cells were observed using fluorescence microscopy for vacuole morphology.

nonselective autophagy, was used to trigger nonselective autophagy in WT and *crd1Δ* at 30°C. FM 4-64 staining was performed to observe vacuole morphology. As seen in Fig. 4.4, both *crd1Δ* and WT exhibited enlarged vacuoles, raising the possibility that nonselective autophagy triggered by rapamycin results in enlarged vacuoles in even WT. However, rapamycin has downstream effects other than autophagy. If the vacuole enlargement triggered by rapamycin in *crd1Δ* and WT was due to increased nonselective autophagy, but not to other downstream effects of rapamycin, deletion of the nonselective autophagy genes in these strains should rescue vacuole morphology. However, with rapamycin, *atg8Δ* and *crd1Δatg8Δ* exhibited enlarged vacuoles similar to that in *crd1Δ* and WT, indicating that blocking autophagy does not rescue vacuole enlargement triggered by rapamycin. Thus, the vacuole enlargement induced by rapamycin is probably not due to increased nonselective autophagy. In addition to triggering nonselective autophagy via the TOR1 pathway (Li et al., 2012; Yorimitsu et al., 2007), rapamycin may be involved in other cellular processes that regulate vacuole size.

4.2 Is the vacuole defect caused by perturbation of the FAB pathway in *crd1Δ* ?

The FAB pathway regulates the synthesis of phosphatidylinositol 3-phosphate (PI3P) and phosphatidylinositol 3,5-bisphosphate ($PI(3,5)P_2$), which affects the size and acidification of the vacuole. Interestingly, the *fab1Δ* mutant, in which $PI(3,5)P_2$ is undetectable, displays growth and vacuole defects that are similar to those in *crd1Δ*, including decreased growth at elevated temperature, vacuole enlargement and loss of

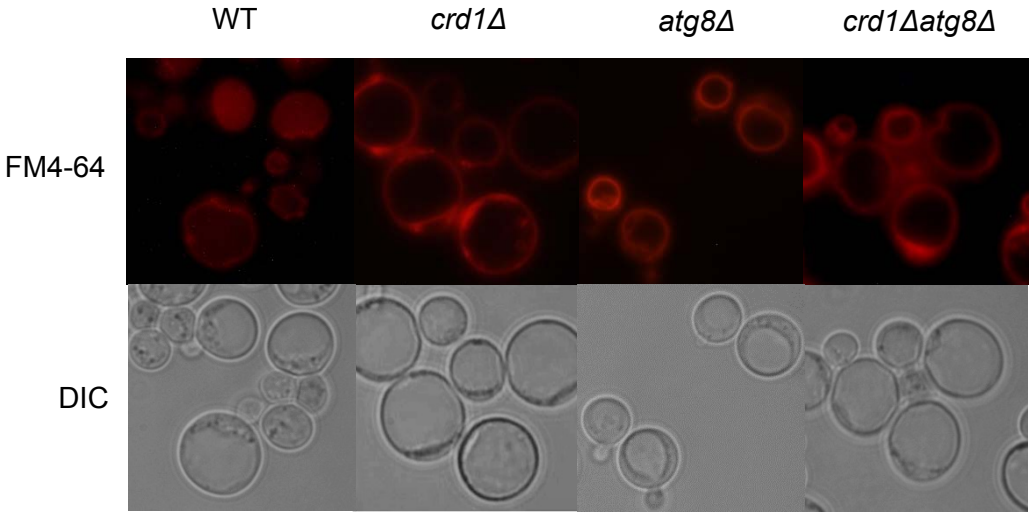

Fig. 4.4 Rapamycin triggers enlargement of vacuoles in both WT and *crd1Δ*, which is not rescued by deletion of *ATG8*. Cells were pre-cultured at 30 ℃ to the early log phase and then transferred to medium containing 10nM rapamycin at a starting A_{550} of 0.5 for 8h. FM4-64 staining was performed and cells were observed using fluorescence microscopy for vacuole morphology.

vacuole acidification (Bonangelino et al., 2002; Gary et al., 1998; Yamamoto et al., 1995). Thus, Chen et al. suggested that perturbation of the FAB pathway in CL deficient cells may explain the vacuole defects. Chen determined that mRNA levels of the FAB pathway genes were not affected in *crd1Δ* cells (Chen et al., 2008b). However, *FAB1* is not transcriptionally regulated (Gary et al., 1998). Therefore, non-transcriptional regulation of the FAB pathway may be defective in *crd1Δ*. Further studies are necessary to address this possibility.

4.2.1 The FAB pathway

As shown in Fig. 4.5, the first step of the FAB pathway is the synthesis of PI3P from PI, catalyzed by phosphatidylinositol (PI) 3-kinase, Vps34p (Auger et al., 1989; Slessareva et al., 2006). Fab1p, which localizes to the vacuole membrane, catalyzes the second step, converting vacuolar PI3P to PI(3,5)P_2 (Dove et al., 2002; Gary et al., 1998; Yamamoto et al., 1995). The reverse reaction to dephosphorylate PI(3,5)P_2 to PI3P is catalyzed by PI(3,5)P_2 phosphatase, Fig4p (Rudge et al., 2004), which is also needed for maximum function of Fab1p (Duex et al., 2006). Fab1p can be activated by Vac7p and Vac14p (Bonangelino et al., 1997; Duex et al., 2006; Gary et al., 2002), the latter of which is physically associated with Fig4p (Duex et al., 2006). Atg18p negatively regulates Vac7p (Efe et al., 2005). This regulatory pathway controls levels of PI(3,5)P_2, which affect vacuole size and acidification. It is known that hyperosmotic stress leads to increased PI(3,5)P_2, resulting in shrunken and fragmented vacuoles (Bonangelino et al., 2002; Dove et al., 1997), while loss of PI(3,5)P_2 by deletion of

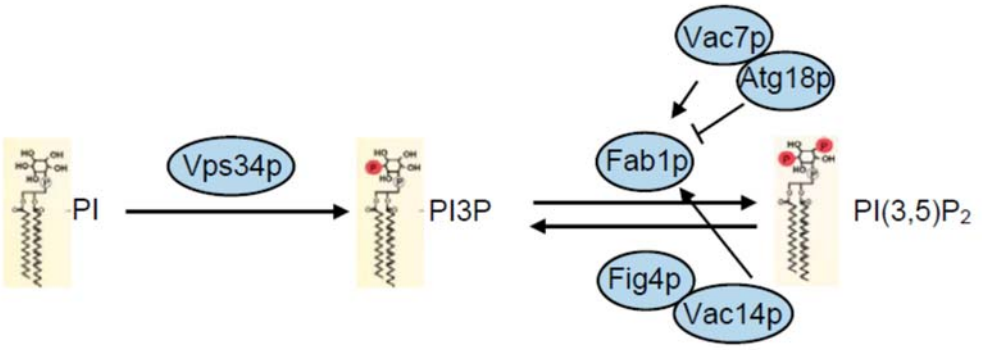

Fig. 4.5 The FAB pathway and its regulation. Revised from Efe et al., 2005.

FAB1 leads to enlarged vacuoles (Gary et al., 1998; Odorizzi et al., 1998).

4.2.2 Is the FAB pathway perturbed in *crd1Δ* ?

To determine if there is perturbation of the FAB pathway in *crd1Δ*, I assessed genetic interaction between *crd1Δ* and *fig4Δ*, because Fig4p is essential for both synthesis and turn over of PI(3,5)P_2. If the FAB pathway in *crd1Δ* is perturbed, no matter whether there is altered synthesis of PI(3,5)P_2, or altered turn-over of PI(3,5)P_2, I should see genetic interaction between *FIG4* and *CRD1*. The ability of single cells to form colonies was observed, using our lab generated *crd1Δfig4Δ*, *fig4Δ*, *crd1Δ* and WT strains in the FGY background. As shown in Fig. 4.6, deletion of *FIG4* partially rescued the *crd1Δ* growth defect at 37.5°C, suggesting that the FAB pathway may be perturbed in *crd1Δ*. Levels of PI(3,5)P_2 may be decreased, and deletion of FIG4 may rescue the growth defects of *crd1Δ* by blocking the dephosphorylation of PI(3,5)P_2.

4.2.3 PI3P and PI(3,5)P_2 are localized normally on the vacuole membrane of *crd1Δ*.

The findings described in section 4.2.2 provided a clue that the growth and vacuole defects in *crd1Δ* may be due to perturbation of the FAB pathway. Thus, it was necessary to determine if PI3P and PI(3,5)P_2 on the vacuole membrane of *crd1Δ* are decreased.

To directly observe if there is loss of PI3P or PI(3,5)P_2 on the vacuole membrane, both *crd1Δ* and WT cells were transformed with the pRS415-GFP-FYVE and pRS415-GFP-*ATG18* plasmids (kindly provided by Rania Deranieh), while *fab1Δ* containing the

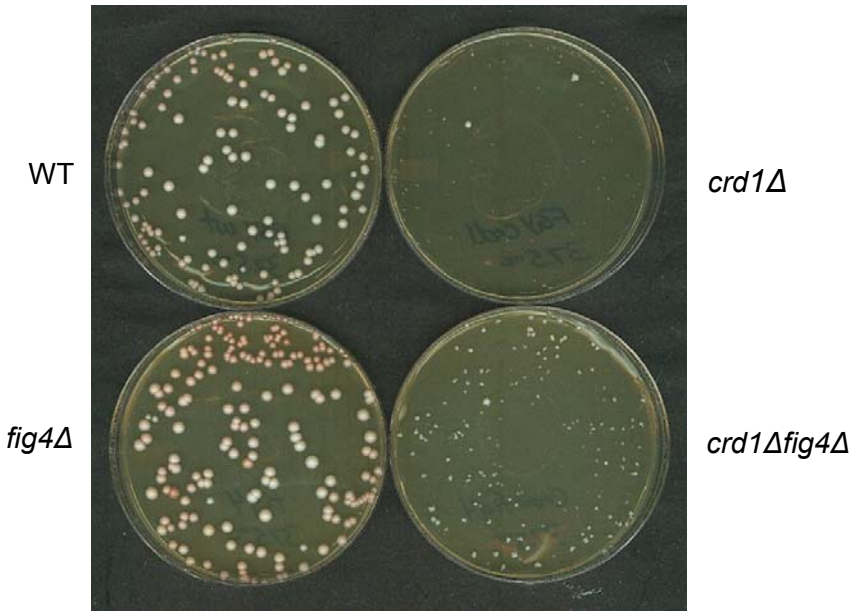

Fig. 4.6 Deletion of *FIG4* partially rescues *crd1Δ* temperature sensitivity. Cells were pre-cultured in liquid YPD at 30˚C to the mid-log phase. Approximately 200 cells of each strain were plated on YPD plates and incubated at 37.5°C for 3 days.

pRS415-GFP-*ATG18* plasmid (kindly provided by Rania Deranieh) was used as a negative control. The pRS415-GFP-FYVE plasmid expresses a protein in which GFP is fused to the FYVE zinc finger domain. Binding of the FYVE domain of this probe to PI3P enables the monitoring of PI3P intracellular localization. The pRS415-GFP-*ATG18* plasmid expresses a PI(3,5)P_2 specific fluorescent lipid-associated reporter (FLARE), on which GFP is fused to the PI(3,5)P_2 binding domain of Atg18p. At elevated temperature, PI3P and PI(3,5)P_2 vacuolar localization in *crd1Δ* was similar to that of WT (Fig 4.7). In contrast, there is a loss of PI(3,5)P_2 on the vacuole membrane in *fab1Δ* (Fig 4.8), suggesting that loss of vacuolar PI(3,5)P_2 may be the cause of the vacuole defects in *fab1Δ* but not *crd1Δ*. However, normal PI3P and PI(3,5)P_2 vacuole localization does not exclude the possibility that PI(3,5)P_2 levels are slightly decreased in *crd1Δ*, which would not be discernible by comparison of fluorescence intensity. Analysis of PI3P and PI(3,5)P_2 levels by HPLC would be required to conclusively show altered FAB pathway function.

4.2.4 Are protein levels of the FAB pathway regulators altered in *crd1Δ* ?

Although overexpression of *FAB1* did not increase PI(3,5)P_2 levels (Gary et al., 1998), overexpression of *FAB1* suppressed the vacuole defects in *vac14Δ* (Dove et al., 2002). This finding suggests that, other than regulating synthesis of PI(3,5)P_2, Fab1p also directly controls vacuole size and acidification by a mechanism still unkown. Thus, the protein levels of the FAB pathway regulators are also important for vacuole morphology and acidification. Although Chen showed that the mRNA levels of *FAB1*,

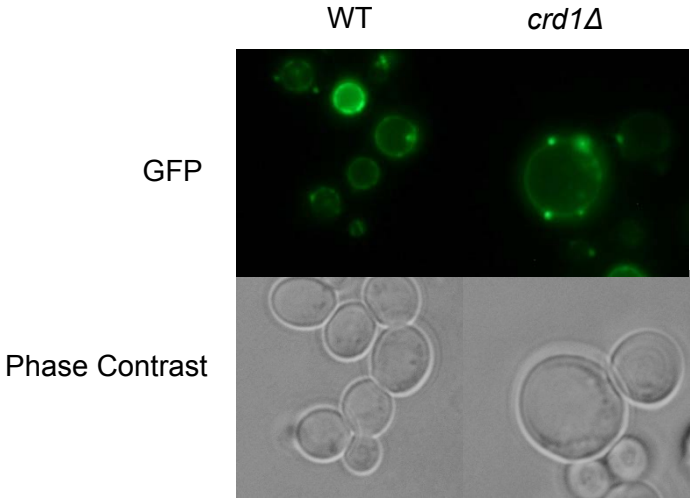

Fig. 4.7 *crd1Δ* exhibits normal PI3P localization at the vacuolar membrane. Cells were pre-cultured at 30 ℃ to the early log phase and then transferred to 37℃ at a starting A_{550} of 0.5 for 8h. PI3P localization was then observed using fluorescence microscopy.

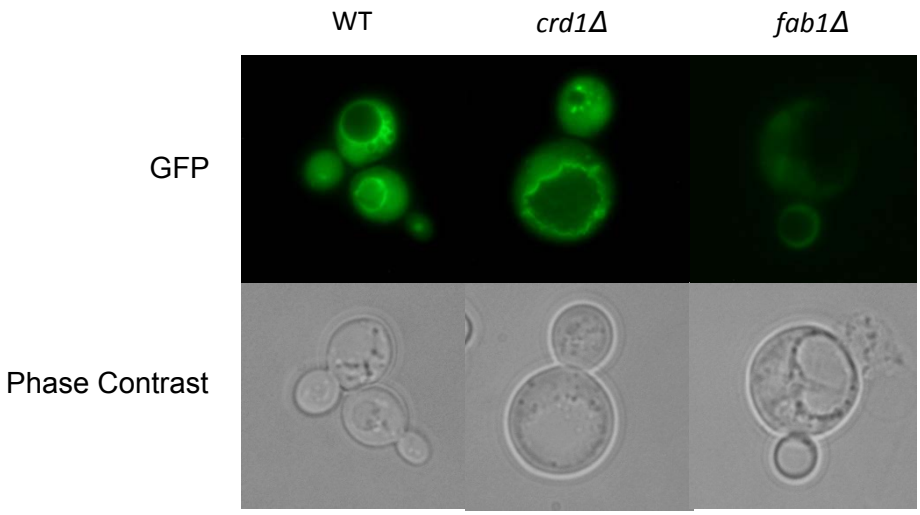

Fig. 4.8 Normal vacuolar localization of PI(3,5)P_2 in *crd1Δ*. Cells were pre-cultured at 30℃ to the early log phase and then transferred to 37℃ at a starting A_{550} of 0.5 for 8h. Cells were then observed using fluorescence microscopy to determine PI(3,5)P_2 localization.

VAC7, *VAC14*, *VPS15*, *VPS34*, *FIG4*, and *ATG18* were not affected in *crd1Δ* cells, the protein levels were not examined (Chen et al., 2008b).

The optimal way to address this question is to detect the protein levels of these regulators by Western blot. However, primary antibodies against these proteins are not commercially available. Thus, I employed an indirect approach to address this question. If overexpression of *FAB1* or *VAC7* suppresses the vacuole defects in *crd1Δ*, it suggests that Fab1p or Vac7p protein levels may be decreased in the mutant, which may account for the vacuole defects. *crd1Δ* in the BY4742 background was transformed with vectors expressing either *FAB1* or *VAC7* (or empty pYPGK18 vector as a negative control), plated on leu^- plates, and incubated at 30ºC or 38ºC. The ability of single cells to form colonies was observed. Overexpression of *FAB1* and *VAC7* in *crd1Δ* did not rescue the growth defects of *crd1Δ* (Fig 4.9), indicating that Fab1p and Vac7p protein levels may be unaltered in *crd1Δ*. However, it is possible that there is targeted degradation of the *FAB1* and *VAC7* mRNA in *crd1Δ*, resulting in not only degradation of endogenous *FAB1* and *VAC7* mRNA, but also *FAB1* and *VAC7* mRNA that is expressed from the overexpression vector.

To definitively ascertain if protein levels of FAB pathway regulators are altered in CL deficient cells, Western blot detections of these proteins are required. Because the primary antibodies against these proteins are not commercially available, an alternative approach is to tag each FAB pathway regulator with the hemagglutinin (HA) tag to enable the detection of these proteins by Western blot.

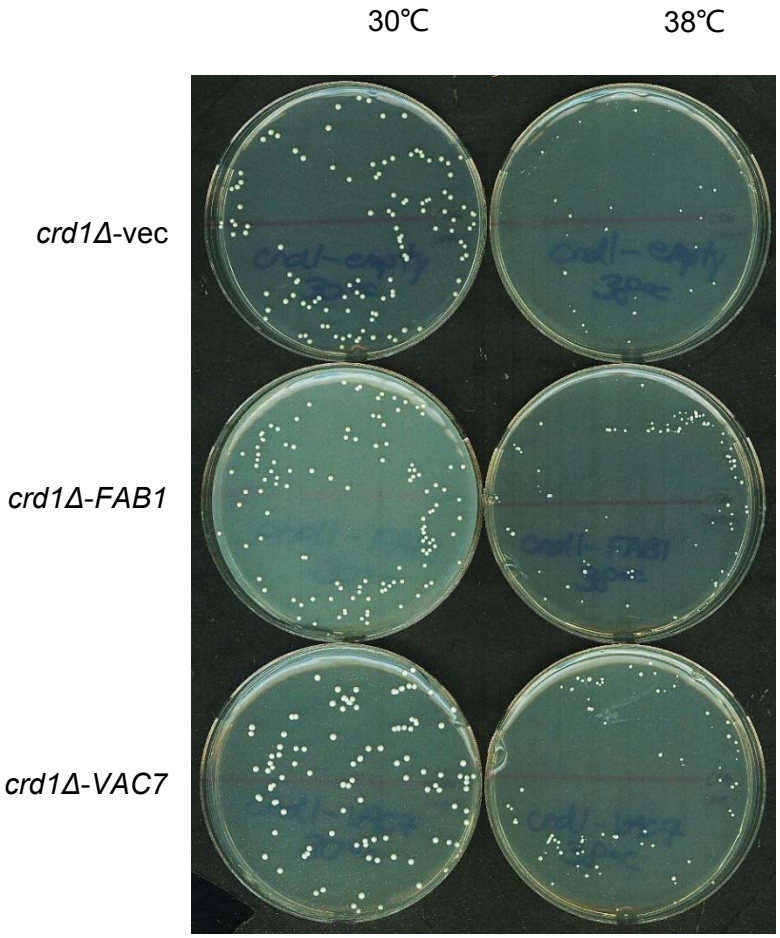

crd1Δ-vec

crd1Δ-FAB1

crd1Δ-VAC7

Fig. 4.9 Overexpression of *FAB1* and *VAC7* does not rescue *crd1Δ* temperature sensitivity. Cells were pre-cultured in liquid SC leu$^-$ at 30˚C to the mid-log phase. Approximately 200 cells of each strain were plated on SC leu$^-$ plates and incubated at 38°C for 3 days.

4.3 Are the vacuole defects in *crd1Δ* caused by perturbation of the Ena1 Na^+-ATPase exporter?

Vacuole size and acidification are regulated by $PI(3,5)P_2$, as well as ion pumps and channels presented in the vacuole membrane. These include the H^+-Ca^{2+} exchanger Vcx1p, the Ca^{2+} pump Pmc1p, the Ca^{2+} channel Yvc1p, the H^+-Na^+ exchanger Nhx1p, and the voltage-sensitive Cl^- channel Gef1p (Bonilla and Cunningham, 2002; Ke et al., 2013; Li and Kane, 2009). Deletion of *NHX1*, but not the genes encoding the other pumps or channels, suppresses vacuole defects and temperature sensitivity of *crd1Δ* (Chen et al., 2008b). There is defective vacuolar V-ATPase activity and reduced proton transport in *crd1Δ*, causing decreased intra-vacuolar H^+ levels (Chen et al., 2008b). Deletion of *NHX1* blocks the vacuolar efflux of H^+ and influx of Na^+, which may counteract the decreased vacuolar H^+ level. However, the mechanism whereby deletion of *NHX1* rescues the vacuole morphology remains to be elucidated.

Because deletion of *NHX1* blocks the influx of Na^+ into the vacuole, it is reasonable to speculate that there may be excessive Na^+ in the vacuole of *crd1Δ*. Na^+ is sequestered in the vacuole when intracellular Na^+ levels are increased (Li et al., 2012). If there is excessive intra-vacuolar Na^+ in *crd1Δ*, it may indicate increased intracellular Na^+ in this strain.

The amount of intracellular Na^+ in *Saccharomyces cerevisiae* is tightly *regulated* by activity of the ion pumps and channels on the cell membrane. The cell membrane influx of Na^+ is mainly induced by the Na^+-K^+ transporter Trk system and the non-

specific cation channel Nsc1. Conversely, the efflux of Na^+ is induced by the Na^+/K^+-ATPase Ena1p and the Na^+, K^+/H^+ antiporter Nha1p (Ke et al., 2013). Although Ena1p and Nha1p are both involved in cell Na^+ efflux, Nha1p plays a larger role in K^+ extrusion and cell survival under acidic conditions, while Ena1p is more involved in Na^+ extrusion and cell survival under alkaline conditions (Jung et al., 2012). In WT cells, heat shock stimulates activity of the Na^+-K^+ pump (the Trk system) without affecting intracellular Na^+ levels (Boonstra et al., 1984), suggesting that the efflux of Na^+ may be upregulated to counteract stimulation of the Na^+-K^+ pump at elevated temperature. Thus, Na^+ efflux is essential for cell survival under heat stress.

4.3.1 Deletion of *ENA1* does not exacerbate *crd1Δ* temperature sensitivity

I hypothesized that Na^+ efflux is defective in *crd1Δ* at 39˚C, resulting in increased intracellular Na^+. To alleviate toxicity caused by increased intracellular Na^+, vacuolar Na^+ influx is increased, resulting in increased osmotic pressure and vacuole enlargement. To test my hypothesis, I investigated if there is genetic interaction between *CRD1* and *ENA1*, which encodes the major Na^+ efflux transporter. Synthetic lethality would suggest that Ena1p is defective in *crd1Δ.* A *crd1Δena1Δ* double mutant was constructed by tetrad dissection and examined for temperature sensitivity. Deletion of *ENA1* did not exacerbate *crd1Δ* temperature sensitivity (Fig. 4.10), suggesting that Ena1p may not be defective in *crd1Δ.*

4.3.2 Upregulation of *ENA1* expression may be partially impaired in *crd1Δ*

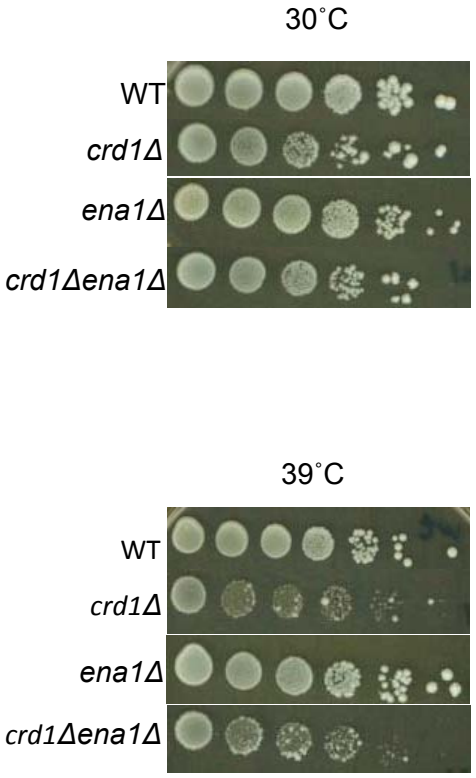

Fig. 4.10 Deletion of *ENA1* does not affect *crd1Δ* temperature sensitivity. Cells were pre-cultured in liquid YPD at 30˚C to the mid-log phase. Aliquots were adjusted to $2x10^8$ cells/ml and then diluted in a 10X serial dilution. Cells were spotted on YPD plates with the most diluted spot containing 2000 cells, and the plates were incubated at 30˚C or 39˚C for 2 days.

Ena1p is regulated at the transcriptional level (Ke et al., 2013; Márquez JA and R., 1996; Platara et al., 2006). To determine if there is defective Na^+ efflux in *crd1Δ* at 39˚C, it is necessary to determine if *ENA1* gene expression is decreased in *crd1Δ* compared to WT at 39˚C. This would suggest that Na^+ efflux will be decreased, leading to increased intracellular Na^+. WT and *crd1Δ* cells were incubated at either 30˚C or 39˚C for 2 hours. *ENA1* expression in these strains was determined by RT-PCR. At 39˚C, *ENA1* expression was upregulated in both WT and *crd1Δ.* However, upregulation of *ENA1* expression in *crd1Δ* was less than in WT (Fig. 4.11), suggesting that upregulation of *ENA1* expression may be partially impaired in *crd1Δ* at elevated temperature. Impaired *ENA1* upregulation may lead to inadequate Na^+ efflux and accumulation of intracellular Na^+, leading to vacuole enlargement.

4.3.3 Overexpression of *ENA1* does not rescue *crd1Δ* temperature sensitivity

As seen in Fig.4.11, there may be impaired upregulation of *ENA1* in *crd1Δ* at 39˚C. I then determined if overexpression of *ENA1* rescues *crd1Δ*. *crd1Δ* was transformed with a vector (pYPGK18) overexpressing *ENA1*, spotted on the leu^- plates and incubated at 30˚C or 39˚C. Overexpression of *ENA1* did not affect *crd1Δ* temperature sensitivity (Fig. 4.12), indicating that the growth and vacuole defects in *crd1Δ* at elevated temperature are probably not due to impaired upregulation of *ENA1* in *crd1Δ*.

The findings in Section 4.3.2 and 4.3.3 are controversial. To conclusively address if there is increased intracellular Na^+, the total Na^+ level in *crd1Δ* at 39˚C should be

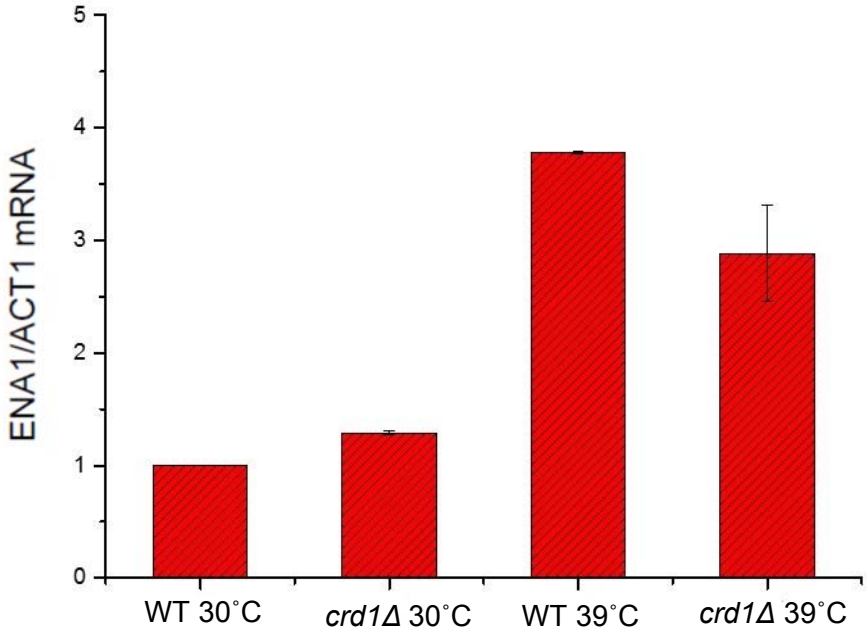

Fig. 4.11 Inadequate *ENA1* upregulation in *crd1Δ* compared to WT, at elevated temperature. WT and *crd1Δ* cells were cultured in YPD medium to the mid-log phase at 30˚C and then incubated at either 30˚C or 39˚C for 2 hours. *ENA1* expression was determined by RT-PCR.

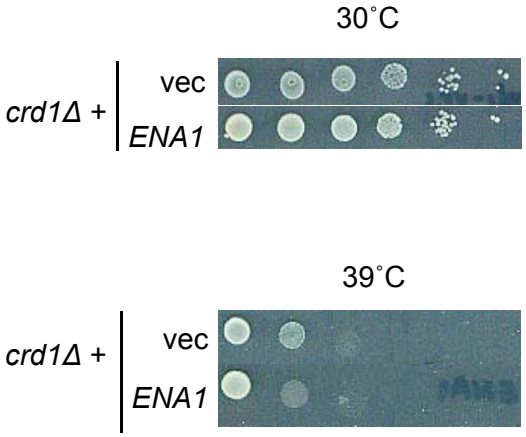

Fig. 4.12 Overexpression of *ENA1* does not rescue *crd1Δ* temperature sensitivity. Cells were pre-cultured in liquid SC leu$^-$ at 30˚C to the mid-log phase. Aliquots were adjusted to 2x10^8 cells/ml and then diluted in a 10X serial dilution. Cells were spotted on YPD plates with the most diluted spot containing 2000 cells, and the plates were incubated at 30˚C or 39˚C for 2 days.

directly measured by isotachophoresis (Nakamura et al., 1993), an analytical chemistry technique used for quantification of ionic analytes.

5. Summary

In this chapter, I suggest future experiments to elucidate how CL regulates mitophagy and MAPK pathways. In addition, experiments to investigate the role of CL in vacuole homeostasis were described, and future directions related to this work have been proposed. Much about CL remains to be elucidated. I encourage my junior labmates to continue to explore the mystery of how CL contributes to human life and health.

REFERENCES

Aoki, Y., T. Kanki, Y. Hirota, Y. Kurihara, T. Saigusa, T. Uchiumi, and D. Kang. 2011. Phosphorylation of Serine 114 on Atg32 mediates mitophagy. *Molecular Biology of the Cell*. 22:3206-3217.

Auger, K.R., C.L. Carpenter, L.C. Cantley, and L. Varticovski. 1989. Phosphatidylinositol 3-kinase and its novel product, phosphatidylinositol 3-phosphate, are present in Saccharomyces cerevisiae. *Journal of Biological Chemistry*. 264:20181-20184.

Baba M, Takeshige K, Baba N, and O. Y. 1994. Ultrastructural analysis of the autophagic process in yeast: detection of autophagosomes and their characterization. *The Journal of Cell Biology*. 124:903-913.

Baba, M., M. Osumi, and Y. Ohsumi. 1995. Anaysis of the Membrane Structures Involved in Autophagy in Yeast by Freeze-Replica Method. *Cell Structure and Function*. 20:465-471.

Backues, S.K., M.A. Lynch-Day, and D.J. Klionsky. 2012. The Ume6-Sin3-Rpd3 complex regulates ATG8 transcription to control autophagosome size. *Autophagy*. 8:1835-1836.

Baile, M.G., M. Sathappa, Y.-W. Lu, E. Pryce, K. Whited, J.M. McCaffery, X. Han, N.N. Alder, and S.M. Claypool. 2014. Unremodeled and Remodeled Cardiolipin Are Functionally Indistinguishable in Yeast. *The Journal of Biological Chemistry*. 289:1768-1778.

Baile, M.G., K. Whited, and S.M. Claypool. 2013. Deacylation on the matrix side of

the mitochondrial inner membrane regulates cardiolipin remodeling. *Molecular Biology of the Cell*. 24:2008-2020.

Barth PG, Scholte HR, Berden JA, Van der Klei-Van Moorsel JM, Luyt-Houwen IE, Van 't Veer-Korthof ET, Van der Harten JJ, and S.-P. MA. 1983. An X-linked mitochondrial disease affecting cardiac muscle, skeletal muscle and neutrophil leucocytes. *Journal of the Neurological Sciences*. 62.

Barth, P.G., R.J. Wanders, and P. Vreken. 1999. X-linked cardioskeletal myopathy and neutropenia (Barth syndrome)-MIM 302060. *The Journal of pediatrics*. 135:273-276.

Beranek, A., G. Rechberger, H. Knauer, H. Wolinski, S.D. Kohlwein, and R. Leber. 2009. Identification of a Cardiolipin-specific Phospholipase Encoded by the Gene CLD1 (YGR110W) in Yeast. *The Journal of Biological Chemistry*. 284:11572-11578.

Beyer K, and K. M. 1985. ADP/ATP carrier protein from beef heart mitochondria has high amounts of tightly bound cardiolipin, as revealed by 31P nuclear magnetic resonance. *Biochemistry*. 24:3821-3826.

Bione, S., P. D'Adamo, E. Maestrini, A.K. Gedeon, P.A. Bolhuis, and D. Toniolo. 1996. A novel X-linked gene, G4.5. is responsible for Barth syndrome. *Nat Genet*. 12:385-389.

Bochkov, V.N., O.V. Oskolkova, K.G. Birukov, A.-L. Levonen, C.J. Binder, and J. Stöckl. 2010. Generation and Biological Activities of Oxidized Phospholipids. *Antioxidants & Redox Signaling*. 12:1009-1059.

Bonangelino, C.J., N.L. Catlett, and L.S. Weisman. 1997. Vac7p, a novel vacuolar protein, is required for normal vacuole inheritance and morphology. *Molecular and Cellular Biology*. 17:6847-6858.

Bonangelino, C.J., J.J. Nau, J.E. Duex, M. Brinkman, A.E. Wurmser, J.D. Gary, S.D. Emr, and L.S. Weisman. 2002. Osmotic stress–induced increase of phosphatidylinositol 3,5-bisphosphate requires Vac14p, an activator of the lipid kinase Fab1p. *The Journal of Cell Biology*. 156:1015-1028.

Bonilla, M., and K.W. Cunningham. 2002. Calcium Release and Influx in Yeast: TRPC and VGCC Rule Another Kingdom. pe17-pe17 pp.

Boonstra, J., D.H.J. Schamhart, S.W. de Laat, and R. van Wijk. 1984. Analysis of K+ and Na+ Transport and Intracellular Contents during and after Heat Shock and Their Role in Protein Synthesis in Rat Hepatoma Cells. *Cancer Research*. 44:955-960.

Buckland, A.G., A.R. Kinkaid, and D.C. Wilton. 1998. Cardiolipin hydrolysis by human phospholipases A2: The multiple enzymatic activities of human cytosolic phospholipase A2. *Biochimica et Biophysica Acta (BBA) - Lipids and Lipid Metabolism*. 1390:65-72.

Budovskaya, Y.V., J.S. Stephan, F. Reggiori, D.J. Klionsky, and P.K. Herman. 2004. The Ras/cAMP-dependent Protein Kinase Signaling Pathway Regulates an Early Step of the Autophagy Process in Saccharomyces cerevisiae. *The Journal of biological chemistry*. 279:20663-20671.

Camougrand, N., A. Grelaud-Coq, E. Marza, M. Priault, J.-J. Bessoule, and S.

Manon. 2003. The product of the UTH1 gene, required for Bax-induced cell death in yeast, is involved in the response to rapamycin. *Molecular Microbiology*. 47:495-506.

Cao, J., Y. Liu, J. Lockwood, P. Burn, and Y. Shi. 2004. A Novel Cardiolipin-remodeling Pathway Revealed by a Gene Encoding an Endoplasmic Reticulum-associated Acyl-CoA:Lysocardiolipin Acyltransferase (ALCAT1) in Mouse. *Journal of Biological Chemistry*. 279:31727-31734.

Carden, D.L., and D.N. Granger. 2000. Pathophysiology of ischaemia–reperfusion injury. *The Journal of Pathology*. 190:255-266.

Chang, S.-C., P.N. Heacock, E. Mileykovskaya, D.R. Voelker, and W. Dowhan. 1998a. Isolation and Characterization of the Gene (CLS1) Encoding Cardiolipin Synthase in Saccharomyces cerevisiae. *Journal of Biological Chemistry*. 273:14933-14941.

Chang, S.C., P.N. Heacock, E. Mileykovskaya, D.R. Voelker, and W. Dowhan. 1998b. Isolation and characterization of the gene (CLS1) encoding cardiolipin synthase in Saccharomyces cerevisiae. *The Journal of biological chemistry*. 273:14933-14941.

Chatfield, K.C., G.C. Sparagna, C.C. Sucharov, S.D. Miyamoto, J.E. Grudis, R.D. Sobus, J. Hijmans, and B.L. Stauffer. Dysregulation of cardiolipin biosynthesis in pediatric heart failure. *Journal of Molecular and Cellular Cardiology*. 74:251-259.

Chen, D., X.-Y. Zhang, and Y. Shi. 2006. Identification and functional characterization

of hCLS1, a human cardiolipin synthase localized in mitochondria. *Biochemical Journal*. 398:169-176.

Chen, R., T. Tsuji, F. Ichida, K.R. Bowles, X. Yu, S. Watanabe, K. Hirono, S. Tsubata, Y. Hamamichi, J. Ohta, Y. Imai, N.E. Bowles, T. Miyawaki, J.A. Towbin, and c. Noncompaction study. 2002. Mutation analysis of the G4.5 gene in patients with isolated left ventricular noncompaction. *Molecular genetics and metabolism*. 77:319-325.

Chen, S., Q. He, and M.L. Greenberg. 2008a. Loss of tafazzin in yeast leads to increased oxidative stress during respiratory growth. *Molecular Microbiology*. 68:1061-1072.

Chen, S., D. Liu, R.L. Finley, and M.L. Greenberg. 2010. Loss of Mitochondrial DNA in the Yeast Cardiolipin Synthase crd1 Mutant Leads to Up-regulation of the Protein Kinase Swe1p That Regulates the G2/M Transition. *Journal of Biological Chemistry*. 285:10397-10407.

Chen, S., M. Tarsio, P.M. Kane, and M.L. Greenberg. 2008b. Cardiolipin Mediates Cross-Talk between Mitochondria and the Vacuole. *Molecular Biology of the Cell*. 19:5047-5058.

Cheng, H., D.J. Mancuso, X. Jiang, S. Guan, J. Yang, K. Yang, G. Sun, R.W. Gross, and X. Han. 2008. Shotgun Lipidomics Reveals the Temporally Dependent, Highly Diversified Cardiolipin Profile in the Mammalian Brain: Temporally Coordinated Postnatal Diversification of Cardiolipin Molecular Species with Neuronal Remodeling. *Biochemistry*. 47:5869-5880.

Conboy, M.J., and M.S. Cyert. 2000. Luv1p/Rki1p/Tcs3p/Vps54p, a Yeast Protein That Localizes to the Late Golgi and Early Endosome, Is Required for Normal Vacuolar Morphology. *Molecular Biology of the Cell*. 11:2429-2443.

D'Adamo, P., L. Fassone, A. Gedeon, E.A. Janssen, S. Bione, P.A. Bolhuis, P.G. Barth, M. Wilson, E. Haan, K.H. Orstavik, M.A. Patton, A.J. Green, E. Zammarchi, M.A. Donati, and D. Toniolo. 1997. The X-linked gene G4.5 is responsible for different infantile dilated cardiomyopathies. *American journal of human genetics*. 61:862-867.

D'Silva, P.D., B. Schilke, W. Walter, A. Andrew, and E.A. Craig. 2003. J protein cochaperone of the mitochondrial inner membrane required for protein import into the mitochondrial matrix. *Proceedings of the National Academy of Sciences*. 100:13839-13844.

Davey, K.M., J.S. Parboosingh, D.R. McLeod, A. Chan, R. Casey, P. Ferreira, F.F. Snyder, P.J. Bridge, and F.P. Bernier. 2006. Mutation of DNAJC19, a human homologue of yeast inner mitochondrial membrane co-chaperones, causes DCMA syndrome, a novel autosomal recessive Barth syndrome-like condition. *Journal of Medical Genetics*. 43:385-393.

De Bruijn, J.H. 1966. Chemical structure and serological activity of natural and synthetic cardiolipin and related compounds. *British Journal of Venereal Diseases*. 42:125-128.

Dennis, E.A., J. Cao, Y.-H. Hsu, V. Magrioti, and G. Kokotos. 2011. Phospholipase A(2) Enzymes: Physical Structure, Biological Function, Disease Implication,

Chemical Inhibition, and Therapeutic Intervention. *Chemical reviews*. 111:6130-6185.

Deprez, P., I. Baholet, S. Burlet, G. Lange, R. Amengual, B. Schoot, A. Vermond, E. Mandine, and D. Lesuisse. 2002. Discovery of highly potent Src SH2 binders: structure-activity studies and X-ray structures. *Bioorganic & medicinal chemistry letters*. 12:1291-1294.

Dove, S.K., F.T. Cooke, M.R. Douglas, L.G. Sayers, P.J. Parker, and R.H. Michell. 1997. Osmotic stress activates phosphatidylinositol-3,5-bisphosphate synthesis. *Nature*. 390:187-192.

Dove, S.K., R.K. McEwen, A. Mayes, D.C. Hughes, J.D. Beggs, and R.H. Michell. 2002. Vac14 Controls PtdIns(3,5)P2 Synthesis and Fab1-Dependent Protein Trafficking to the Multivesicular Body. *Current Biology*. 12:885-893.

Duex, J.E., F. Tang, and L.S. Weisman. 2006. The Vac14p–Fig4p complex acts independently of Vac7p and couples PI3,5P(2) synthesis and turnover. *The Journal of Cell Biology*. 172:693-704.

Efe, J.A., R.J. Botelho, and S.D. Emr. 2005. The Fab1 phosphatidylinositol kinase pathway in the regulation of vacuole morphology. *Current Opinion in Cell Biology*. 17:402-408.

Eilers, M., T. Endo, and G. Schatz. 1989. Adriamycin, a drug interacting with acidic phospholipids, blocks import of precursor proteins by isolated yeast mitochondria. *Journal of Biological Chemistry*. 264:2945-2950.

Endo, T., M. Eilers, and G. Schatz. 1989. Binding of a tightly folded artificial

mitochondrial precursor protein to the mitochondrial outer membrane involves a lipid-mediated conformational change. *Journal of Biological Chemistry*. 264:2951-2956.

Endo, T., and G. Schatz. 1988. Latent membrane perturbation activity of a mitochondrial precursor protein is exposed by unfolding. *The EMBO Journal*. 7:1153-1158.

Farré, J.-C., A. Burkenroad, S.F. Burnett, and S. Subramani. 2013. Phosphorylation of mitophagy and pexophagy receptors coordinates their interaction with Atg8 and Atg11. *EMBO Reports*. 14:441-449.

Ferrari, R., C. Ceconi, S. Curello, A. Cargnoni, E. Pasini, F. De Giuli, and A. Albertini. 1991. Role of oxygen free radicals in ischemic and reperfused myocardium. *The American Journal of Clinical Nutrition*. 53:215S-222S.

Ferrigno, P., F. Posas, D. Koepp, H. Saito, and P.A. Silver. 1998. Regulated nucleo/cytoplasmic exchange of HOG1 MAPK requires the importin beta homologs NMD5 and XPO1. *The EMBO Journal*. 17:5606-5614.

Fobker, M., R. Voss, H. Reinecke, C. Crone, G. Assmann, and M. Walter. 2001. Accumulation of cardiolipin and lysocardiolipin in fibroblasts from Tangier disease subjects. *FEBS Lett*. 500:157-162.

Frank, M., S. Duvezin-Caubet, S. Koob, A. Occhipinti, R. Jagasia, A. Petcherski, M.O. Ruonala, M. Priault, B. Salin, and A.S. Reichert. 2012. Mitophagy is triggered by mild oxidative stress in a mitochondrial fission dependent manner. *Biochimica et Biophysica Acta (BBA) - Molecular Cell Research*.

1823:2297-2310.

Fredrickson, D.S. 1964. The Inheritance of High Density Lipoprotein Deficiency (Tangier Disease). *The Journal of clinical investigation*. 43:228-236.

Frostegård, A.G., J. Su, X. Hua, M. Vikström, U. de Faire, and J. Frostegård. 2014. Antibodies against Native and Oxidized Cardiolipin and Phosphatidylserine and Phosphorylcholine in Atherosclerosis Development. *PLoS ONE*. 9:e111764.

Fry, M., and D.E. Green. 1981. Cardiolipin requirement for electron transfer in complex I and III of the mitochondrial respiratory chain. *Journal of Biological Chemistry*. 256:1874-1880.

Gary, J.D., T.K. Sato, C.J. Stefan, C.J. Bonangelino, L.S. Weisman, and S.D. Emr. 2002. Regulation of Fab1 Phosphatidylinositol 3-Phosphate 5-Kinase Pathway by Vac7 Protein and Fig4, a Polyphosphoinositide Phosphatase Family Member. *Molecular Biology of the Cell*. 13:1238-1251.

Gary, J.D., A.E. Wurmser, C.J. Bonangelino, L.S. Weisman, and S.D. Emr. 1998. Fab1p Is Essential for PtdIns(3)P 5-Kinase Activity and the Maintenance of Vacuolar Size and Membrane Homeostasis. *The Journal of Cell Biology*. 143:65-79.

Gasch, A.P., P.T. Spellman, C.M. Kao, O. Carmel-Harel, M.B. Eisen, G. Storz, D. Botstein, and P.O. Brown. 2000. Genomic Expression Programs in the Response of Yeast Cells to Environmental Changes. *Molecular Biology of the Cell*. 11:4241-4257.

Gebert, N., A.S. Joshi, S. Kutik, T. Becker, M. McKenzie, X.L. Guan, V.P. Mooga, D.A. Stroud, G. Kulkarni, M.R. Wenk, P. Rehling, C. Meisinger, M.T. Ryan, N. Wiedemann, M.L. Greenberg, and N. Pfanner. 2009. Mitochondrial cardiolipin involved in outer membrane protein biogenesis: implications for Barth syndrome. *Current biology : CB*. 19:2133-2139.

Gillooly, D.J., I.C. Morrow, M. Lindsay, R. Gould, N.J. Bryant, J.-M. Gaullier, R.G. Parton, and H. Stenmark. 2000. Localization of phosphatidylinositol 3-phosphate in yeast and mammalian cells. *The EMBO Journal*. 19:4577-4588.

Gohil, V.M., P. Hayes, S. Matsuyama, H. Schägger, M. Schlame, and M.L. Greenberg. 2004. Cardiolipin Biosynthesis and Mitochondrial Respiratory Chain Function Are Interdependent. *Journal of Biological Chemistry*. 279:42612-42618.

Gohil, V.M., M.N. Thompson, and M.L. Greenberg. 2005. Synthetic Lethal Interaction of the Mitochondrial Phosphatidylethanolamine and Cardiolipin Biosynthetic Pathways in Saccharomyces cerevisiae. *Journal of Biological Chemistry*. 280:35410-35416.

Gu, Z., F. Valianpour, S. Chen, F.M. Vaz, G.A. Hakkaart, R.J.A. Wanders, and M.L. Greenberg. 2004. Aberrant cardiolipin metabolism in the yeast taz1 mutant: a model for Barth syndrome. *Molecular Microbiology*. 51:149-158.

Han, X., D.R. Abendschein, J.G. Kelley, and R.W. Gross. 2000. Diabetes-induced changes in specific lipid molecular species in rat myocardium. *Biochemical Journal*. 352:79-89.

Han, X., J. Yang, H. Cheng, K. Yang, D.R. Abendschein, and R.W. Gross. 2005. Shotgun Lipidomics Identifies Cardiolipin Depletion in Diabetic Myocardium Linking Altered Substrate Utilization with Mitochondrial Dysfunction†. *Biochemistry*. 44:16684-16694.

Han, X., J. Yang, K. Yang, Z. Zhao, D.R. Abendschein, and R.W. Gross. 2007. Alterations in Myocardial Cardiolipin Content and Composition Occur at the Very Earliest Stages of Diabetes: A Shotgun Lipidomics Study. *Biochemistry*. 46:6417-6428.

He, Q., and X. Han. 2014. Cardiolipin remodeling in diabetic heart. *Chemistry and Physics of Lipids*. 179:75-81.

Heinisch, J.J., A. Lorberg, H.-P. Schmitz, and J.J. Jacoby. 1999. The protein kinase C-mediated MAP kinase pathway involved in the maintenance of cellular integrity in Saccharomyces cerevisiae. *Molecular Microbiology*. 32:671-680.

Helliwell, S.B., A. Schmidt, Y. Ohya, and M.N. Hall. 1998. The Rho1 effector Pkc1, but not Bni1, mediates signalling from Tor2 to the actin cytoskeleton. *Current Biology*. 8:1211-1214.

Herskowitz, I. 1995. MAP kinase pathways in yeast: For mating and more. *Cell*. 80:187-197.

Hijikata, A., K. Yura, O. Ohara, and M. Go. 2015. Structural and functional analyses of Barth syndrome-causing mutations and alternative splicing in the tafazzin acyltransferase domain. *Meta Gene*. 4:92-106.

Hoppins, S., S.R. Collins, A. Cassidy-Stone, E. Hummel, R.M. DeVay, L.L. Lackner,

B. Westermann, M. Schuldiner, J.S. Weissman, and J. Nunnari. 2011. A mitochondrial-focused genetic interaction map reveals a scaffold-like complex required for inner membrane organization in mitochondria. *The Journal of Cell Biology*. 195:323-340.

Hostetler, K.Y., H. van den Bosch, and L.L. van Deenen. 1972. The mechanism of cardiolipin biosynthesis in liver mitochondria. *Biochimica et biophysica acta*. 260:507-513.

Houtkooper, R.H., H. Akbari, H. van Lenthe, W. Kulik, R.J.A. Wanders, M. Frentzen, and F.M. Vaz. 2006. Identification and characterization of human cardiolipin synthase. *FEBS Letters*. 580:3059-3064.

Houtkooper, R.H., and F.M. Vaz. 2008. Cardiolipin, the heart of mitochondrial metabolism. *Cell. Mol. Life Sci.* 65:2493-2506.

Hsu, Y.-H., D.S. Dumlao, J. Cao, and E.A. Dennis. 2013. Assessing Phospholipase A(2) Activity toward Cardiolipin by Mass Spectrometry. *PLoS ONE*. 8:e59267.

Jiang, F., H.S. Rizavi, and M.L. Greenberg. 1997. Cardiolipin is not essential for the growth of Saccharomyces cerevisiae on fermentable or non-fermentable carbon sources. *Molecular Microbiology*. 26:481-491.

Jiang, F., M.T. Ryan, M. Schlame, M. Zhao, Z. Gu, M. Klingenberg, N. Pfanner, and M.L. Greenberg. 2000. Absence of Cardiolipin in the crd1 Null Mutant Results in Decreased Mitochondrial Membrane Potential and Reduced Mitochondrial Function. *Journal of Biological Chemistry*. 275:22387-22394.

Joshi, A.S., J. Zhou, V.M. Gohil, S. Chen, and M.L. Greenberg. 2009. Cellular

functions of cardiolipin in yeast. *Biochimica et biophysica acta*. 1793:212-218.

Journo, D., A. Mor, and H. Abeliovich. 2009. Aup1-mediated Regulation of Rtg3 during Mitophagy. *The Journal of Biological Chemistry*. 284:35885-35895.

Jung, K.-W., A.K. Strain, K. Nielsen, K.-H. Jung, and Y.-S. Bahn. 2012. Two cation transporters Ena1 and Nha1 cooperatively modulate ion homeostasis, antifungal drug resistance, and virulence of Cryptococcus neoformans via the HOG pathway. *Fungal Genetics and Biology*. 49:332-345.

Köfinger, J., Michael J. Ragusa, I.-H. Lee, G. Hummer, and James H. Hurley. 2015. Solution Structure of the Atg1 Complex: Implications for the Architecture of the Phagophore Assembly Site. *Structure*. 23:809-818.

Kadenbach, B., P. Mende, H.V.J. Kolbe, I. Stipani, and F. Palmieri. 1982. The mitochondrial phosphate carrier has an essential requirement for cardiolipin. *FEBS Letters*. 139:109-112.

Kalogeris, T., Y. Bao, and R.J. Korthuis. 2014. Mitochondrial reactive oxygen species: A double edged sword in ischemia/reperfusion vs preconditioning. *Redox Biology*. 2:702-714.

Kanki, T., D. Kang, and D.J. Klionsky. 2009a. Monitoring mitophagy in yeast: The Om45-GFP processing assay. *Autophagy*. 5:1186-1189.

Kanki, T., K. Wang, M. Baba, C.R. Bartholomew, M.A. Lynch-Day, Z. Du, J. Geng, K. Mao, Z. Yang, W.-L. Yen, and D.J. Klionsky. 2009b. A Genomic Screen for Yeast Mutants Defective in Selective Mitochondria Autophagy. *Molecular Biology of the Cell*. 20:4730-4738.

Kanki, T., K. Wang, Y. Cao, M. Baba, and D.J. Klionsky. 2009c. Atg32 Is a Mitochondrial Protein that Confers Selectivity during Mitophagy. *Developmental Cell*. 17:98-109.

Ke, R., P.J. Ingram, and K. Haynes. 2013. An Integrative Model of Ion Regulation in Yeast. *PLoS Computational Biology*. 9:e1002879.

Kirisako, T., M. Baba, N. Ishihara, K. Miyazawa, M. Ohsumi, T. Yoshimori, T. Noda, and Y. Ohsumi. 1999. Formation Process of Autophagosome Is Traced with Apg8/Aut7p in Yeast. *The Journal of Cell Biology*. 147:435-446.

Kissová, I., M. Deffieu, S. Manon, and N. Camougrand. 2004. Uth1p Is Involved in the Autophagic Degradation of Mitochondria. *Journal of Biological Chemistry*. 279:39068-39074.

Kiššová, I.B., B. Salin, J. Schaeffer, S. Bhatia, S. Manon, and N. Camougrand. 2007. Selective and Non-Selective Autophagic Degradation of Mitochondria in Yeast. *Autophagy*. 3:329-336.

Kito, M., S. Aibara, M. Kato, and T. Hata. 1972. Differences in fatty acid composition among phosphatidylethanolamine, phosphatidylglycerol and cardiolipin of Escherichia coli. *Biochimica et Biophysica Acta (BBA) - Lipids and Lipid Metabolism*. 260:475-478.

Kloner, R.A., K. Przyklenk, and P. Whittaker. 1989. Deleterious effects of oxygen radicals in ischemia/reperfusion. Resolved and unresolved issues. *Circulation*. 80:1115-1127.

Knight, B.L. 2004. ATP-binding cassette transporter A1: Regulation of cholesterol

efflux. *Biochemical Society Transactions*. 32:124-127.

Korytowski, W., L.V. Basova, A. Pilat, R.M. Kernstock, and A.W. Girotti. 2011. Permeabilization of the Mitochondrial Outer Membrane by Bax/Truncated Bid (tBid) Proteins as Sensitized by Cardiolipin Hydroperoxide Translocation: MECHANISTIC IMPLICATIONS FOR THE INTRINSIC PATHWAY OF OXIDATIVE APOPTOSIS. *The Journal of Biological Chemistry*. 286:26334-26343.

Koshkin, V., and M.L. Greenberg. 2002. Cardiolipin prevents rate-dependent uncoupling and provides osmotic stability in yeast mitochondria. *Biochemical Journal*. 364:317-322.

Kutik, S., M. Rissler, X.L. Guan, B. Guiard, G. Shui, N. Gebert, P.N. Heacock, P. Rehling, W. Dowhan, M.R. Wenk, N. Pfanner, and N. Wiedemann. 2008. The translocator maintenance protein Tam41 is required for mitochondrial cardiolipin biosynthesis. *The Journal of cell biology*. 183:1213-1221.

Lands, W.E.M. 1960. Metabolism of Glycerolipids: II. THE ENZYMATIC ACYLATION OF LYSOLECITHIN. *Journal of Biological Chemistry*. 235:2233-2237.

Le, C.H., C.M. Mulligan, M.A. Routh, G.J. Bouma, M.A. Frye, K.M. Jeckel, G.C. Sparagna, J.M. Lynch, R.L. Moore, S.A. McCune, M. Bristow, S. Zarini, R.C. Murphy, and A.J. Chicco. 2014. Delta-6-desaturase Links Polyunsaturated Fatty Acid Metabolism With Phospholipid Remodeling and Disease Progression in Heart Failure. *Circulation: Heart Failure*. 7:172-183.

Lesnefsky, E.J., T.J. Slabe, M.S.K. Stoll, P.E. Minkler, and C.L. Hoppel. 2001.

Myocardial ischemia selectively depletes cardiolipin in rabbit heart subsarcolemmal mitochondria. H2770-H2778 pp.

Levin, D.E., and B. Errede. 1995. The proliferation of MAP kinase signaling pathways in yeast. *Current Opinion in Cell Biology*. 7:197-202.

Li, S.C., T.T. Diakov, J.M. Rizzo, and P.M. Kane. 2012. Vacuolar H(+)-ATPase Works in Parallel with the HOG Pathway To Adapt Saccharomyces cerevisiae Cells to Osmotic Stress. *Eukaryotic Cell*. 11:282-291.

Li, S.C., and P.M. Kane. 2009. The Yeast Lysosome-like Vacuole: Endpoint and Crossroads. *Biochimica et biophysica acta*. 1793:650-663.

Li, X.-X., B. Tsoi, Y.-F. Li, H. Kurihara, and R.-R. He. 2015. Cardiolipin and Its Different Properties in Mitophagy and Apoptosis. *Journal of Histochemistry & Cytochemistry*.

Linton, P.-J., M. Gurney, D. Sengstock, R.M. Mentzer Jr, and R.A. Gottlieb. This old heart: Cardiac aging and autophagy. *Journal of Molecular and Cellular Cardiology*.

Lopez, D., K. Kobayashi, J.T. Merrill, E. Matsuura, and L.R. Lopez. 2003. IgG Autoantibodies against β(2)-Glycoprotein I Complexed with a Lipid Ligand Derived from Oxidized Low-Density Lipoprotein are Associated with Arterial Thrombosis in Antiphospholipid Syndrome. *Clinical and Developmental Immunology*. 10:203-211.

Lu, B., F.Y. Xu, Y.J. Jiang, P.C. Choy, G.M. Hatch, C. Grunfeld, and K.R. Feingold. 2006. Cloning and characterization of a cDNA encoding human cardiolipin

synthase (hCLS1). *Journal of Lipid Research*. 47:1140-1145.

Márquez JA, and S. R. 1996. Multiple transduction pathways regulate the sodium-extrusion gene PMR2/ENA1 during salt stress in yeast. *FEBS Lett.* 11:89-92.

Ma, L., F.M. Vaz, Z. Gu, R.J.A. Wanders, and M.L. Greenberg. 2004. The Human TAZ Gene Complements Mitochondrial Dysfunction in the Yeast taz1Δ Mutant: IMPLICATIONS FOR BARTH SYNDROME. *Journal of Biological Chemistry*. 279:44394-44399.

Maack, C., and B. O'Rourke. 2007. Excitation-contraction coupling and mitochondrial energetics. *Basic research in cardiology*. 102:369-392.

Malhotra, A., Y. Xu, M. Ren, and M. Schlame. 2009. Formation of molecular species of mitochondrial cardiolipin. 1. A novel transacylation mechanism to shuttle fatty acids between sn-1 and sn-2 positions of multiple phospholipid species. *Biochimica et biophysica acta*. 1791:314-320.

Mao, K., K. Wang, M. Zhao, T. Xu, and D.J. Klionsky. 2011. Two MAPK-signaling pathways are required for mitophagy in Saccharomyces cerevisiae. *The Journal of Cell Biology*. 193:755-767.

Marai, I., M. Shechter, P. Langevitz, B. Gilburd, A. Rubenstein, E. Matssura, Y. Sherer, and Y. Shoenfeld. 2008. Anti-Cardiolipin Antibodies and Endothelial Function in Patients With Coronary Artery Disease. *The American Journal of Cardiology*. 101:1094-1097.

McMurray, J.J.V., and M.A. Pfeffer. Heart failure. *The Lancet*. 365:1877-1889.

Meldrum, D.R., J.C. Cleveland, Jr., X. Meng, B.C. Sheridan, F. Gamboni, B.S. Cain,

A.H. Harken, and A. Banerjee. Protein Kinase C Isoform Diversity in Preconditioning. *Journal of Surgical Research*. 69:183-187.

Mellor, H., and P.J. Parker. 1998. The extended protein kinase C superfamily. *Biochemical Journal*. 332:281-292.

Mileykovskaya, E., and W. Dowhan. 2014a. Cardiolipin-Dependent Formation of Mitochondrial Respiratory Supercomplexes. *Chemistry and physics of lipids*. 179:42-48.

Mileykovskaya, E., and W. Dowhan. 2014b. Cardiolipin-dependent formation of mitochondrial respiratory supercomplexes. *Chemistry and Physics of Lipids*. 179:42-48.

Mokranjac, D., M. Sichting, W. Neupert, and K. Hell. 2003. Tim14, a novel key component of the import motor of the TIM23 protein translocase of mitochondria. 4945-4956 pp.

Moyzis, A.G., J. Sadoshima, and Å.B. Gustafsson. 2015. Mending a broken heart: the role of mitophagy in cardioprotection. H183-H192 pp.

Munakata M, Stamm C, Friehs I, Zurakowski D, Cowan DB, Cao-Danh H, McGowan FX Jr, and d.N. PJ. 2002. Protective effects of protein kinase C during myocardial ischemia require activation of phosphatidyl-inositol specific phospholipase C. *Ann Thorac Surg.* 73:1236-1245.

Nair, U., and D.J. Klionsky. 2005. Molecular Mechanisms and Regulation of Specific and Nonspecific Autophagy Pathways in Yeast. *Journal of Biological Chemistry*. 280:41785-41788.

Nakai, A., O. Yamaguchi, T. Takeda, Y. Higuchi, S. Hikoso, M. Taniike, S. Omiya, I. Mizote, Y. Matsumura, M. Asahi, K. Nishida, M. Hori, N. Mizushima, and K. Otsu. 2007. The role of autophagy in cardiomyocytes in the basal state and in response to hemodynamic stress. *Nat Med*. 13:619-624.

Nakamura, T., Y. Liu, D. Hirata, H. Namba, S. Harada, T. Hirokawa, and T. Miyakawa. 1993. Protein phosphatase type 2B (calcineurin)-mediated, FK506-sensitive regulation of intracellular ions in yeast is an important determinant for adaptation to high salt stress conditions. *The EMBO Journal*. 12:4063-4071.

Narendra, D., A. Tanaka, D.-F. Suen, and R.J. Youle. 2008. Parkin is recruited selectively to impaired mitochondria and promotes their autophagy. *The Journal of Cell Biology*. 183:795-803.

Nathan, D.M. 1993. Long-Term Complications of Diabetes Mellitus. *New England Journal of Medicine*. 328:1676-1685.

Noda, T., and D.J. Klionsky. 2008. Chapter 3 The Quantitative Pho8Δ60 Assay of Nonspecific Autophagy. *In* Methods in Enzymology. Vol. Volume 451. J.K. Daniel, editor. Academic Press. 33-42.

Nomoto S, Watanabe Y, Ninomiya-Tsuji J, Yang LX, Nagai Y, Kiuchi K, Hagiwara M, Hidaka H, Matsumoto K, and I. K. 1997. Functional analyses of mammalian protein kinase C isozymes in budding yeast and mammalian fibroblasts. *Genes Cells*. 2:601-614.

Nowikovsky, K., S. Reipert, R.J. Devenish, and R.J. Schweyen. 2007. Mdm38 protein depletion causes loss of mitochondrial K+//H+ exchange activity, osmotic

swelling and mitophagy. *Cell Death Differ*. 14:1647-1656.

O'Rourke, S.M., and I. Herskowitz. 2004. Unique and Redundant Roles for HOG MAPK Pathway Components as Revealed by Whole-Genome Expression Analysis. *Molecular Biology of the Cell*. 15:532-542.

Odorizzi, G., M. Babst, and S.D. Emr. 1998. Fab1p PtdIns(3)P 5-Kinase Function Essential for Protein Sorting in the Multivesicular Body. *Cell*. 95:847-858.

Okamoto, K. 2014. Organellophagy: Eliminating cellular building blocks via selective autophagy. *The Journal of Cell Biology*. 205:435-445.

Okamoto, K., N. Kondo-Okamoto, and Y. Ohsumi. 2009. Mitochondria-Anchored Receptor Atg32 Mediates Degradation of Mitochondria via Selective Autophagy. *Developmental Cell*. 17:87-97.

Oram, J.F. 2000. Tangier disease and ABCA1. *Biochimica et Biophysica Acta (BBA) - Molecular and Cell Biology of Lipids*. 1529:321-330.

Osman, C., M. Haag, F.T. Wieland, B. Brugger, and T. Langer. 2010. A mitochondrial phosphatase required for cardiolipin biosynthesis: the PGP phosphatase Gep4. *The EMBO journal*. 29:1976-1987.

Pan, H.-J., Y. Lin, Y.E. Chen, D.E. Vance, and E.H. Leiter. 2006. Adverse hepatic and cardiac responses to rosiglitazone in a new mouse model of type 2 diabetes: Relation to dysregulated phosphatidylcholine metabolism. *Vascular Pharmacology*. 45:65-71.

Paradies, G., G. Petrosillo, M. Pistolese, N. Di Venosa, A. Federici, and F.M. Ruggiero. 2004. Decrease in Mitochondrial Complex I Activity in

Ischemic/Reperfused Rat Heart: Involvement of Reactive Oxygen Species and Cardiolipin. *Circulation Research*. 94:53-59.

Paradies, G., G. Petrosillo, M. Pistolese, N. Di Venosa, D. Serena, and F.M. Ruggiero. 1999. Lipid peroxidation and alterations to oxidative metabolism in mitochondria isolated from rat heart subjected to ischemia and reperfusion. *Free Radical Biology and Medicine*. 27:42-50.

Paradies, G., and F.M. Ruggiero. 1988. The effect of doxorubicin on the transport of pyruvate in rat-heart mitochondria. *Biochemical and Biophysical Research Communications*. 156:1302-1307.

Petrosillo, G., F.M. Ruggiero, N. Di Venosa, and G. Paradies. 2003. Decreased complex III activity in mitochondria isolated from rat heart subjected to ischemia and reperfusion: role of reactive oxygen species and cardiolipin. *The FASEB Journal*.

Pfeiffer, K., V. Gohil, R.A. Stuart, C. Hunte, U. Brandt, M.L. Greenberg, and H. Schägger. 2003. Cardiolipin Stabilizes Respiratory Chain Supercomplexes. *Journal of Biological Chemistry*. 278:52873-52880.

Platara, M., A. Ruiz, R. Serrano, A. Palomino, F. Moreno, and J. Ariño. 2006. The Transcriptional Response of the Yeast Na+-ATPase ENA1 Gene to Alkaline Stress Involves Three Main Signaling Pathways. *Journal of Biological Chemistry*. 281:36632-36642.

Proft, M., and K. Struhl. 2004. MAP Kinase-Mediated Stress Relief that Precedes and Regulates the Timing of Transcriptional Induction. *Cell*. 118:351-361.

Raingeaud, J., S. Gupta, J.S. Rogers, M. Dickens, J. Han, R.J. Ulevitch, and R.J. Davis. 1995. Pro-inflammatory Cytokines and Environmental Stress Cause p38 Mitogen-activated Protein Kinase Activation by Dual Phosphorylation on Tyrosine and Threonine. *Journal of Biological Chemistry*. 270:7420-7426.

Ranieri, A., D. Millo, G. Di Rocco, G. Battistuzzi, C. Bortolotti, M. Borsari, and M. Sola. 2015. Immobilized cytochrome c bound to cardiolipin exhibits peculiar oxidation state-dependent axial heme ligation and catalytically reduces dioxygen. *J Biol Inorg Chem*:1-10.

Reggiori, F., T. Shintani, U. Nair, and D.J. Klionsky. 2005. Atg9 Cycles between Mitochondria and the Pre-Autophagosomal Structure in Yeasts. *Autophagy*. 1:101-109.

Reggiori, F., K.A. Tucker, P.E. Stromhaug, and D.J. Klionsky. 2004. The Atg1-Atg13 Complex Regulates Atg9 and Atg23 Retrieval Transport from the Pre-Autophagosomal Structure. *Developmental Cell*. 6:79-90.

Rehling, P., N. Pfanner, and C. Meisinger. 2003. Insertion of Hydrophobic Membrane Proteins into the Inner Mitochondrial Membrane—A Guided Tour. *Journal of Molecular Biology*. 326:639-657.

Reibel, D.K., B. O'Rourke, K.A. Foster, H. Hutchinson, C.E. Uboh, and R.L. Kent. 1986. Altered phospholipid metabolism in pressure-overload hypertrophied hearts. *American Journal of Physiology - Heart and Circulatory Physiology* 250:H1-H6.

Rep, M., M. Krantz, J.M. Thevelein, and S. Hohmann. 2000. The Transcriptional

Response of Saccharomyces cerevisiae to Osmotic Shock: Hot1p AND Msn2p/Msn4p ARE REQUIRED FOR THE INDUCTION OF SUBSETS OF HIGH OSMOLARITY GLYCEROL PATHWAY-DEPENDENT GENES. *Journal of Biological Chemistry*. 275:8290-8300.

Richter-Dennerlein, R., A. Korwitz, M. Haag, T. Tatsuta, S. Dargazanli, M. Baker, T. Decker, T. Lamkemeyer, Elena I. Rugarli, and T. Langer. 2014. DNAJC19, a Mitochondrial Cochaperone Associated with Cardiomyopathy, Forms a Complex with Prohibitins to Regulate Cardiolipin Remodeling. *Cell Metabolism*. 20:158-171.

Roberts, C., C. Raymond, C. Yamashiro, and T. Stevens. 1991. Methods for studying the yeast vacuole. *Methods Enzymol*. 194:644-661.

Rosca, M., P. Minkler, and C.L. Hoppel. 2011. Cardiac mitochondria in heart failure: Normal cardiolipin profile and increased threonine phosphorylation of complex IV. *Biochimica et Biophysica Acta (BBA) - Bioenergetics*. 1807:1373-1382.

Ross, R. 1993. The pathogenesis of atherosclerosis: a perspective for the 1990s. *Nature*. 362:801-809.

Rudge, S.A., D.M. Anderson, and S.D. Emr. 2004. Vacuole Size Control: Regulation of PtdIns(3,5)P(2) Levels by the Vacuole-associated Vac14-Fig4 Complex, a PtdIns(3,5)P(2)-specific Phosphatase. *Molecular Biology of the Cell*. 15:24-36.

Rust, S., M. Rosier, H. Funke, J. Real, Z. Amoura, J.-C. Piette, J.-F. Deleuze, H.B. Brewer, N. Duverger, P. Denefle, and G. Assmann. 1999. Tangier disease is

caused by mutations in the gene encoding ATP-binding cassette transporter 1. *Nat Genet*. 22:352-355.

Sack, M.N. 2009. Type 2 Diabetes, Mitochondrial Biology and the Heart. *Journal of molecular and cellular cardiology*. 46:842-849.

Saini-Chohan, H.K., M.G. Holmes, A.J. Chicco, W.A. Taylor, R.L. Moore, S.A. McCune, D.L. Hickson-Bick, G.M. Hatch, and G.C. Sparagna. 2009. Cardiolipin biosynthesis and remodeling enzymes are altered during development of heart failure. *Journal of Lipid Research*. 50:1600-1608.

Saito, H., and K. Tatebayashi. 2004. Regulation of the Osmoregulatory HOG MAPK Cascade in Yeast. *Journal of Biochemistry*. 136:267-272.

Sakoh-Nakatogawa, M., H. Kirisako, H. Nakatogawa, and Y. Ohsumi. 2015. Localization of Atg3 to autophagy-related membranes and its enhancement by the Atg8-family interacting motif to promote expansion of the membranes. *FEBS Letters*. 589:744-749.

Schlame, M., S. Brody, and K.Y. Hostetler. 1993. Mitochondrial cardiolipin in diverse eukaryotes. *European Journal of Biochemistry*. 212:727-733.

Schlame, M., R.I. Kelley, A. Feigenbaum, J.A. Towbin, P.M. Heerdt, T. Schieble, R.J. Wanders, S. DiMauro, and T.J. Blanck. 2003. Phospholipid abnormalities in children with Barth syndrome. *Journal of the American College of Cardiology*. 42:1994-1999.

Schlame, M., and M. Ren. 2006. Barth syndrome, a human disorder of cardiolipin metabolism. *FEBS Letters*. 580:5450-5455.

Schlame, M., J.A. Towbin, P.M. Heerdt, R. Jehle, S. DiMauro, and T.J. Blanck. 2002. Deficiency of tetralinoleoyl-cardiolipin in Barth syndrome. *Annals of neurology*. 51:634-637.

Shintani, T., and D.J. Klionsky. 2004. Autophagy in Health and Disease: A Double-Edged Sword. *Science (New York, N.Y.)*. 306:990-995.

Slessareva, J.E., S.M. Routt, B. Temple, V.A. Bankaitis, and H.G. Dohlman. 2006. Activation of the Phosphatidylinositol 3-Kinase Vps34 by a G Protein α Subunit at the Endosome. *Cell*. 126:191-203.

Sparagna, G.C., A.J. Chicco, R.C. Murphy, M.R. Bristow, C.A. Johnson, M.L. Rees, M.L. Maxey, S.A. McCune, and R.L. Moore. 2007. Loss of cardiac tetralinoleoyl cardiolipin in human and experimental heart failure. *Journal of Lipid Research*. 48:1559-1570.

Steven P. Marso, and D.M. Stern. 2003. Diabetes and Cardiovascular Disease: Integrating Science and Clinical Medicine. Lippincott Williams & Wilkins.

Su, J., A.G. Frostegård, X. Hua, T. Gustafsson, T. Jogestrand, I. Hafström, and J. Frostegård. 2013. Low Levels of Antibodies Against Oxidized but not Nonoxidized Cardiolipin and Phosphatidylserine Are Associated with Atherosclerotic Plaques in Systemic Lupus Erythematosus. *The Journal of Rheumatology*. 40:1856-1864.

Su, J., A. Georgiades, R. Wu, T. Thulin, U. de Faire, and J. Frostegård. 2006. Antibodies of IgM subclass to phosphorylcholine and oxidized LDL are protective factors for atherosclerosis in patients with hypertension.

Atherosclerosis. 188:160-166.

Suzuki, K., T. Kirisako, Y. Kamada, N. Mizushima, T. Noda, and Y. Ohsumi. 2001. The pre-autophagosomal structure organized by concerted functions of APG genes is essential for autophagosome formation. *The EMBO Journal*. 20:5971-5981.

Suzuki, K., Y. Kubota, T. Sekito, and Y. Ohsumi. 2007. Hierarchy of Atg proteins in pre-autophagosomal structure organization. *Genes to Cells*. 12:209-218.

Türkoğlu, O., N. Barış, N. Kütükçüler, Ö. Şenarslan, S. Güneri, and G. Atilla. 2008. Evaluation of Serum Anti-Cardiolipin and Oxidized Low-Density Lipoprotein Levels in Chronic Periodontitis Patients With Essential Hypertension. *Journal of Periodontology*. 79:332-340.

Takeshige K, Baba M, Tsuboi S, Noda T, and O. Y. 1992. Autophagy in yeast demonstrated with proteinase-deficient mutants and conditions for its induction. *The Journal of Cell Biology*. 119:301-311.

Tamura, Y., Y. Harada, S. Nishikawa, K. Yamano, M. Kamiya, T. Shiota, T. Kuroda, O. Kuge, H. Sesaki, K. Imai, K. Tomii, and T. Endo. 2013. Tam41 is a CDP-diacylglycerol synthase required for cardiolipin biosynthesis in mitochondria. *Cell metabolism*. 17:709-718.

Taylor, W.A., and G.M. Hatch. 2009. Identification of the Human Mitochondrial Linoleoyl-coenzyme A Monolysocardiolipin Acyltransferase (MLCL AT-1). *The Journal of Biological Chemistry*. 284:30360-30371.

Tian, H.F., J.M. Feng, and J.F. Wen. 2012. The evolution of cardiolipin biosynthesis

and maturation pathways and its implications for the evolution of eukaryotes. *BMC evolutionary biology*. 12:32.

Tong, A.H.Y., M. Evangelista, A.B. Parsons, H. Xu, G.D. Bader, N. Pagé, M. Robinson, S. Raghibizadeh, C.W.V. Hogue, H. Bussey, B. Andrews, M. Tyers, and C. Boone. 2001. Systematic Genetic Analysis with Ordered Arrays of Yeast Deletion Mutants. *Science*. 294:2364-2368.

Tuller, G., C. Hrastnik, G. Achleitner, U. Schiefthaler, F. Klein, and G. Daum. 1998. YDL142c encodes cardiolipin synthase (Cls1p) and is non-essential for aerobic growth of Saccharomyces cerevisiae. *FEBS Letters*. 421:15-18.

Tuominen, A., Y.I. Miller, L.F. Hansen, Y.A. Kesäniemi, J.L. Witztum, and S. Hörkkö. 2006. A Natural Antibody to Oxidized Cardiolipin Binds to Oxidized Low-Density Lipoprotein, Apoptotic Cells, and Atherosclerotic Lesions. *Arteriosclerosis, Thrombosis, and Vascular Biology*. 26:2096-2102.

Valianpour, F., R.J. Wanders, H. Overmars, P. Vreken, A.H. Van Gennip, F. Baas, B. Plecko, R. Santer, K. Becker, and P.G. Barth. 2002. Cardiolipin deficiency in X-linked cardioskeletal myopathy and neutropenia (Barth syndrome, MIM 302060): a study in cultured skin fibroblasts. *The Journal of pediatrics*. 141:729-733.

Vaz, F.M., R.H. Houtkooper, F. Valianpour, P.G. Barth, and R.J.A. Wanders. 2003. Only One Splice Variant of the Human TAZ Gene Encodes a Functional Protein with a Role in Cardiolipin Metabolism. *Journal of Biological Chemistry*. 278:43089-43094.

Walker, G.M. 1998. Yeast Physiology and Biotechnology. John Wiley & Sons Ltd. 150.

Wan, M., X. Hua, J. Su, D. Thiagarajan, A.G. Frostegård, J.Z. Haeggström, and J. Frostegård. 2014. Oxidized but not native cardiolipin has pro-inflammatory effects, which are inhibited by Annexin A5. *Atherosclerosis*. 235:592-598.

Wang, K., and D.J. Klionsky. 2011. Mitochondria removal by autophagy. *Autophagy*. 7:297-300.

Wang, N., D.L. Silver, C. Thiele, and A.R. Tall. 2001. ATP-binding cassette transporter A1 (ABCA1) functions as a cholesterol efflux regulatory protein. *Journal of Biological Chemistry*. 276:23742-23747.

Welter, E., M. Montino, R. Reinhold, P. Schlotterhose, R. Krick, J. Dudek, P. Rehling, and M. Thumm. 2013. Uth1 is a mitochondrial inner membrane protein dispensable for post-log-phase and rapamycin-induced mitophagy. *FEBS Journal*. 280:4970-4982.

Winkler, A., C. Arkind, C.P. Mattison, A. Burkholder, K. Knoche, and I. Ota. 2002. Heat Stress Activates the Yeast High-Osmolarity Glycerol Mitogen-Activated Protein Kinase Pathway, and Protein Tyrosine Phosphatases Are Essential under Heat Stress. *Eukaryotic Cell*. 1:163-173.

Wu, X., and B.P. Tu. 2011. Selective regulation of autophagy by the Iml1-Npr2-Npr3 complex in the absence of nitrogen starvation. *Molecular Biology of the Cell*. 22:4124-4133.

Xiao, J., J.L. Engel, J. Zhang, M.J. Chen, G. Manning, and J.E. Dixon. 2011.

Structural and functional analysis of PTPMT1, a phosphatase required for cardiolipin synthesis. *Proceedings of the National Academy of Sciences of the United States of America*. 108:11860-11865.

Xie, Z., and D.J. Klionsky. 2007. Autophagosome formation: core machinery and adaptations. *Nat Cell Biol*. 9:1102-1109.

Xu, Y., R.I. Kelley, T.J.J. Blanck, and M. Schlame. 2003. Remodeling of Cardiolipin by Phospholipid Transacylation. *Journal of Biological Chemistry*. 278:51380-51385.

Yamamoto, A., D.B. DeWald, I.V. Boronenkov, R.A. Anderson, S.D. Emr, and D. Koshland. 1995. Novel PI(4)P 5-kinase homologue, Fab1p, essential for normal vacuole function and morphology in yeast. *Molecular Biology of the Cell*. 6:525-539.

Yamashita, A., T. Sugiura, and K. Waku. 1997. Acyltransferases and Transacylases Involved in Fatty Acid Remodeling of Phospholipids and Metabolism of Bioactive Lipids in Mammalian Cells. *Journal of Biochemistry*. 122:1-16.

Ye, C., W. Lou, Y. Li, I.A. Chatzispyrou, M. Hüttemann, I. Lee, R.H. Houtkooper, F.M. Vaz, S. Chen, and M.L. Greenberg. 2014a. Deletion of the Cardiolipin-specific Phospholipase Cld1 Rescues Growth and Life Span Defects in the Tafazzin Mutant: IMPLICATIONS FOR BARTH SYNDROME. *The Journal of Biological Chemistry*. 289:3114-3125.

Ye, C., Z. Shen, and M. Greenberg. 2014b. Cardiolipin remodeling: a regulatory hub for modulating cardiolipin metabolism and function. *J Bioenerg Biomembr*:1-

11.

Yorimitsu, T., S. Zaman, J.R. Broach, and D.J. Klionsky. 2007. Protein Kinase A and Sch9 Cooperatively Regulate Induction of Autophagy in Saccharomyces cerevisiae. *Molecular Biology of the Cell*. 18:4180-4189.

Zhang, J., Z. Guan, A.N. Murphy, S.E. Wiley, G.A. Perkins, C.A. Worby, J.L. Engel, P. Heacock, O.K. Nguyen, J.H. Wang, C.R. Raetz, W. Dowhan, and J.E. Dixon. 2011. Mitochondrial phosphatase PTPMT1 is essential for cardiolipin biosynthesis. *Cell metabolism*. 13:690-700.

Zhang, M., E. Mileykovskaya, and W. Dowhan. 2002. Gluing the Respiratory Chain Together: CARDIOLIPIN IS REQUIRED FOR SUPERCOMPLEX FORMATION IN THE INNER MITOCHONDRIAL MEMBRANE. *Journal of Biological Chemistry*. 277:43553-43556.

Zhang, M., E. Mileykovskaya, and W. Dowhan. 2005. Cardiolipin Is Essential for Organization of Complexes III and IV into a Supercomplex in Intact Yeast Mitochondria(). *The Journal of biological chemistry*. 280:29403-29408.

Zhong, H., J. Lu, L. Xia, M. Zhu, and H. Yin. 2014. Formation of electrophilic oxidation products from mitochondrial cardiolipin in vitro and in vivo in the context of apoptosis and atherosclerosis. *Redox Biology*. 2:878-883.

Zhong, Q., J. Gvozdenovic-Jeremic, P. Webster, J. Zhou, and M.L. Greenberg. 2005. Loss of Function of KRE5 Suppresses Temperature Sensitivity of Mutants Lacking Mitochondrial Anionic Lipids. *Molecular Biology of the Cell*. 16:665-675.

Zhong, Q., G. Li, J. Gvozdenovic-Jeremic, and M.L. Greenberg. 2007. Up-regulation of the Cell Integrity Pathway in Saccharomyces cerevisiae Suppresses Temperature Sensitivity of the pgs1Δ Mutant. *Journal of Biological Chemistry*. 282:15946-15953.

Zhou, J., Q. Zhong, G. Li, and M.L. Greenberg. 2009. Loss of Cardiolipin Leads to Longevity Defects That Are Alleviated by Alterations in Stress Response Signaling. *Journal of Biological Chemistry*. 284:18106-18114.

ABSTRACT

CARDIOLIPIN REGULATES MITOPHAGY THROUGH THE PKC PATHWAY

by

ZHENI SHEN

August 2015

Advisor: Dr. Miriam L. Greenberg

Major: Biological Sciences

Degree: Doctor of Philosophy

Cardiolipin (CL), the signature phospholipid of mitochondrial membranes, is important for cardiovascular health. Perturbation of CL metabolism is implicated in cardiovascular disease (CVD). The link between CL and CVD may be explained by the physiological roles of CL in pathways that are cardioprotective, such as autophagy/mitophagy and the mitogen-activated protein kinase (MAPK) pathways. My dissertation work focuses on elucidating how CL influences mitophagy and MAPK pathways.

crd1Δ was synthetically lethal/sick with the general autophagy mutants *atg8Δ*, *atg18Δ* and mitophagy mutant *atg32Δ*, suggesting that autophagy/mitophagy may be deficient in cells lacking CL. Microscopic examination of mitophagy revealed decreased translocation of GFP-tagged mitochondrial proteins into the vacuole of *crd1Δ* cells. This was confirmed by a decreased level of free GFP generated by

cleavage of GFP-tagged mitochondrial protein after delivery into the vacuole by mitophagy. These findings indicated that mitophagy is decreased in CL-deficient cells. Expression of *ATG8* was increased in *crd1Δ* cells at 37˚C, suggesting that nonselective autophagy was upregulated to compensate for decreased mitophagy.

The PKC and HOG MAPK pathways are known to be required for mitophagy. *crd1Δ* growth defects are exacerbated by deletion of HOG pathway genes *SHO1*, *SSK1*, *STE50* and *HOG1*, and rescued by stimulating the HOG pathway and upregulating the PKC pathway. These findings suggested the possibility that MAPK pathways are defective in *crd1Δ* cells. Phosphorylation of Slt2p and Hog1p in response to stimulants was decreased in *crd1Δ*, consistent with defective activation of these MAPK pathways. Interestingly, upregulating PKC by transforming the cell with a vector expressing a constitutively activated Pkc1p rescued defective mitophagy in *crd1Δ*.

These results suggest that the mechanism underlying defective mitophagy caused by loss of CL is a defective PKC pathway.

AUTOBIOGRAPHICAL STATEMENT

ZHENI SHEN

EDUCATION:

Ph.D. Biological Sciences, June 2015
Wayne State University, Detroit, Michigan, USA

M.S. Biochemistry and Molecular Biology, June 2009
Sichuan University West China Medical Center, Chengdu, Sichuan, China

B. M. Basic Medical Sciences, Jun 2006
Sichuan University West China Medical Center, Chengdu, Sichuan, China

AWARDS and FELLOWSHIPS:

- Wayne State University Outstanding Graduate Teaching Assistant Award, 2013
- Wayne State University Travel Awards, 2013
- Sichuan University First Class Honor Scholarship, 2001, 2003, 2004, 2005
- Sichuan University Excellent Student Leader, 2002,2003

PUBLICATIONS and SELECTED PRESENTATIONS:

1. Zheni Shen, Cunqi Ye, Keanna McCain, and Miriam L. Greenberg. The role of cardiolipin in cardiovascular health. *Biomed Research International (Journal of Biomedicine and Biotechnology)*: under revision.
2. Cunqi Ye, Zheni Shen, and Miriam L. Greenberg. Cardiolipin remodeling: a regulatory hub for modulating cardiolipin metabolism and function. *Journal of Bioenergetics and Biomembranes (JOBB)*, Special Edition : **2014** Nov 29.
3. Zheni Shen, Xiaosu Wang, Ping Fan et al. Analysis of UCP-1 gene A-3826G polymorphism in Chinese non-obese and obese populations. *Chinese Journal of Medical Genetics*, **2009**, 26 (5):555-61
4. Zheni Shen, Lihua Li, Yi Qu et al. The change of the expression level of VEGF in newborn-rat HIE Model. **The communication document for the 14th National Paediatrics Academic Conference[C].**
5. Zheni Shen, Zhijuan Luo. RNA interference and the feasibility in antiviral use. *Chinese Bulletin of Life Science*. **2006.** 18 (1): 41-44.
6. Zheni Shen, Wei Hao. Problems in the revolution of higher education. *Northwest Medical Education*. **2005**. 13(S): **The focal recommended communication document for the Third Chinese Educationist Conference.**
7. Zheni Shen, Dingzhi Fang. Problems and reform in education: Some personal opinion. *Research in Higher Education development*. **2004***.* 21(3): 62-68.